Exoplanet radius measurements for short-period exoplanets observed by the *CHEOPS* mission

Braeden Marie Harris

B.Sc. (Hons.) Kent, M.Sc. Cardiff

Master of Philosophy

Department of Physics, Keele University

March 2024

Abstract

Context. Scheduling observing time for the *CHEOPS* mission leaves short gaps in which the telescope goes unused. If data collected during these gaps provided quality results, they could be utilised to make observing time more efficient.

Aims. The aim of this study is to determine if the data collected during gaps in allocated observing time can produce publishable quality planetary radius measurements.

Methods. A bespoke method was created using `pycheops` to analyse short-period exoplanets observed during these observing gaps alongside *TESS* data analysis. Six exoplanetary systems were chosen to test this method: WASP-3, WASP-14, WASP-16, WASP-24, WASP-29, and WASP-74. The planetary radius measurements from each system were compared against published papers in order to determine their accuracy and precision.

Results. The planetary radius measurements were found to be comparable to literature for the exoplanets in this study. Furthermore, the radius measurements of WASP-3b, WASP-14b, WASP-16b, and WASP-29b were more precise than current literature values.

Conclusions. While it requires additional information to fill in missing pieces, precise radius measurements can be made using as little as one *CHEOPS* dataset. By adding these "filler programmes" to observing schedules, *CHEOPS* can be used more efficiently.

Acknowledgements

This research could not have been completed without the guidance and support of my supervisor, Dr Pierre Maxted. For patiently answering all of my questions and dedicating your time to helping me, I truly am grateful. I would like to thank all those within the School of Chemical and Physical Sciences at Keele University for every email, letter, and conversation. I knew I could ask for anything and you would all do your best to support me. To the *CHEOPS* mission consortium, thank you for allowing me to be a part of your research. I would also like to thank Prof Don Pollaco for being my *CHEOPS* sponsor.

I cannot express my gratitude enough to Dame Jocelyn Bell Burnell. It was through your encouragement that I pursued this degree, and your words to me are the guiding light I need when I begin to doubt myself. I could not have undertaken this research without the support of Prof Paul Roche and Dr Richard Lewis from Cardiff University. Your support during my MSc degree allowed me to move forward into this position. Finally, to Matthew Swayne, all of your advice and guidance was more helpful than you realise.

Personally, I would first like to thank my grandparents, Tom and Sally Harris as well as Don and Barb Baldwin. Your enthusiasm in my work has brought me joy beyond comprehension. To my parents, Tom and Gretchen, and my sisters, Spenser and Chesney, your laughter and love reminded me why I set out on this path in the first place.

Connor, for every late night and cup of coffee you made me, for every dinner you cooked at midnight because I forgot to eat, for believing in me when I could not do it myself, *thank you.*

Contents

iv

List of Figures

List of Tables

x

1   Introduction

1.1   Studying exoplanets

Exoplanet research has been ongoing for decades, with the first confirmed discoveries of planet-mass objects in the 1990's [Wolszczan and Frail, 1992, Mayor and Queloz, 1995]. This has lead to understanding how the Solar System compares to other planetary systems. A common occurrence which is not present in our own system is a class of exoplanets known as hot Jupiters. These are Jupiter-sized planets orbiting their host star once every few days or less. Their size and location make them particularly good subjects to observe and study, which will be explained further in this chapter.

High precision observation provides a wealth of information about exoplanetary systems [Santos et al., 2020]. While missions like *Kepler* and the Transiting Exoplanet Survey Satellite (*TESS*) have discovered thousands of confirmed planets, their characterisation capability is limited by the lack of focus on a single target [Borucki et al., 2009, Ricker et al., 2015, Gaidos et al., 2017]. To fill this gap, the CHaracterising ExOPlanets Satellite (*CHEOPS*) was launched on December 18, 2019 [Benz et al., 2021]. *CHEOPS* observes previously discovered systems and provides accurate planetary radius measurements [Broeg et al., 2014, Benz et al., 2018]. Analysing data from both *TESS* and *CHEOPS* broadens their individual capabilities and bridges gaps [Garai et al., 2022, Oddo et al., 2023].

The precision from *CHEOPS* results makes it an excellent tool for atmospheric characterisation [Lendl et al., 2020, Wilson et al., 2022]. The composition of the atmosphere can affect the opacity at certain wavelengths, which can be observed as a change in the measured planetary radius at varying wavelengths [Sing et al., 2011]. Because *CHEOPS* observes in the optical to near-infrared range (330 nm to 1100 nm) and *TESS* covers only the red to near-infrared range (600 nm to 1100 nm), comparing the results from these sources can provide information on how wavelength correlates with the radius of a planet [Ricker et al., 2014, Deline et al., 2020].

1.1.1 Observations

There are a number of methods to detect and study planetary systems, from direct observation to gravitational lensing, but the most successful type (in terms of number of planets detected) is the transit method [Sackett, 1999, Wright and Gaudi, 2013, Winn and Fabrycky, 2015]. The transit method observes a star over a period of time and detects the small decrease in light that occurs when a planet passes between the star and our line of sight [Carter et al., 2008].

TESS is a space-based telescope that searches for exoplanets using the transit method [Ricker et al., 2014]. The mission objective was to discover planets for further study, and it has far exceeded this goal. It has identified over 6000 exoplanet candidates, much greater than the predicted 1250 candidates [Guerrero et al., 2021, Barclay et al., 2018]. It has become a staple source of data on transiting exoplanetary systems.

CHEOPS observes transiting exoplanets using ultrahigh precision photometry [Broeg et al., 2014]. Precision is obtained by a single frame-transfer backside illuminated CCD. The photometric precision capability is 20 ppm in a 6 hour integration time, the precision needed to observe an Earth-sized planet orbiting a G5 dwarf star [Beck et al., 2017a]. This exceeds ground-based telescopes; a single Next Generation Transit Survey (NGTS) telescope has a precision of 400 ppm over a 30 minute integration [Bayliss et al., 2022]. The design is an improvement on previous exoplanet satellites, showcased in its similarity and use of *CoRoT* design [Beck et al., 2017b].

Raw images from *CHEOPS* observations go through an automated processing called the Data Reduction Pipeline (DRP) to calibrate and correct the images, then transform them into science-ready data [Hoyer et al., 2020]. Calibration removes instrumental noise from the images and correction removes environmental effects. Aperture photometry is then used to produce light curves. Aperture photometry is a method of measuring the flux within a circular area of a CCD frame [Da Costa, 1992, Mighell, 1999]. Finally, a report is produced which summarises the DRP process and provides multiple light curves for different sized apertures. Following the report and choosing an aperture size, the light curve can be analysed.

pycheops is a software package written in PYTHON which is designed to analyse *CHEOPS* data [Maxted et al., 2021]. pycheops has been successful in the analyses it has performed thus far. There are an estimated 40 published papers which use pycheops in some capacity, as of June 2023. These tend to (roughly) fall in one of two categories. The first category consists of studies which utilise pycheops for its ability to download and process the data (i.e. decorrelating and detrending) [Barragán et al., 2022, Wilson et al., 2022]. The second category goes beyond the first to use the modelling and analysis capabilities as well as the initial steps [Lendl et al., 2020, Bonfanti et al., 2021]. The studies are split almost in half, with a few outliers making use of other specific features included in the pycheops module. A particularly telling result of this survey of studies is that no papers, including those of the first category, suggest any major flaws or inconsistencies in their use of pycheops. With the *CHEOPS* mission extended to at least 2026, potentially 2029, there is a multitude of data to be analysed, for which a fast and accurate analysis tool such as pycheops is perfectly suited [Lea, 2023].

1.1.2 Light curve analysis

Analysing the light curve of a transiting exoplanet independent from any other information can provide data on orbital period, ratio of radii, and mean stellar density [Seager and Mallén-Ornelas, 2003]. These are obtained using the light curve observables: the depth of the transit, the total transit time (the time of the entire dip, including the ingress/ egress), and the transit duration (time spent inside the ingress/ egress) [Enoch et al., 2010]. These observables, as well as their relationship with the impact parameter, can be seen in Figure 1.1. Further, a complete orbit is required to independently complete the analysis because the light curve will show the orbital period by measuring the time between the start of one transit to the start of the next [Seager and Mallén-Ornelas, 2003]. If consecutive transits are not observed, external data (such as literature values or calculations using a series of mid-transit times) are required to determine the period [Bouchy, 2005, Torres et al., 2008a].
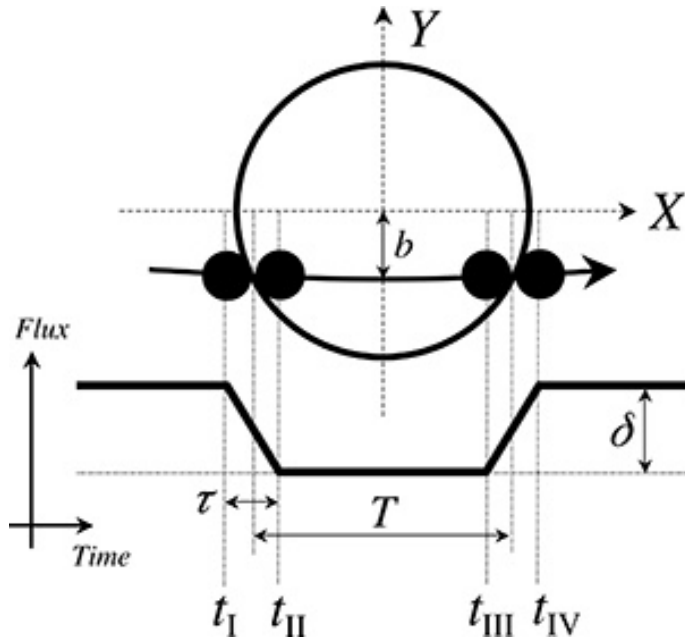
Figure 1.1: Diagram of the transit method analysis technique showing the observables and their relationships. This includes the depth, δ, the four points of contact, and the impact parameter, b [Santos et al., 2020]. The total transit time, t_T, is measured from t_I to t_{IV}, whereas t_F is the time between t_{II} and t_{III}. The ingress is measured from t_I to t_{II} (shown as τ), while the egress is between points t_{III} and t_{IV}.

While eccentricity is typically included in light curve analysis, it is usually not possible to make an accurate measurement of the eccentricity from the transit alone and must come from outside sources. When studying large objects with short orbital periods, such as hot Jupiter systems, a circular orbit is generally the case, so an assumed eccentricity of $e = 0$ is reasonable [Seager and Mallén-Ornelas, 2003]. The following equations are derived for circular orbits. This information can also be extracted for systems with eccentric orbits, if the eccentricity is correctly accounted for [Kipping, 2008]. Another property that is often ignored is the flux from/ reflected from the planet. Observed flux is dependent on radius, and therefore the small planet-star radius ratio leads to a small planet-star flux ratio ~ 100 ppm at optical wavelengths [Seager et al., 2005].

The first observable is the depth of the light curve. This is represented either by δ, as it is in Figure 1.1, or simply as D. This is the dip in the amount of flux received from the star due to the planet blocking light during its transit [Csizmadia et al., 2013]. In the simplest case, all variables contributing to flux remain the same during the transit other than the surface area, therefore the difference in flux depends only on the area of the disc blocked by the transiting planet. In reality, the shape of the transit is also influenced by stellar activity and limb darkening, which is discussed in more detail in Section 1.1.4 [Heller, 2019]. Since the area of a disc is equal to πR^2, the depth of the transit (ignoring limb darkening) is

$$\delta = \left(\frac{R_{\mathrm{p}}}{R_\star}\right)^2 = k^2,$$

where R_{p} is planetary radius, $R_\star$ is the host star radius, and k is the planet-star radius ratio.

The two time measurements pertaining to the transit are the total transit time, t_T, and the transit duration, t_F. These are measured with reference to four points of contact [Seager and Mallén-Ornelas, 2003, Hippke and Heller, 2019]. The first to the second point of contact is the ingress, in which the planet is partially blocking the stellar disc as it moves in front of the star. On the light curve, this is seen as the decrease in flux. From the second to the third point of contact the planet is entirely in front of the star, blocking the same amount of light throughout the transit (ignoring limb darkening). This gives the flat portion at the bottom of the light curve. The third to the fourth point of contact is the egress, where the planet is leaving the stellar disc, giving the light curve an increase in flux. Measuring from the first point of contact, t_{I}, to the fourth, t_{IV}, gives t_T, and the second to the third point of contact (t_{II} to t_{III}) gives t_F. The ratio of these time measurements gives information on the shape of the light curve. It is used determine the impact parameter,

$$b \equiv \left(\frac{a}{R_\star}\right)\cos\left(i\right) = \left[\frac{(1-k)^2 - \left(\frac{t_F}{t_T}\right)^2 (1+k)^2}{1 - \left(\frac{t_F}{t_T}\right)^2}\right]^{1/2},$$

which is also equivalent to the ratio of semi-major axis, a, to $R_\star$ multiplied by the cosine of inclination angle, i [Winn, 2008]. Impact parameter describes where on the light disc the planet appears to transit ($b = 0$ refers to the planet transiting through the centre of the stellar disc, $b = 1$ corresponds to a grazing transit where the centre of the planet coincides with the limb of the star at mid-transit) [Carter et al., 2008].

The last of the four observables is the period, P. This is used to calculate $\frac{a}{R_\star}$,

$$\frac{a}{R_\star} = \frac{2P}{\pi}\sqrt{\frac{k}{(t_T^2 - t_F^2)}},$$

using k, t_T, and t_F [Seager and Mallén-Ornelas, 2003, Enoch et al., 2010]. Introducing Kepler's law,

$$P^2 = \frac{4\pi^2}{G(M_\star + M_\mathrm{p})}a^3,$$

allows for the calculation of mean stellar density. Rearranging Kepler's law for mass, where $M_\star$ is stellar mass and M_p is planetary mass, and dividing by radius cubed gives mean stellar density

$$\rho_\star = \frac{4\pi^2}{GP^2}\left(\frac{a}{R_\star}\right)^3 - \frac{M_\mathrm{p}}{R_\star^3}$$

[Torres et al., 2008a]. The second term in this equation is generally negligible. Substituting in the equation for $\frac{a}{R_\star}$ and simplifying produces

$$\frac{\rho_\star}{\rho_\odot} = \frac{32P}{G\pi}\left[\frac{k}{(t_T^2 - t_F^2)}\right]^{3/2},$$

which can be solved without external information since it contains only observables and constants [Seager and Mallén-Ornelas, 2003].

1.1.3 Beyond the light curve

Beyond the transit method, the radial velocity method is another common way to observe and study exoplanetary systems. The radial velocity method looks for the small Doppler shift of a star's spectrum to uncover the wobble produced by the gravitational interactions between a planet and its star [Lovis and Fischer, 2010]. This interaction

is measured using $K_\star$, which describes the wobble in terms of kms^{-1}. The velocity of the star is the only one required, which is beneficial because the velocity of the planet is generally unobservable due to the planet-to-star flux ratio. Because radial velocity analysis can provide data that the transit method cannot, combining information from both methods allows the conclusions to go further [Gaidos et al., 2017]. The surface gravity of the planet is

$$g_\mathrm{p} = \frac{2\pi}{P} \frac{(1 - e^2)^{1/2} K_\star}{r_\mathrm{p}^2 \sin(i)},$$

where $r_\mathrm{p} = \frac{R_\mathrm{p}}{a}$. This equation combines information from both techniques [Southworth et al., 2007]. Eccentricity and semi-amplitude, e and $K_\star$, respectively, are determined by fitting a Keplerian orbit model to the graph of radial velocity against time [Boisse et al., 2011, Mayor and Queloz, 1995]. The period, P, can be obtained from either method. Inclination, i, and the fractional planetary radius, r_p, are measured through the transit method [Southworth, 2008].

If data on the host star is available the remaining variables can be calculated. For example, substituting stellar radius into $\delta = \left(\frac{R_\mathrm{p}}{R_\star}\right)^2$ gives the radius of the planet precisely (rather than as a fraction of stellar radius). To obtain the mass of the planet is slightly more difficult, as it requires both methods and the stellar mass, $M_\star$, to complete the calculation [Southworth et al., 2007, Endl, 2014]. The stellar mass is often estimated using evolutionary models or empirical relations obtained from effective temperature, T_eff, and metallicity, [Fe/H] [Enoch et al., 2010, Torres et al., 2010]. As well as stellar mass, the calculation for planetary mass,

$$M_\mathrm{p} = \sqrt[3]{\frac{PK_\star^3}{2\pi G} \frac{M_\star^2}{\sin^3(i)} (1 - e^2)^{3/2}},$$

also uses $K_\star$ and e from the radial velocity method, i from the transit method, and P from either. If there is no precise measurement for e, setting it to zero gives the minimum mass of the planet [Udry and Santos, 2007].

1.1.4 Limb darkening

A major challenge in light curve analysis is limb darkening [Morello et al., 2017]. This is an optical effect where the star appears brighter in the centre of the stellar disc and dimmer towards the edge (limb). As illustrated in Figure 1.2, the non-uniform distribution of light seen on the stellar disc causes the transit light curve to have a rounded dip [Southworth, 2008]. Uncertainty in the second and third points of contact increases error in almost all further calculations, as seen by the dependence on the t_F parameter (as well as i which is dependent on t_F) in the above equations. A lack of sufficient parameters to constrain the model fit can lead to inaccurate interpretation of results [Csizmadia et al., 2013].
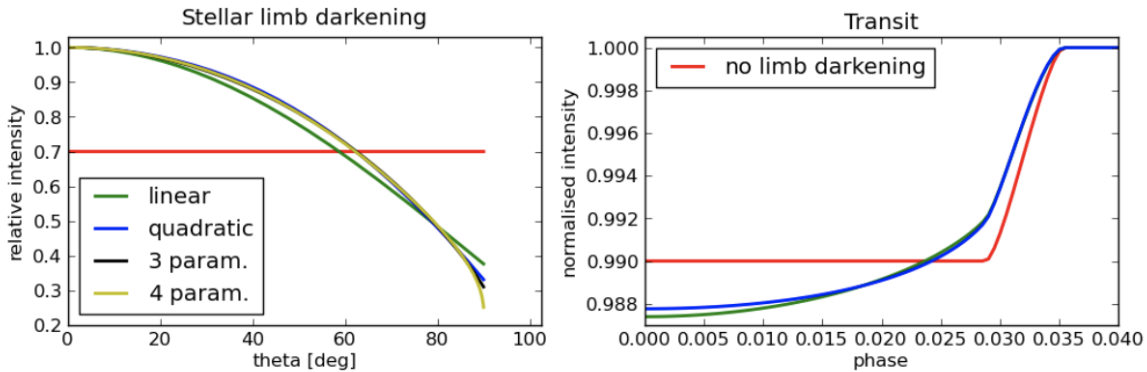
Figure 1.2: *Left*: The decrease in intensity observed from the centre of the stellar disc towards the edge, showing how various limb-darkening laws replicate the optical effect. *Right*: A model light curve with and without the effect of limb darkening [Odunlade and Pauline, 2010].

Limb-darkening laws typically parameterise the variation in specific intensity at some wavelength λ, $\lambda(\mu)$, as a function of $\mu = \cos(\theta)$, where θ is the angle between the line of sight and the surface normal vector. Several limb-darkening laws have been proposed, including linear [Schwarzschild, 1906, Milne, 1921], quadratic [Kopal, 1950], logarithmic [Klinglesmith and Sobieski, 1970], square root [Diaz-Cordoves and

Gimenez, 1992], power-2 [Hestroffer, 1997, Maxted, 2018] and Claret's 4-parameter [Claret, 2000] laws. The power-2 law, employed here, is $I_X(\mu) = 1 - c(1 - \mu^\alpha)$. While it describes limb darkening well, analysis shows a strong correlation between c and α, which makes defining these parameters individually difficult. Maxted [2018] found that using $h_1 = 1 - c(1 - 2^{-\alpha})$ and $h_2 = c2^{-\alpha}$ could accurately model the limb darkening in transit curves while reducing the correlation between c and α. Figure 1.3 illustrates how h_1 influences the entire light curve, while h_2 primarily affects the ingress/ egress.
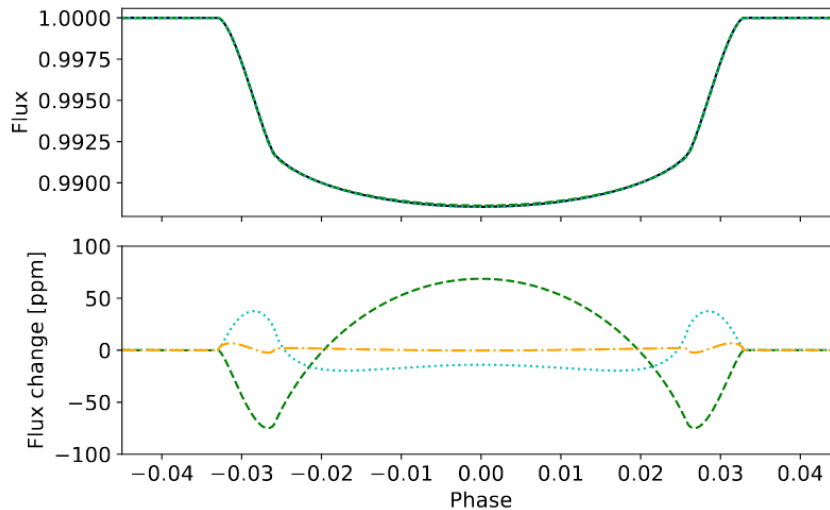
Figure 1.3: An illustration of the power-2 limb-darkening law for a simulated light curve [Maxted, 2018]. *Upper*: The simulated light curve using nominal values for h_1 (0.75 ± 0.01) and h_2 (0.25 ± 0.05). *Lower*: The effect on flux of perturbing h_1 (dashed line) and h_2 (dotted line) by $+1\sigma$. The dot-dashed line is not relevant to this study.

The issue of limb darkening is further complicated by stellar activity which can physically affect limb darkening, such as temperature variations across the stellar disc caused by convection [Pereira et al., 2013]. In many cases the coefficients in the limb-darkening law are left as free parameters to allow for these potential additional effects [Espinoza and Jordán, 2016]. However, to increase the accuracy of the results, priors to the coefficients can be added. These priors are determined by the stellar atmosphere using STAGGER-grid models and information on T_{eff}, log g, and [Fe/H] [Maxted, 2018].

1.1.5   Transit time variation

Mid-transit time is used as a reference point in the observation of transiting exoplanets. In a two-body Keplerian system the mid-transit time would occur at consistent intervals equal to the length of the orbital period. Therefore, if observed mid-transit times do not align with this interval, it can indicate a perturbation in the system [Agol et al., 2005, Miralda-Escudé, 2002]. This is why transit time variation (TTV) can be used to detect additional planets in a system [Holman and Murray, 2005, Winn and Fabrycky, 2015]. Another cause of TTV is the orbital decay of the planet, because period decreases with the shrinking orbit [Levrard et al., 2009]. TTV provides a method to study tidal interactions between stars and short-period planets [Weinberg et al., 2023].

1.2   Problem

An important problem in astronomical observation is the efficient use of time. This is a particular problem for *CHEOPS* because almost all the observations it performs are time-critical and of fixed duration, from a few hours to several days. This leaves gaps in the schedule of a few hours between observations in the Guaranteed Observing Time (GTO) as well as the Guest Observer (GO) programmes. A variety of "filler programmes" have been devised to make use of these gaps in the schedule, including the programme ID-052: Short-period EBLM and hot-Jupiter systems (PI: Maxted) that is the focus of this thesis. It is currently unknown exactly how useful data from this filler programme might be. If the data can produce good results, there is a potential to increase the science output of the mission by adding more of these filler programmes during the mission extension.

As technology improves, the quality of data continues to increase. Both *CHEOPS* and *TESS* are space-based missions producing high-quality data. The results produced from analysing the data from these missions have proven to be extremely precise. Increasing the accuracy of the results enables further studies which rely on those results.

For instance, studying the atmospheric composition of an exoplanet requires a solid understanding of the planet's parameters. Further studies cannot reliably be built on ambiguous data. Therefore, it is extremely important to understand the accuracy and precision of the measurements, i.e. to quantify the level of systematic errors in the measurements based on data from these missions.

There are many software packages based on a variety of different algorithms available to analyse the data from *CHEOPS* and *TESS*, all producing results of varying accuracy. If the data were analysed using the same method, the results could be combined while minimising errors caused by using multiple analysis methods.

1.3   Aim

The aim of this study is to compare exoplanetary radius measurements using *CHEOPS* and *TESS* data against each other and against literature values to determine their accuracy and precision. These results will allow for quantification of the quality of filler programme data. Further, by analysing *TESS* and *CHEOPS* data using the same method the uncertainties can be minimised while improving the accuracy and precision of the results. If the final results are an improvement on current literature values, these can be updated in preparation for future missions.

For this study a method to analyse *CHEOPS* and *TESS* data needs to be created. The method should be efficient and accurate to keep up with the quantity and quality of the data. It must also have a robust system for calculating uncertainties to ensure precision is not a result of underestimated errors. The method should be run on the *CHEOPS* filler programme data to determine if the data are useful. The method should also be run on available *TESS* data to compare and combine with the *CHEOPS* results. The comparison will allow for understanding how *CHEOPS* and *TESS* data differ; the combination will provide additional information to the "filler" data in order to produce more accurate results.

1.4   Significance and limitations

A filler programme focused on observing hot-Jupiter transits could potentially produce a significant amount of data. These observations will not be high-priority compared to scheduled observations in the GTO and GO programmes, so it is important to have a quick-and-easy method to analyse these data so that they can be published on a reasonable timescale (without sacrificing accuracy and precision). This method will need to cope with the unusual observing strategy for these filler programme observations, i.e. multiple short visits of a few hours, rather than the more usual strategy of observing a single transit from beginning to end.

The main limitation of this study is the availability of data. The *CHEOPS* data will consist entirely of data under programme ID-052 on DACE (Data & Analysis Center for Exoplanets), which will limit the amount of data available for use. Furthermore, the *TESS* data will be gathered from what is publicly available on MAST (The Mikulski Archive for Space Telescopes). Since the analysis works best when given multiple datasets, the small data pool presents a challenge. The effect of this limited data pool must therefore be further explored.

The method will be based in `pycheops`, and utilise most of its features relating to transits. This module is adaptable and easy to use, so most of its associated constraints were mitigated with simple procedures and supplementary modules. Therefore, the method itself did not present limitations which could not be overcome.

1.5   Structure

Following this introductory chapter, this paper is structured as follows. Chapter 2 explores the literature available relating to the concept of homogeneous studies, as well as information about the current state of research on the exoplanets chosen for this study and their transit times. The method created for analysing the *CHEOPS* filler programme data alongside *TESS* transits can be found in Chapter 3. This chapter also

discusses important investigations relating to the creation of the analysis method. The final results for all systems have been placed in Chapter 4. Following this is Chapter 5, where the results are analysed alongside literature values. It also discusses the impact of data quality and improvements for the future. Finally, Chapter 6 summarises the findings and concludes the study.

2 Literature Review

2.1 Homogeneous studies

The analysis of transiting exoplanets relies on the use of models to determine non-observable parameters (e.g. impact parameter and density). Modelling transit curves is a complex process, and even minor variations can cause dramatic effects [Southworth, 2008]. There is no unified method for creating these models, as there is still a lot to learn about these systems [Maxted and Gill, 2019, Saha, 2023]. They require many decisions and assumptions about parameters and errors which alter the results, further amplified when the parameters in question correlate with other parameters [Mandel and Agol, 2002].

There is so much inherent variation that it can be quite difficult to discern what effects relate to which causes [Mancini and Southworth, 2016]. Furthermore, analysing multiple objects and/or using multiple instruments introduces additional variations [Oddo et al., 2023]. It is therefore imperative to minimise any adverse effects caused by subtle differences in the analysis process [Southworth, 2009]. Using as similar a method as possible allows the results to be compared fairly and without additional uncertainties associated with inconsistent methods [Torres et al., 2008b]. This is the basis of homogeneous studies: to ensure the comparison of results relates to changes in the data rather than differences in method.

There are four major aspects of model analysis methods which commonly vary with different methods: instrumental noise, parameter assumptions (including model parameter priors and limb darkening), stellar parameters, and error estimation [Winn, 2008]. The effect on the result for each of these ranges from minor changes in the final calculation to fundamental differences throughout the process. An homogeneous study aims to keep these aspects consistent across all analyses. `pycheops` has been designed with this in mind, and accounts for these variations where possible [Maxted et al., 2022].

The first step in analysing exoplanet data is correcting for instrumental noise. As it is the first step, it has an important impact on the analysis as a whole. For *CHEOPS* data, sources of instrumental noise are removed during the DRP process [Hoyer et al., 2020]. To account for residual instrumental noise `pycheops` uses a linear model with the coefficients as free parameters and the basis vectors are parameters determined by data or meta-data, such as spacecraft roll angle. [Maxted et al., 2022]. For *TESS*, the Science Processing Operations Center (SPOC) at NASA Ames Research Center performs calibrations and corrections before data is added to MAST [Jenkins et al., 2016]. Given the quality of the data after the SPOC pipeline, additional corrections risk over-correcting the light curve [Oddo et al., 2023]. Thus, a *TESS*-specific noise correction is not required within `pycheops`.

The parameters used to determine the shape of a model are crucial to obtaining accurate results. Adding priors to model parameters help to make informed decisions during the modelling process [Maxted et al., 2022]. The choice of adding priors, and which to add, depends on the quality of data as well as the desired outcome. For example, in this study the *CHEOPS* data often do not contain full transits, so an accurate width measurement is difficult to obtain. To help the analysis a prior is given for width, so the model can adapt appropriately. On the other hand, the aim is to measure depth accurately, so it would not be appropriate to add a prior to depth. Doing so would give biased results and if the prior was inaccurate the result could be significantly incorrect.

One particular parameter which is not straight-forward to implement is limb darkening. As discussed in Section 1.1.4, there are multiple limb-darkening laws which aim to correctly model the curvature of light curves [Mandel and Agol, 2002]. If implemented correctly, limb darkening parameters increase the accuracy of the results [Oddo et al., 2023]. However, with research still ongoing to determine the best laws and priors, there is also the potential to decrease accuracy [Csizmadia et al., 2013, Espinoza and Jordán, 2016]. All analyses in this study makes use of one single limb-darkening law, the power-2 law, to maintain consistency [Maxted and Gill, 2019, Maxted et al., 2022].

Determining limb darkening relies on stellar parameters, and how they are obtained can impact the accuracy of results. The coefficients in limb-darkening laws, including the one used by `pycheops`, are derived from information regarding the stellar atmosphere [Maxted, 2018]. Accurate stellar atmospheric models themselves rely on an understanding of stellar parameters. These are namely effective temperature, T_{eff}, the logarithm of the surface gravity, $\log g$ (normally given in cgs units), and the log of the metal abundance relative to the Sun, [Fe/H], where iron is normally taken as a proxy for the total metal abundance [Sing, 2010, Magic et al., 2015]. Compound uncertainties caused by the accuracy of stellar parameters as well as stellar models will affect the results of limb-darkening coefficients, therefore it is important to use consistent and well-studied sources [Maxted, 2023].

Stellar parameters are also required for calculating planetary mass and, the focus of this study, radius (see Section 1.1.3). Before the era of *Gaia*, measuring stellar radius directly was inaccurate or not possible at all [Seager and Mallén-Ornelas, 2003]. To bridge the gap studies used estimations to determine exoplanetary radius, however this introduced uncertainties that lead to inaccuracies [Winn, 2008]. Now though, stellar radii are able to be determined accurately through measurements [Stassun et al., 2017]. It is important to be mindful of the method a study uses to obtain a stellar radius value. An incorrectly estimated value can lead to an erroneous planetary radius result, as occurred in a 2008 study of the planet XO-3b [Johns-Krull et al., 2008].

It is vital to ensure the final results do not underestimate the uncertainties [Carter et al., 2008]. There are multiple methods for estimating uncertainties, such as the Levenberg-Marquardt or Markov chain Monte Carlo (MCMC) methods [Newville et al., 2014, Foreman-Mackey et al., 2013]. `pycheops` performs thorough error estimation using an MCMC method, as discussed in Section 3.1.4 [Maxted et al., 2021].

2.2 Exoplanetary Systems

The following sections contain background information on the exoplanets that were chosen in this study. All of these exoplanets are hot Jupiters with orbital periods of less than five days. While some systems have been studied more than others, all have been observed with *CHEOPS* and at least one other telescope.

2.2.1 WASP-3

WASP-3b is a hot Jupiter exoplanet (radius: 1.31 ± 0.011 R_{Jup} and mass: 1.76 ± 0.011 M_{Jup}) orbiting an F7 type star with a roughly 1.8 day orbit [Pollacco et al., 2008]. The majority of studies on WASP-3b were between its discovery in 2008 and 2013, with a strong focus on the TTV signal. There was uncertainty surrounding if the signal was an indication of another body in the system, however this was disproved [Maciejewski et al., 2010, Montalto et al., 2012]. Thermal emissions in infrared and near-infrared have been detected on multiple occasions suggesting an atmosphere with inefficient heat redistribution [Rostron and Wheatley, 2013, Zhao et al., 2012].

2.2.2 WASP-14

WASP-14b, one of the densest hot Jupiters ever discovered (radius: 1.28 ± 0.08 R_{Jup} and mass: 7.3 ± 0.5 M_{Jup}), orbits an F5 type star with a period of 2.2 days [Joshi et al., 2009]. Despite its short orbital period, WASP-14b has been confirmed to have an eccentric orbit ($e = 0.0877 \pm 0.0030$) [Husnoo et al., 2011]. Most studies on WASP-14b focus on its atmosphere. It has been concluded that it is highly irradiated and carbon-rich [Madhusudhan, 2012, Blecic et al., 2013]. While comparing observations with models, the dayside was found to likely have equilibrium chemistry whereas a discrepancy in the nightside emission was attributed to the high carbon content [Wong et al., 2015].

2.2.3   WASP-16

WASP-16 is a typical hot Jupiter system. Orbiting a solar analogue host star (type G3) in just 3.1 days is a planet roughly the size of Jupiter (radius: $1.00 \pm 0.07 \ R_{\mathrm{Jup}}$ and mass: $0.86 \pm 0.06 \ M_{\mathrm{Jup}}$) [Lister et al., 2009]. WASP-16b has barely been studied at all. Confirmation of its moderate albedo was included in one Spitzer Space Telescope (*Spitzer*) study [Kilpatrick et al., 2017].

2.2.4   WASP-24

WASP-24b (radius: $1.3 \pm 0.04 \ R_{\mathrm{Jup}}$ and mass: $1.07 \pm 0.04 \ M_{\mathrm{Jup}}$) orbits a late F-star (type F8/9) with a period of 2.3 days [Street et al., 2010]. Studies have yet to find anything particularly unusual about this planet. It was determined to have a well-aligned and prograde orbit, also known as a "normal" orbit, and most properties remained consistent across studies [Simpson et al., 2011]. Observations are consistent for thermal inversion as well as without the inversion [Turner et al., 2017, Smith et al., 2012]. The age of its host star would allow WASP-24b to have a relatively large moon (mass: $0.4 M_{\oplus}$) [Weidner and Horne, 2010].

2.2.5   WASP-29

Out of the systems chosen for this study, WASP-29 has both the coldest star and the smallest planet. Orbiting a K4 dwarf star (temperature: 4875 ± 65 K) with a period of about 3.9 days is the roughly Saturn-sized planet (radius: $0.775 \pm 0.031 \ R_{\mathrm{Jup}}$ and mass: $0.244 \pm 0.020 \ M_{\mathrm{Jup}}$) discovered by Hellier et al. [2010]. Studies on the atmosphere of WASP-29b have consistently found a featureless transmission spectrum with no particularly intriguing results [dos Santos et al., 2021, Gibson et al., 2013, Wong et al., 2022].

2.2.6   WASP-74

The most recently discovered of the exoplanets in this study is WASP-74b. Found orbiting a type F9 star with a period of roughly 2 days in 2015, WASP-74b has a mass of roughly 0.95 M_{Jup} and a radius of 1.5 R_{Jup} [Hellier et al., 2015]. There have been few studies on it, the focus being the atmospheric composition [Fu et al., 2021, Lira-Barria et al., 2022, Spyratos et al., 2023]. One potential reason for having very few studies of this system could be its location outside of the *TESS* field of view, which could be a limiting factor in its study.

2.3   Ephemerides

Accurate mid-transit times and period measurements are vital to light curve analyses. These ephemerides need to be updated regularly to account for any temporal changes in the periods of exoplanets in order for all subsequent calculations and TTV to be accurate. The reference ephemerides used in this study can be found in Table 2.1.

System	Time of mid-transit [BJD]	Period [days]
WASP-3	2455362.76229(009)	1.84683510(020) [a]
WASP-14	2455632.57865(010)	2.24376644(022) [b]
WASP-16	2454584.42898(038)	3.11860680(120) [c]
WASP-24	2454945.58944(009)	2.34122188(030) [d]
WASP-29	2458356.41487(003)	3.92271218(025) [e]
WASP-74	2457173.87198(018)	2.13774453(077) [f]

Table 2.1: The reference ephemerides used in this study. The uncertainty in the final decimal place of each value is given in brackets following the value itself. Ephemerides are from the following: [a]Wong et al. [2021], [b]Baştürk et al. [2022], [c]Southworth et al. [2013], [d]Turner et al. [2017], [e]Saha and Sengupta [2021], and [f]Mancini et al. [2019].

3   Methodology

This project uses `pycheops` version 1.0.9 to analyse *CHEOPS* data of hot-Jupiter class exoplanets. The *CHEOPS* data in this study consists entirely of filler programme data collected for GTO programme ID-052. While the filler observations do not generally contain enough data to make reliable measurements of the transit width and impact parameter, they can provide reliable transit depth measurements. To fill the gaps in the filler data, *TESS* light curves were analysed to give width and impact parameter which were then used as priors for the *CHEOPS* data so the analysis could measure transit depth.

For this process to work, a list was compiled of exoplanets that had both *CHEOPS* and *TESS* data. This resulted in the following list of systems: WASP-3, WASP-14, WASP-16, WASP-24, WASP-29, and WASP-74. It was later discovered that the *TESS* data were not available for WASP-74, so an analysis based in *Spitzer* observations was used to set priors on the width of the transit and impact parameter instead for this system.

For all systems excluding WASP-74 the *TESS* data were downloaded, split into individual transits, and analysed with `pycheops`. This produced the priors that would be set on the *CHEOPS* data analysis. It was also used to create TTV plots to determine if there were any potential for extra bodies in the system (or other phenomenon) which might affect the results. Once the *CHEOPS* data were downloaded, they were analysed using priors on width and impact parameter. After all the *CHEOPS* data were analysed separately they were analysed together using the `MultiVisit` function. Finally, the `MultiVisit` results were run through the `massradius` function to estimate the planet's mass and radius.

Target	Start date [UTC]	Length [hours]	Effic. [%]	File key
WASP-03				
	2022-06-22 02:29	3.17	66.5	CH_PR120052_TG002201_V0200
	2022-06-23 23:39	2.57	79.3	CH_PR120052_TG002202_V0200
	2022-06-25 18:42	3.17	58.6	CH_PR120052_TG002203_V0200
	2022-07-14 06:01	2.68	77.7	CH_PR120052_TG002204_V0200
WASP-14				
	2022-05-18 23:14	3.72	73.6	CH_PR120052_TG009901_V0200
	2022-06-05 22:35	2.58	67.3	CH_PR120052_TG011801_V0200
WASP-16				
	2022-06-02 17:24	2.63	64.1	CH_PR120052_TG011901_V0200
WASP-24				
	2022-05-26 18:04	3.80	87.7	CH_PR120052_TG010101_V0200
	2022-06-14 12:45	2.60	75.1	CH_PR120052_TG012001_V0200
	2022-07-03 05:06	3.62	60.5	CH_PR120052_TG012003_V0200
WASP-29				
	2021-10-18 04:52	3.17	59.7	CH_PR120052_TG006801_V0200
	2021-10-22 04:43	3.17	58.1	CH_PR120052_TG006401_V0200
WASP-74				
	2021-09-16 11:32	3.17	63.3	CH_PR120052_TG002301_V0200
	2022-07-10 16:14	3.17	90.5	CH_PR120052_TG002302_V0200

Table 3.1: Observing log of *CHEOPS* observations for all systems in this study.

3.1 Final method

To analyse the data a series of Jupyter notebooks were created. Each notebook contained one step of the process, and most relied on the outcomes of preceding notebooks. Each of the following sections (3.1.1 to 3.1.6) outlines the details of one notebook. The list of *CHEOPS* observations used for this analysis is located in Table 3.1. This does not include datasets which were available but unused because they did not contain any part of the transit.

3.1.1 User Inputs

To minimise the need to manually edit every section of code, a text file containing all of the parameters which were subject to change was created. This file could then be called by all other notebooks. This was done to reduce errors, maintain consistency, and make the process more efficient. The inputs in this file were divided into three sections: basic inputs, *CHEOPS* inputs, and external parameters which could not be queried within the code.

The system name, *TESS* catalogue ID number (TIC), and folder path comprised the basic inputs. The TIC number could be queried using the system name, however after experiencing some retrieval errors, it was added to the input file so it could be used should the error reoccur. The folder path was the path to the data folder within the pycheops folder. This was required to separate the *TESS* datasets.

The next section was devoted to *CHEOPS*-specific inputs. The Program ID number was essential to ensure the only data used were those which permission to analyse was granted. The aperture setting was also set in this file, to maintain consistency. Further information on the aperture can be found in Section 3.1.4. This was only for the *CHEOPS* data. The *TESS* data could only be set to default aperture, so was hard-coded in the *TESS* notebooks. The number of datasets available on DACE[1] (for the given Program ID) was important for downloading and compiling the *CHEOPS* data [Buchschacher et al., 2015]. Rather than changing the dataset number manually, a loop was made to automatically download the dataset if it had not already been downloaded and terminate when it reached the total number of available datasets.

The last section included radial velocity (from the NASA Exoplanet Archive[2]), stellar mass, and stellar radius for `massradius` [Akeson et al., 2013]. It also included the question to query DACE for parameters or look elsewhere for property values, such as TEPCat[3] and SWEET-Cat[4] [Southworth, 2011, Santos et al., 2013].

---

[1]https://dace.unige.ch/
[2]https://exoplanetarchive.ipac.caltech.edu
[3]https://www.astro.keele.ac.uk/jkt/tepcat/
[4]https://sweetcat.iastro.pt

3.1.2 Creating the individual *TESS* datasets

`pycdata`[5] was used to query the *TESS* Catalogue for transit data. After downloading all available data, each transit was saved as a separate dataset. A function was written which would loop over a *TESS* data file and create datasets for each transit it found. The data for each transit are divided by a straight line fit to each side of the transit to remove any trends in the data. This was saved as its own dataset, and the loop continued for the next transit. To call this function required the file path and the TIC number to find the correct datasets. It also needed to be given transit properties downloaded from TEPCat. These were the reference mid-transit time (BJD), the period (days), and the transit width (normalised phase units). Once all the *TESS* data were saved as individual transits, the analysis could be performed.

3.1.3 Analysing *TESS* transits

To model the transits, `pycheops` uses the qpower2 algorithm [Maxted and Gill, 2019]. This is implemented as a `lmfit`[6] model. `lmfit` combines a non-linear least-squares optimisation with the Levenberg-Marquardt method to determine the most probable model parameters [Newville et al., 2014]. While `lmfit` does not give reliable error estimates, this is rectified by taking the mean and standard error of the mean over the fits to all the transits for each system. The limb-darkening parameters were calculated using the STAGGER-grid models and the following stellar parameters found on SWEET-Cat: effective temperature, surface gravity, and metallicity [Maxted, 2018]. The results for the limb-darkening coefficients, h_1 and h_2, were then given Gaussian priors with four times the necessary uncertainty, following the advice in Maxted [2018]. The period and ephemeris were taken from TEPCat. While the period was held constant, the mid-transit time was calculated by increasing from the ephemeris in steps equal to the period. The impact parameter was free within is its full range (0 to 1).

---

[5]https://github.com/Jayshil/pycdata
[6]https://lmfit.github.io/lmfit-py/

To check for transits greatly affected by instrumental noise or with poor phase coverage, the plots for every transit were returned at the end of the analysis. This made it easy to scroll through the plots and catch any obvious sections of bad data. Additionally, the primary parameters (depth, width and impact parameter) for each transit were printed in a table after completing analysis for all transits. Again, this allowed for a simple visual analysis to determine outliers. If any outlying transits were found, the culprit could be excluded from the analysis by entering it into the "ignore cycles" term. When the function was rerun, the outlying transits would be skipped and thus would not skew the results.

The weighted mean and standard error of the mean were calculated from the `lmfit` analysis results using the `pycheops.combine` function. This function calculates a weighted mean value accounting for any additional scatter in the values beyond that expected based on the quoted error bars. These were then saved in a csv file to be used in the *CHEOPS* analysis. The results of depth, width, impact parameter, limb darkening, and log stellar density were plotted to show the deviation from the weighted mean for each dataset.

The mid-transit time for every cycle produced by the `lmfit` analysis was subtracted from the expected mid-transit time (calculated from the reference mid-transit time and the orbital period). The results were plotted to show the TTV. High variations in TTV could suggest a possible additional body in the system causing gravitational fluctuations thus changing the period of each orbit, as mentioned in Section 1.1.5. Smaller variations were also important to note, while not necessarily an indication of perturbations in the system, these suggested a need to update the ephemeris.

It was following this step that systems without *TESS* data would begin their analysis. For such systems (i.e. WASP-74) the literature values were used in place of any "*TESS* analysis result" parameters. From this point forward, mentions of *TESS* analysis results can be assumed as interchangeable with literature values in such cases.

3.1.4   *CHEOPS* analysis

The *CHEOPS* data were downloaded by querying DACE. Since the data had gone through the DRP, the initial calibration and corrections were done automatically. Once downloaded, the dataset was checked for potential unresolved causes of contamination by reading through the Data Reduction Report for information on the calibration and correction process. The report also provided information on the apertures. In an attempt to keep much of the analysis the same for each system, apertures were all set at DEFAULT, which is an aperture with a radius of 25 pixels = 25 arcsec, once they were all found free of large contamination. After performing an outlier rejection for extreme outlying data points, the initial plot of the data was created.

The data were fit using *TESS* or *Spitzer* analysis results, SWEET-Cat, and TEPCat parameters. The mid-transit time from the dataset was combined with the TEPCat values for period and T_0 to produce the relative mid-transit time. This parameter as well as period were fixed variables in the transit fit. The limb-darkening coefficients were again calculated with STAGGER-grid models. The parameter h_1 was used as a free parameter with a prior while h_2 remained fixed, because it has very little effect on the shape of the transit. Width and impact parameter were given priors from the *TESS* or *Spitzer* analysis; most of the *CHEOPS* datasets contained incomplete transits which makes the measurements of these parameters unreliable. If `pycheops` was given initial values, it was less likely to mistake small trends in noise as physical trends in the data. Depth was left as a free parameter.

The results of the first least-squares fit were used to select which parameters to use to model the instrumental noise. The noise parameters relate to three types of errors: roll angle, CCD effects, and a linear trend with time. The roll angle, described further in Section 3.2.2.1, describes the effect of the movement of the spacecraft around the line of sight. CCD effects relate to the errors caused by the background, frame transfer (the lack of a shutter causes smear), and contamination from nearby stars. Trends on the timescale of hours to days are expected for magnetically active stars. A linear trend with time is sufficient to account for this effect in short duration obbservations, as are

used here. The selection of noise parameters was done by calculating Bayes factors for each decorrelation parameter and using them in the detrending process [Maxted et al., 2021]. Given the short visits, it was determined that the term regarding the fluctuation of flux against time, *dfdt*, hindered the accuracy of the result and was therefore removed. The decorrelation parameters were then used in the re-run of `lmfit`.

The final fit was done using `emcee`, an affine-invariant Markov chain Monte Carlo ensemble sampler [Foreman-Mackey et al., 2013]. The idea behind MCMC is to take random "walks" around the parameter space, and progressively getting closer to the answer by determining if each step is better or worse than the last [Goodman and Weare, 2010]. This process takes the results from the `lmfit` model and Gaussian priors to sample the posterior probability function. While the Probability Distribution Function (PDF) describes the probability of the outcomes of a study, the posterior PDF uses prior information to understand the probability from a more informed standpoint. This produces accurate uncertainty estimations for each parameter as well as giving information on correlations between the model parameters. It came to its conclusion using 100 walkers and 100 steps after a burn-in time of 400 steps. Burn-in time is used to make sure the sampler converged so the results within the burn-in time are discarded. Convergence is double checked by inspecting the trail plots to ensure a lack of any trends in the mean or variance of the walkers, which shows that the sampler was "well-mixed." Finally, corner plots were produced to show the correlation between parameters.

The data were saved in two ways. The dataset itself was saved, as well as a csv file of the parameter results of the `emcee` analysis. One step was added to the end of the notebook which would check if all the available datasets had been analysed. If this was the case it would use the combine function on all parameter results to give the weighted mean and standard error for each. If it determined that not all the available datasets had been analysed it would advise the user to rerun the notebook to continue the analysis.

3.1.5   Compiling the data with `MultiVisit`

The `MultiVisit` function in `pycheops` was used to analyse data from multiple visits to the same target using a single transit model, while allowing the individual noise models for each visit to remain independent. SWEET-Cat stellar properties (effective temperature, surface gravity, and metallicity) were used to calculate the limb-darkening coefficients. TEPCat period and mid-transit time were used in the `MultiVisit` function to give mid-transit time in phase units. The *TESS* analysis result for transit width was used as an initial value for the fit. Two additional parameters were added to this transit fit. log_sigma_w, a noise model parameter, was set at a reasonable range for all transits, because it is assumed that the "white noise" is the same for all data points due to unknown noise sources. The second was N_{roll}. This parameter is related to the number of terms in the harmonic function used to model trends correlated with the roll angle of the spacecraft during the observation, as this motion causes trends in the data. `pycheops` avoids the inconvenience of explicitly sampling multiple parameters using implicit decorrelation from Luger et al. [2017]. More detail on how N_{roll} was handled in this study can be found in Section 3.2.2.1.

After running the `emcee` sampler the resulting fit was plotted for each transit, as well as phase-folded. Trail and corner plots for the analysis were shown and the results saved in the same method as the *CHEOPS* csv file.

3.1.6   Planet mass and radius estimates

The `massradius` function was used to estimate mass and radius of the planet. The results from the `MultiVisit` step k, aR, and $\sin i$, were used alongside the radial velocity, stellar mass, and stellar radius from the user inputs file. After analysing the results, it was decided to calculate the planetary mass and its radius using *TESS* data. While the *CHEOPS*-calculated planetary radii were influenced by *TESS* data through the priors, the *TESS*-calculated R_{p} were independent of *CHEOPS*. For the calculation, k, aR, and $\sin i$ were input from the *TESS* analysis step.

The focus of this study, planetary radius measurements, were calculated in this function using only the radius ratio k (derived from the depth measurement) and stellar radius $R_\star$. This method for calculating planetary radius avoids relying on as many estimations and assumptions as possible, rather than estimating planetary radius using stellar density estimations from the light curve and assuming stellar mass.

3.2 Method Development

3.2.1 Building the foundation: WASP-29

WASP-29 was the first exoplanet system studied. The process used for its analysis became the foundation for the final method. To begin, the analysis was originally performed on the *CHEOPS* data only. It followed the basic structure outlined in a recent paper [Maxted et al., 2021]. To evaluate the results obtained by `pycheops`, the results were compared to literature results of *TESS* analyses. There were two main papers used as the literature comparison. These were the WASP-29b discovery paper [Hellier et al., 2010] and a recent *TESS* study [Saha and Sengupta, 2021], as these papers contained the most comprehensive results.

The main comparable parameters, depth, D, transit width, W, and impact parameter, b, are shown in Table 3.2. These are all consistent and generally within the error bounds. The exception to this is the abnormally small uncertainties given for *TESS* (up to 100 times more precise than this work and Hellier et al. 2010) and it is unknown how the precision was obtained. Since the method in this study to estimate the uncertainties is robust (using the standard error of the mean from independent datasets), the discrepancy in the precision is not an issue with this method. The consistency of the results with literature values proved enough confidence in the accuracy of the `pycheops` script compilation that it could be used as the template for further studies.

Parameter	This work	SA2021	HE2010
D [%]	0.9813 ± 0.0442	$0.9332^{+0.0004}_{-0.0005}$	1.02 ± 0.04
W [hr]	2.5630 ± 0.0246	$2.6178^{+0.0016}_{-0.0014}$	2.6592 ± 0.0360
b	0.15238 ± 0.13361	$0.11600^{+0.00360}_{-0.00390}$	0.26 ± 0.15

Table 3.2: `pycheops`-analysed results and literature results for WASP-29 parameters (SA2021: Saha and Sengupta [2021], HE2010: [Hellier et al., 2010]).

Parameter	*TESS* Set 1	*TESS* Set 2	SA2021
D [%]	0.9807 ± 0.0342	0.9595 ± 0.0265	$0.9332^{+0.0004}_{-0.0005}$
W [hr]	2.6163 ± 0.0282	2.6182 ± 0.0198	$2.6178^{+0.0016}_{-0.0014}$
b	0.32804 ± 0.15139	0.25351 ± 0.14714	$0.11600^{+0.00360}_{-0.00390}$

Table 3.3: *TESS* values for WASP-29 parameters: `pycheops`-analysed *TESS* results against literature (SA2021: [Saha and Sengupta, 2021]).

Could `pycheops` be used to analyse non-*CHEOPS* data? If so, would the results be better or worse than other methods? Two sets of *TESS* data were available for WASP-29, one with six transits and the other with five. The datasets were kept separate to avoid compounding any errors. The data were downloaded using `pycdata` to create datasets in a format `pycheops` could analyse. The 2021 paper was used as a literature comparison because it contained *TESS* data [Saha and Sengupta, 2021]. Therefore, Table 3.3 should show similar results in theory. The values in both sets of *TESS* data and the literature are consistent within a reasonable degree, however there is some discrepancy especially with the impact parameter b. The impact parameter has shown to be a poorly constrained value for WASP-29, both with the *TESS* data and the *CHEOPS* data, so the discrepancy can be attributed to this issue.

3.2.1.1 Investigation: exposure time

Using `pycheops` on non-*CHEOPS* data brought up the question of whether exposure time affected the `pycheops` analysis. An investigation was set up to determine if exposure time needed to be accounted for in the analysis process, because `pycheops` does not account for it. Examination of the results determined exposure time did not have a significant negative impact on the accuracy of `pycheops`, therefore the code did not require any implementations to handle exposure time.

Simulated data were produced using known system parameters. The data were produced by first creating a transit model from the system parameters as found on TEPCat and using `pycheops.models.TransitModel`. A Gaussian distribution of error was then added to the model to give a more realistic portrayal of the data. Finally, the data were binned using `pycheops.utils.lcbin` to simulate the exposure time. While binning the data is known to cause smearing in the ingress/ egress, the loss of information was not a major concern for the scope of this investigation as the motive was to understand if `pycheops` could handle low-quality data [Kipping, 2010]. Further, the focus of this study was to measure the depth of the light curve, which is not as affected by the distortions as the width or impact parameter. `lmfit` was run on the binned data to estimate the depth, width, and impact parameter of the transit which could be compared to literature to determine if there was a noticeable effect.

The simulation was run for four exposure times: 1 minute, 2 minutes, 10 minutes, and 30 minutes. The lower three durations are used by *CHEOPS* and the largest was used by the *Kepler K2* mission [Howell et al., 2014]. The addition of the *K2* length illustrated importing different mission data into `pycheops` which might use larger exposure times than *CHEOPS*.

Originally the simulation only used WASP-29 parameters, however the results showed a far higher accuracy for the 30 minute exposure time than expected. The simulation was rerun for multiple times between 2 and 30 minutes as well as being run for 35 minutes to gauge the trend. This showed an increased accuracy at times around 30 minutes, ruling out a simple error as the cause. After comparing the exposure time

with the transit duration, a possible explanation was found. The transit duration is around two and a half hours, which corresponds to five data points at a 30 minute exposure time. As it was a simulated set of data the exposure time was aligned with the start of the transit. Likely, this caused the data to represent the transit well because of a lack of contamination from averaging across different sections of the transit (e.g. a data point covering part of the egress as well as part of the outside of the transit would not represent the transit accurately).

Once it was clear that the unexpected accuracy for 30 minutes was due to the correlation with the WASP-29 transit duration, the system parameters for WASP-19 were used instead of WASP-29. WASP-19b was chosen because at about 1.6 hours its transit duration was shorter than WASP-29b [Cortés-Zuleta et al., 2020]. This would further validate if an increase in exposure time would affect the results. This proved successful in showing the decrease of accuracy when exposure time increased, as expected. Further, it gave reliable results to the testing of exposure time. Values produced for three important parameters (depth, width, and impact parameter) by modelling transits with increasing exposure times decreased in accuracy but remained within reasonable uncertainty bounds. Depth and width values were within 10% and 5% of the model values, respectively. Impact parameter, which is often poorly constrained, was within 20% of the uncertainty of the model. WASP-29 also showed favourable results for depth and width (excluding the 30 minute data), keeping within the same bounds as WASP-19. However, the impact parameter results for WASP-29 were so poorly constrained that for a 10 minute exposure time there was over 100% difference between the model and simulated values.

The WASP-29 results were unreliable, however, the results for WASP-19 were able to conclude the following. While there was a decrease in accuracy for increasing exposure times, parameter values were still within reasonable uncertainties as compared to model values up to and including a 30 minute exposure time. The reasonable uncertainties were 10% for depth, 5% for width, and 20% for impact parameter. This showed that `pycheops` did not need to account for exposure time in its transit modelling, as the accuracy was not hindered beyond a reasonable degree.

3.2.2 Refining the process: WASP-3

The analysis performed on WASP-29 showed that the results from using `pycheops` on both *CHEOPS* and *TESS* data were reliable compared to literature. So, the results from *TESS* could be used as priors in the *CHEOPS* analysis to produce more accurate results. To do this, the code had to be restructured to allow the *TESS* data to be analysed first, and then used in the analysis of the *CHEOPS* data. WASP-3 was used as a clean slate to restructure and increase the efficiency of the code. To make the code efficient for use on most exoplanets involved adding the user inputs file, splitting *TESS* datasets automatically, and limiting the need to edit the code wherever possible. This also ensured that each system was analysed in a homogeneous method, enabling more accurate comparisons.

While working on the analysis of WASP-3, two investigations were conducted. The first was to determine the value of N_{roll} that would produce the minimum amount of error without over-fitting the data. For WASP-3 this value was around 4, however it was not certain that this would be the best value for the other systems. Therefore, the N_{roll} investigation was carried out for all systems and determined that a value of 1 was adequate for every system other than WASP-3. The other investigation was as to how much better, if at all, using the priors on the *CHEOPS* analysis made the results. It was determined that for WASP-3, as well as all other systems, using the *TESS* results as priors produced better results than without priors.

3.2.2.1 Investigation: N_{roll}

The *CHEOPS* spacecraft is not stationary in its orbit. A consequence of this is the additional errors associated with roll angle. `pycheops` takes these errors into consideration when performing model selection using Bayes factors. The instrumental noise is typically accounted for using $\Sigma_{j=1}^{n=3}\alpha_j\sin\left(j\cdot\Omega t\right) + \beta_j\cos\left(j\cdot\Omega t\right)$, where α_j and β_j are free parameters and Ω is the angular frequency at which the spacecraft rotates [Maxted et al., 2021]. As the decontamination was performed for the individual

datasets, `MultiVisit` includes its own model to account for the roll angle trends within all datasets. `MultiVisit` allows the user to change the number of terms in this equation from the default value (n=3).

To test the N_{roll} value with the highest accuracy, `MultiVisit` was run repeatedly with increasing N_{roll} values. The BIC (Bayesian information criterion), AIC (Akaike information criterion), and RMS (root mean square) were recorded and compared to quantify the accuracy. This was determined by finding the value of N_{roll} at which the AIC and BIC were at their minimum, and where RMS was reasonably low. Since RMS will continuously decrease the actual minimum for this term is not used. In its place, the point in which the gradient tapers off is considered the "reasonably low." The corresponding N_{roll} value would then be used in the model fit and those results saved.

In Figure 3.1 the statistical parameters all decrease as N_{roll} increases until a value of 4, then the BIC and AIC start to increase. The RMS continues to decrease because increasing the terms in the equation will reduce residuals. The BIC and AIC increase after an N_{roll} value of 4 because the quality of the fit declines. Given the overall decrease finds a minimum at 4, this is the N_{roll} value used.

To further solidify the choice of N_{roll} value, the depth and its error were recorded for each N_{roll} value. These were then plotted to show how the depth result varied according to the given N_{roll} value. Figure 3.2 depicts the depth calculations varying significantly before reaching an N_{roll} of 4, after which it varies only slightly. This shows that using a value of 4 for N_{roll} returns results of the same quality as higher N_{roll} values, without unnecessarily prolonging the equation and thus the run time.

Following the results for WASP-3, this was performed on all other systems to ensure the correct value of N_{roll} was used. In each case the N_{roll} value of 1 produced the minimum AIC and BIC. The plots created to show the effect of N_{roll} on depth, such as Figure 3.2 for WASP-3, showed no significant variation in depth for any value. This confirmed the value of 1 for N_{roll} was sufficient to account for the spacecraft roll angle.
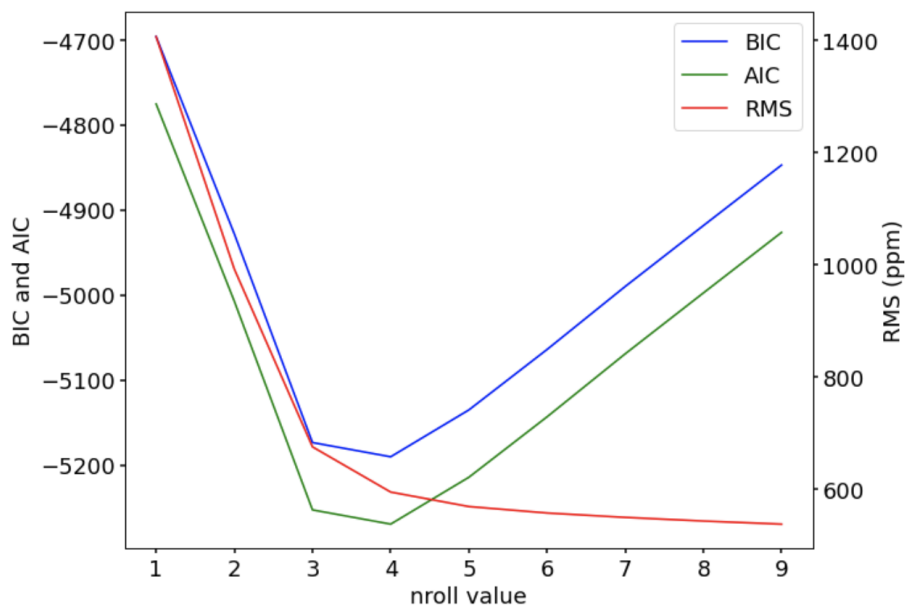
Figure 3.1: The accuracy of the model for increasing N_{roll} values. The accuracy is highest where the BIC, AIC, and RMS values are at their minimum.
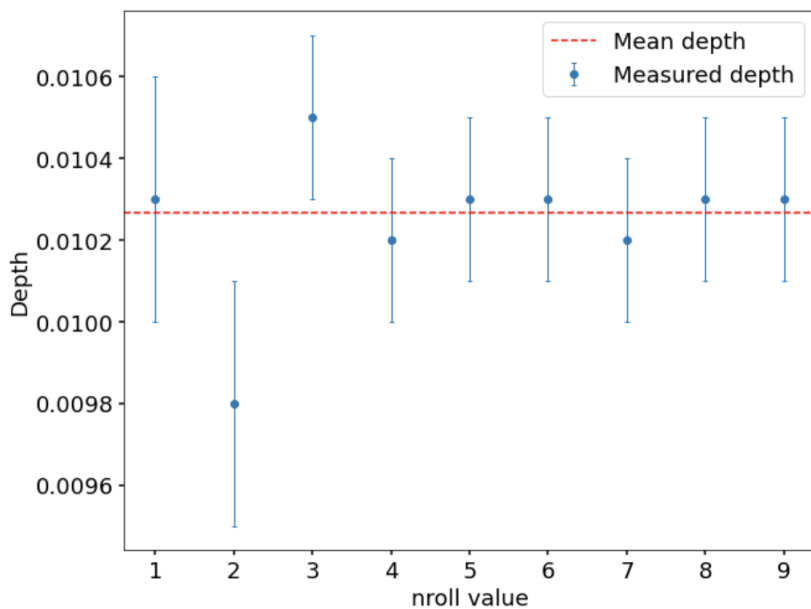
Figure 3.2: The measurements of depth, with errors, given from each model of increasing N_{roll} values. At an N_{roll} of 4 the outlying data points cease, confirming this value is adequate to account for the associated errors.

3.2.2.2   With or without priors

A final analysis was performed to determine if using the *TESS* results as priors produced better results than analysing the *CHEOPS* data without priors. This was done by running the same notebooks on the same data, with the addition/exclusion of priors as the only difference. All systems were run through this process and yielded consistent results as with WASP-3, which can be seen in Table 3.4. Using *TESS* results as priors on *CHEOPS* data produced more accurate and precise results, roughly ten times more precise for depth and width. Impact parameter showed a smaller gap between the uncertainties, at about 1.75 times less precise for the prior. All three parameters were more accurate when using priors. The values for depth and impact parameter when calculated without priors did not agree with literature, whereas the value with priors did. This inconsistency is likely due to the lack of *CHEOPS* data in comparison with the amount of *TESS* data available. Therefore, the final results given were produced using *TESS* priors on *CHEOPS*.

Parameter	With priors	No priors
Depth [%]	1.04 ± 0.02	1.50 ± 0.29
Width	0.0612 ± 0.0002	0.0608 ± 0.0033
Impact parameter	0.5121 ± 0.0443	0.9269 ± 0.0254

Table 3.4: Precision of results for *CHEOPS* analysis results on WASP-3 performed with and without *TESS* priors. For depth and width the result is more precise when priors are used on the *CHEOPS* data, and impact parameter shows only a small difference in precision.

4 Results

There are two main questions the results aim to answer. First, can the filler programme produce publishable quality results? To answer this, it was necessary to understand the quality of data used in the *TESS* analysis and the *CHEOPS* analysis. This was determined by relating the amount of data used from each instrument in Table 4.1 to the precision obtained for the results presented in Table 4.2. The statistical analysis in Table 4.3 was used to study the quality of the results obtained from the data.

The second question was how comparable are *CHEOPS* and *TESS* planetary radius measurements to literature? Since there are no "actual" radius measurements for these planets, a literature comparison was the most logical method to gauge the accuracy of the results. This carries with it a level of uncertainty, because it cannot be assumed that the literature results are correct. The results in Tables 4.6 to 4.10 were analysed in conjunction with findings from the first question.

4.1 *TESS* and *CHEOPS*

Table 4.1 includes the number of observations analysed per system for *TESS* and *CHEOPS* with the average RMS of the residuals of their respective transit fits. The comparison of *CHEOPS* depth against *TESS* depth results is shown in Table 4.2. *CHEOPS* results are products of the `MultiVisit` function, while *TESS* results are taken from the end of the "Analysing *TESS* transits" step. WASP-74 lists no *TESS* results in Table 4.1 nor 4.2, as it contained no *TESS* analysis.

The results in Tables 4.1 and 4.2, alongside the statistical analysis in Table 4.3, were used in determining the effect of the quality of data on the quality of results. Analysing these results involved relating the number of observations used, as well as the quality of each observation, to the precision and accuracy of each result. Figure 4.1 depicts the depth comparison from Table 4.2 as well as literature values.

System		# of observations	Av. RMS [%]
WASP-3			
	CHEOPS	4	0.06
	TESS	44	0.12
WASP-14			
	CHEOPS	2	0.05
	TESS	6	0.07
WASP-16			
	CHEOPS	1	0.08
	TESS	6	0.14
WASP-24			
	CHEOPS	3	0.10
	TESS	4	0.20
WASP-29			
	CHEOPS	2	0.07
	TESS	11	0.11
WASP-74			
	CHEOPS	2	0.04
	TESS	0	-

Table 4.1: Number of *CHEOPS* and *TESS* observations used in the analysis, along with the average RMS of the residuals of the fit.

System	*CHEOPS* depth [%]	*TESS* depth [%]	Literature depth av. [%]
WASP-3	1.040 ± 0.024	1.1113 ± 0.0048	1.07 ± 0.17
WASP-14	0.918 ± 0.016	0.919 ± 0.012	1.01 ± 0.25
WASP-16	1.165 ± 0.033	1.299 ± 0.025	1.20 ± 0.29
WASP-24	1.027 ± 0.018	1.038 ± 0.069	1.00 ± 0.25
WASP-29	1.011 ± 0.036	0.955 ± 0.013	1.01 ± 0.24
WASP-74	0.857 ± 0.028	-	0.96 ± 0.24

Table 4.2: *CHEOPS* depth measurements, *TESS* depth results, and the average of the depth values found on the Exoplanet Archive, for each system.

System	*CHEOPS* t-value	*CHEOPS* Δ_{Lit}	*TESS* t-value	*TESS* Δ_{Lit}	*CHEOPS* vs. *TESS* Δ/σ_Δ
WASP-3	-1.445	-0.0344	7.773	0.0373	-2.95
WASP-14	-5.632	-0.0918	-7.729	-0.0912	-0.03
WASP-16	-1.036	-0.0342	3.952	0.0996	-3.22
WASP-24	1.234	0.0227	0.496	0.0343	-0.16
WASP-29	0.028	0.0010	-4.173	-0.0555	1.47
WASP-74	-3.671	-0.1039	-	-	-

Table 4.3: Statistical look at the results vs. literature. The t-value shows the distance of the measurement to the literature mean in terms of the measurement's uncertainty. Δ_{Lit} is the difference between the measurement and literature mean. Lastly, Δ/σ_Δ, is the standardised difference between the *CHEOPS* and *TESS* measurements.
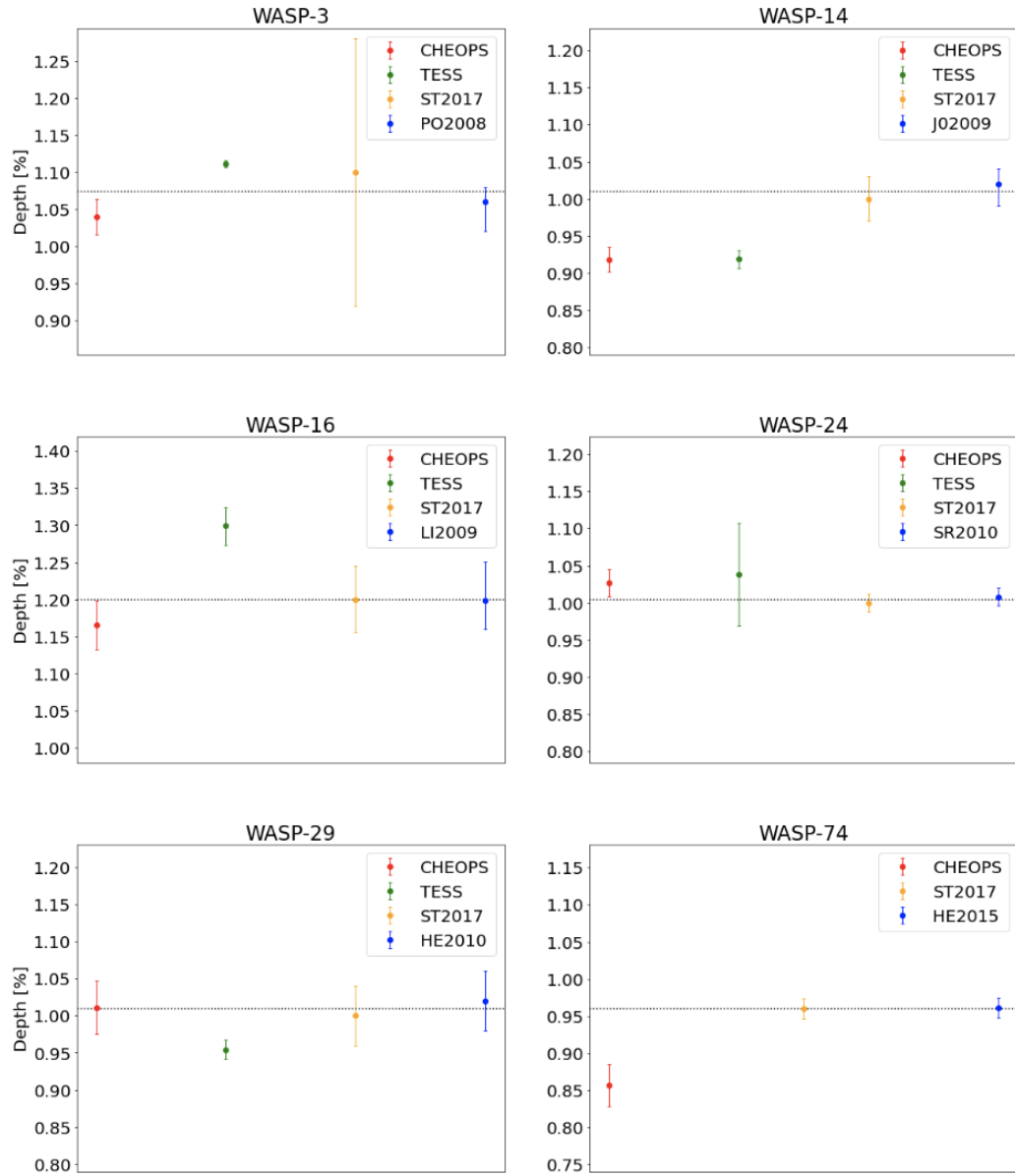
Figure 4.1: The comparison of *TESS* and *CHEOPS* depth results, and their respective errors, against the literature mean. Literature values are also plotted, using the following studies: ST2017 [Stassun et al., 2017], PO2008 [Pollacco et al., 2008], JO2009 [Joshi et al., 2009], LI2009 [Lister et al., 2009], SR2010 [Street et al., 2010], HE2010 [Hellier et al., 2010], and HE2015 [Hellier et al., 2015].

4.2   Radius measurements

The radius measurements were initially calculated using only the `MultiVisit` results, however, since the reliability of these results were unclear the radii were recalculated using the *TESS* results as well. To evaluate the quality of the radius results three parameters are presented: depth (from `MultiVisit` or the *TESS* analysis step), planet-star radius ratio and exoplanetary radius measurements (from `massradius`). These parameters can be found for each system in Tables 4.6 through 4.11. The choice to include all three parameters, rather than only planetary radius, stems from the same reasoning as homogeneous studies. There might be different methods used to calculate each parameter, thus changing the precision and affecting the comparison.

As discussed in Section 1, the mean stellar density, $\langle \rho_\star \rangle$, can be calculated accurately using the depth and width of the transit alongside period. The coverage of the transits within the *TESS* data provided the opportunity to calculate the stellar radius (given a reasonable estimate for stellar mass). Table 4.4 gives the values of the parameters used to calculate the stellar radius, as well as the planetary estimates. The results for these calculations are then given in Table 4.5, with the planetary radii shown again in the individual system results (Tables 4.6 through 4.11).

As the planetary radius is calculated using the stellar radius, its precision is an important factor in the precision of the result. In the case of WASP-3, using the more precise stellar radius value $1.36 \pm 0.02\ R_\odot$ gave a more precise planetary radius value of $1.429 \pm 0.021\ R_{\mathrm{Jup}}$ when using *TESS* data.

Each system's results are compared to three studies, chosen through a survey of the available studies on the NASA Exoplanet Archive. For each system, the literature includes the following: a homogeneous study by Stassun et al. [2017] based on Gaia data for host star properties, the study which presented the most precise value for planetary radius, and the discovery paper. The Stassun et al. [2017] study and discovery papers provided depth measurements as well as planetary radius, to give context for the quality of this work's method for deriving planetary radius from depth measurements. The papers with the most precise planetary radius value was used to gauge how this study's

results compared to the best results. All systems follow this pattern except WASP-24, where the discovery paper itself is the most precise, so an additional paper with a precise value was presented alongside the other two. Figures 4.3 and 4.2 include all three studies against the measured radius of each system, and their respective errors.

System	$M_\star$	K	$\langle \rho_\star \rangle$
	$M_\odot$	ms^{-1}	$\rho_\odot$
WASP-3	1.11 ± 0.07	280.0 ± 8.0	0.53 ± 0.01
WASP-14	1.30 ± 0.06	993.0 ± 3.0	0.46 ± 0.03
WASP-16	0.98 ± 0.05	116.7 ± 2.2	0.81 ± 0.06
WASP-24	1.17 ± 0.08	152.1 ± 3.2	0.55 ± 0.10
WASP-29	0.83 ± 0.03	36.0 ± 3.0	1.75 ± 0.07

Table 4.4: Parameters used to calculate the results in Table 4.5. Stellar mass values were input from TEPCat, whereas radial velocity was found on the Exoplanet Archive.

System	$R_\star$	$M_{\rm p}$	$R_{\rm p}$	$g_{\rm p}$
	$R_\odot$	$M_{\rm Jup}$	$R_{\rm Jup}$	ms^{-2}
WASP-3	1.28 ± 0.03	1.822 ± 0.093	1.349 ± 0.031	25.7 ± 0.9
WASP-14	1.41 ± 0.04	7.69 ± 0.24	1.348 ± 0.034	108.8 ± 4.6
WASP-16	1.06 ± 0.03	0.832 ± 0.034	1.208 ± 0.037	14.5 ± 0.8
WASP-24	1.28 ± 0.08	1.108 ± 0.053	1.302 ± 0.094	16.1 ± 2.2
WASP-29	0.78 ± 0.02	0.246 ± 0.021	0.758 ± 0.016	10.8 ± 1.1

Table 4.5: Results of the *TESS* `massradius` calculations for each system. Following the stellar radius results are the planetary parameters mass, radius, and surface gravity. The associated plots for mass against radius are in Figures C.1 through C.6.

Study	D	$R_{\mathrm{p}}/R_\star$	$R_\star$	R_{p}
	%		$R_\odot$	R_{Jup}
This work				
TESS	1.1113 ± 0.0048	0.1056 ± 0.0002	1.28 ± 0.03	1.349 ± 0.031
CHEOPS	1.040 ± 0.024	0.1015 ± 0.0013	1.28 ± 0.03	1.292 ± 0.035
Literature				
ST2017	1.10 ± 0.18	0.105 ± 0.009	1.44 ± 0.12	1.42 ± 0.17
RO2014	1.11 ± 0.05	0.105 ± 0.002	1.36 ± 0.02	1.40 ± 0.03
PO2008	$1.06^{+0.02}_{-0.04}$	$0.103^{+0.001}_{-0.002}$	$1.31^{+0.05}_{-0.12}$	$1.31^{+0.07}_{-0.14}$

Table 4.6: WASP-3 results for this work against literature values from the following studies: ST2017 [Stassun et al., 2017], RO2014 [Rostron et al., 2014], PO2008 [Pollacco et al., 2008].

Study	D	$R_{\mathrm{p}}/R_\star$	$R_\star$	R_{p}
	%		$R_\odot$	R_{Jup}
This work				
TESS	0.919 ± 0.012	0.0960 ± 0.0005	1.41 ± 0.04	1.348 ± 0.034
CHEOPS	0.918 ± 0.016	0.0958 ± 0.0009	1.41 ± 0.04	1.344 ± 0.040
Literature				
ST2017	1.00 ± 0.03	0.10 ± 0.002	1.40 ± 0.08	1.38 ± 0.08
WO2015	–	0.09 ± 0.0004	–	1.22 ± 0.04
JO2009	$1.02^{+0.02}_{-0.03}$	$0.101^{+0.001}_{-0.002}$	1.306 ± 0.073	1.28 ± 0.08

Table 4.7: WASP-14 results for this work against the following literature: ST2017 [Stassun et al., 2017], WO2015 [Wong et al., 2015], JO2009 [Joshi et al., 2009].

Study	D	$R_{\rm p}/R_\star$	$R_\star$	$R_{\rm p}$
	%		$R_\odot$	$R_{\rm Jup}$
This work				
TESS	1.299 ± 0.025	0.1142 ± 0.0012	1.06 ± 0.03	1.208 ± 0.037
CHEOPS	1.165 ± 0.033	0.1080 ± 0.0015	1.06 ± 0.03	1.138 ± 0.036
Literature				
ST2017	1.200 ± 0.045	0.1095 ± 0.0021	1.14 ± 0.09	1.22 ± 0.10
SO2013	$-$	0.1190 ± 0.0022	1.087 ± 0.042	1.22 ± 0.04
LI2009	$1.199^{+0.052}_{-0.039}$	$0.1095^{+0.0024}_{-0.0018}$	0.946 ± 0.057	$1.01^{+0.08}_{-0.06}$

Table 4.8: WASP-16 results against literature values from the following studies: ST2017 [Stassun et al., 2017], SO2013 [Southworth et al., 2013], LI2009 [Lister et al., 2009].

Study	D	$R_{\rm p}/R_\star$	$R_\star$	$R_{\rm p}$
	%		$R_\odot$	$R_{\rm Jup}$
This work				
TESS	1.038 ± 0.069	0.1021 ± 0.0032	1.28 ± 0.08	1.302 ± 0.094
CHEOPS	1.027 ± 0.018	0.1013 ± 0.0009	1.28 ± 0.08	1.290 ± 0.082
Literature				
ST2017	1.000 ± 0.012	0.1 ± 0.0006	1.42 ± 0.16	1.38 ± 0.16
SO2014	$-$	0.1018 ± 0.0007	1.317 ± 0.041	1.303 ± 0.047
SR2010	1.008 ± 0.012	0.1004 ± 0.0006	1.331 ± 0.032	$1.3^{+0.039}_{-0.038}$

Table 4.9: WASP-24 results for this work against literature values from the following studies: ST2017 [Stassun et al., 2017], SO2014 [Southworth et al., 2014], SR2010 [Street et al., 2010].

Study	D	$R_\mathrm{p}/R_\star$	$R_\star$	R_p
	%		$R_\odot$	R_Jup
This work				
TESS	0.9545 ± 0.013	0.0978 ± 0.0007	0.78 ± 0.02	0.758 ± 0.016
CHEOPS	1.011 ± 0.036	0.1015 ± 0.0013	0.78 ± 0.02	0.792 ± 0.030
Literature				
ST2017	1.00 ± 0.04	0.1 ± 0.002	0.79 ± 0.07	0.77 ± 0.07
GI2013	–	0.0982 ± 0.0015	0.808 ± 0.044	0.776 ± 0.043
HE2010	1.02 ± 0.04	0.101 ± 0.002	0.808 ± 0.044	$0.792^{+0.056}_{-0.035}$

Table 4.10: WASP-29 results for this work against the following studies: ST2017 [Stassun et al., 2017], GI2013 [Gibson et al., 2013], HE2010 [Hellier et al., 2010].

Study	D	$R_\mathrm{p}/R_\star$	$R_\star$	R_p
	%		$R_\odot$	R_Jup
This work				
CHEOPS	0.857 ± 0.028	0.0926 ± 0.0015	$1.536 \pm 0.026^*$	1.418 ± 0.024
Literature				
ST2017	0.960 ± 0.014	0.0980 ± 0.0007	1.42 ± 0.10	1.36 ± 0.10
MA2019	–	0.0903 ± 0.0006	1.536 ± 0.026	1.404 ± 0.022
HE2015	0.961 ± 0.014	0.0980 ± 0.0007	1.64 ± 0.05	1.56 ± 0.06

Table 4.11: WASP-74 radius parameters for this work against literature values from the following studies: ST2017 [Stassun et al., 2017], MA2019 [Mancini et al., 2019], HE2015 [Hellier et al., 2015]. *The stellar radius used for WASP-74 is the literature value also used in MA2019.
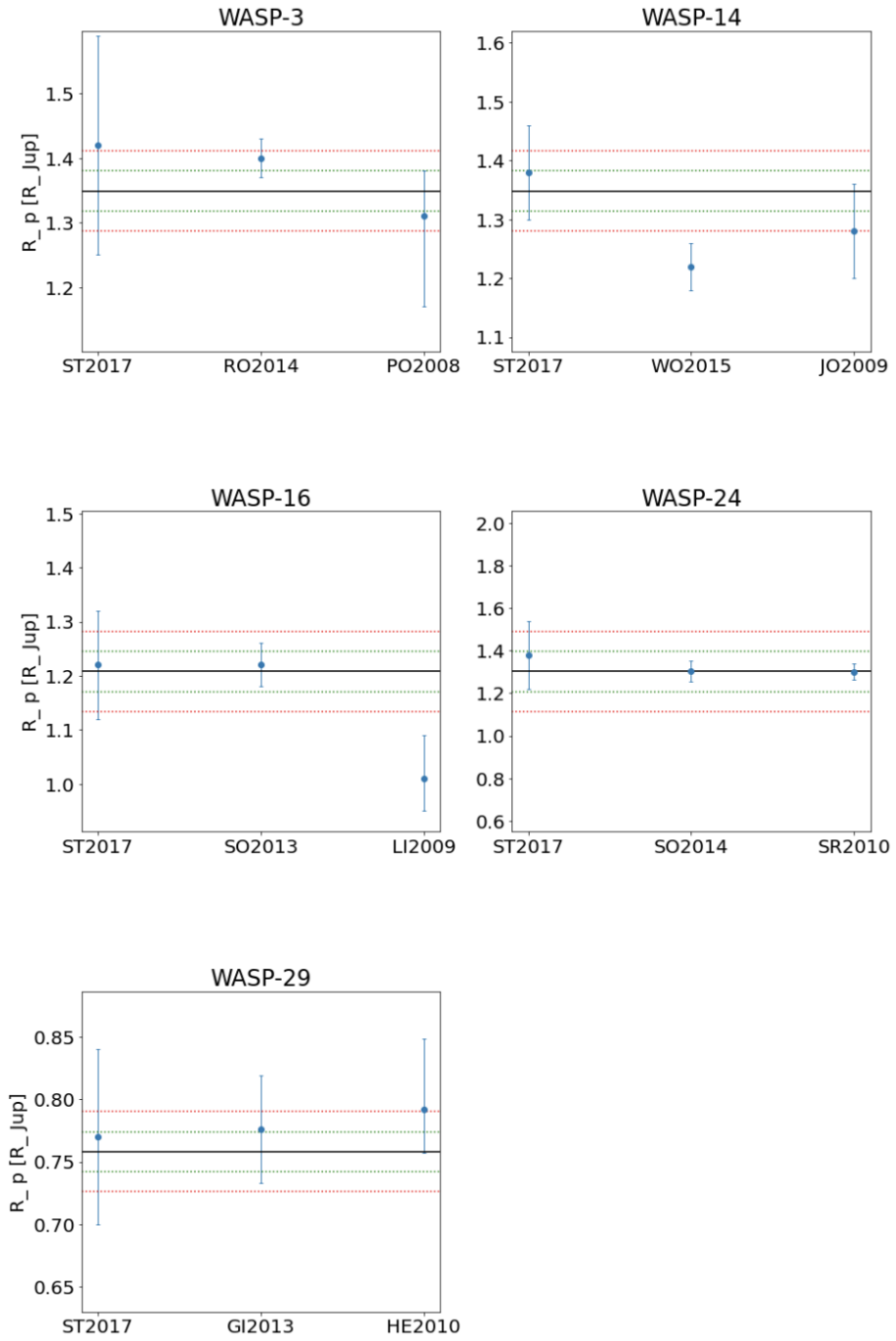
Figure 4.2: Comparison of literature values for planetary radius against the *TESS* measurements within this study. The values for this study are represented by the black horizontal line, with its error shown by the green boundaries (red indicates twice the error, for reference). Keys for each paper are the same as within Tables 4.6 to 4.10.
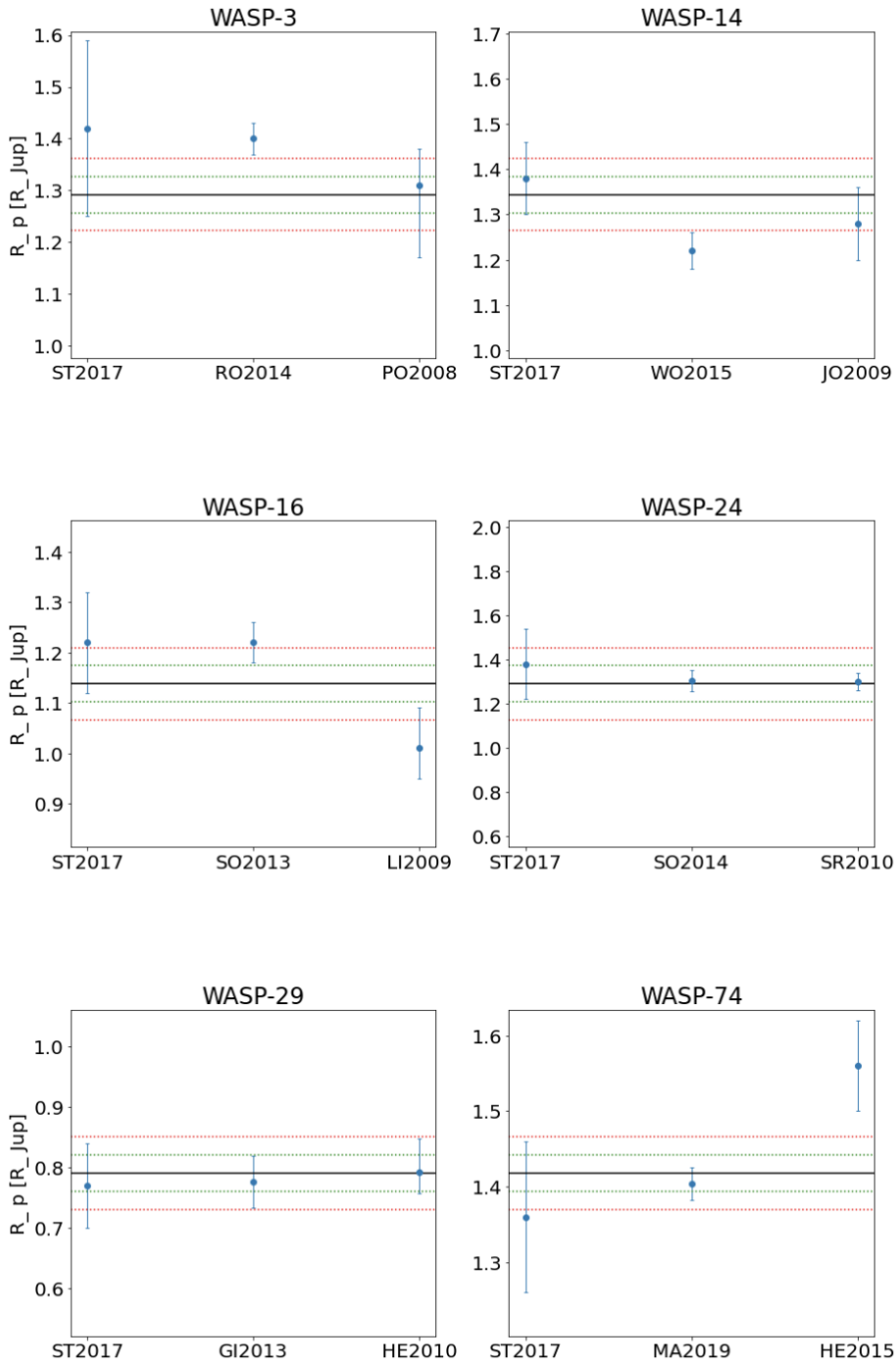
Figure 4.3: Comparison of literature values for planetary radius against those calculated using *CHEOPS* analysis results. The black horizontal line represents the radius results, with all colours following the same meaning as Figure 4.2. Keys for each paper are the same as within Tables 4.6 through 4.11.

4.3 TTV

The *TESS* analysis provided the opportunity to study the TTV of each system. For the TTV seen in Figures D.1 through D.5 an average of the variations for each system are in Table 4.12, as well as the updated ephemerides. WASP-74 did not contain *TESS* analysis, so no TTV plot was made for this system, however an updated ephemeris was still calculated using the *CHEOPS* data. The mid-transit times in Table 4.12 were obtained using the `MultiVisit` function on the *CHEOPS* data. These were then used to calculate the new value of period, and if it was more precise than the literature it is presented in Table 4.12. The literature values used as reference ephemerides can be found in Table 2.1.

The period produced in this study was slightly more precise than literature values in four out of six systems. For WASP-14 and WASP-29 the literature values for period were used in the updated ephemerides, as those were the most precise.

System	AV. TTV [min]	Time of mid-transit [BJD]	Period [days]
WASP-3	0.169 ± 0.074	2459760.07649(020)	1.84683503(009)
WASP-14	0.879 ± 0.165	2459727.45306(052)	2.24376644(022) [a]
WASP-16	1.852 ± 0.306	2459733.23529(193)	3.11859861(119)
WASP-24	-4.864 ± 0.519	2459745.09171(028)	2.34122062(014)
WASP-29	0.030 ± 0.160	2459509.69275(045)	3.92271218(025) [b]
WASP-74	–	2459621.59725(018)	2.13775133(022)

Table 4.12: Results of the TTV analysis alongside the calculated mid-transit time and period. Standard error on the final digit for each value is given in parentheses following the value (for example, the error on the mid transit time of WASP-3 is ± 0.00020). The most precise period values were either from this work or the literature, [a][Baştürk et al., 2022] and [b][Saha and Sengupta, 2021].

5 Discussion

The quality of the data was crucial to understanding the results. However, with only six systems to analyse and limited literature available for each, it was difficult to make confident conclusions regarding the quality of data required to produce good results. The depth measurements for *TESS* and *CHEOPS* were assessed against each other and the literature to understand how different instruments produce different results. Given the lack of measurements from previous studies, quantitative conclusions were difficult to make. The planetary radius results were compared against the literature analytically to determine if there was an improvement in precision. This made drawing quantitative conclusions more straightforward, however the lack of literature values added ambiguity to conclusions. Overall, the minimal literature available was the most significant obstacle when interpreting the results.

The depth measurements from the *CHEOPS* analysis produced consistently smaller results than *TESS*, but with varying magnitudes of difference. The comparison with the literature, seen in Table 4.3, also found differences. The comparison was done using the t-statistic to relate the distance from the literature mean with the precision of the measurement. A simple difference between the literature and measurement was also used in order to distinguish between inaccuracy and high precision.

There is some concern regarding the reliability of the *CHEOPS* measurements, primarily the possibility of over-correcting for noise. If over-correction occurs part of the transit signal can be "fitted out," which leads to underestimation in the transit depth. This was supported by removing the *dfdt* term from the decorrelation process, as discussed in Section 3.1.4. Furthermore, an independent study of the same data for WASP-3 using PSF PIPE photometry (which is less sensitive to instrumental noise) showed good agreement between the *TESS* and *CHEOPS* depth values [Scandariato et al., in prep]. Unlike the *CHEOPS* analysis, the *TESS* analysis had no reliance on calculated priors, and the transit coverage was far more thorough. This makes the *TESS* results potentially more reliable than the *CHEOPS* measurements.

Due to the nature of exoplanet measurements, there are no "actual" values to compare the results against. To determine the accuracy and precision of the radius measurements in this study, they were compared to the findings of previous studies. To better qualify the comparison of results against literature values, it was important to understand how the methods differed from the one used here. Briefly mentioned in Chapter 4, the papers chosen to compare against the results of this work followed a pattern. They all included the discovery paper, the study by Stassun et al. [2017] based on *Gaia* data, and the paper containing the most precise result. First, the 2017 Stassun study presented an opportunity to view these results against another homogeneous study. Next, in the interest of understanding how this work compared to the literature, it was important to investigate the method used to obtain the most precise result. Finally, the discovery paper was used to provide support for the values presented in the other studies, as well as an additional value in case the other papers did not agree.

Following a review of the homogeneous *Gaia* paper, it was confirmed that no method variations were reported for any systems discussed in this study [Stassun et al., 2017]. It focused on obtaining accurate and empirical stellar radius measurements using *Gaia* data. The instrumental noise was handled prior to the data release and no further noise corrections were deemed necessary. In order to calculate stellar radius, bolometric flux (F_{bol}), effective temperature (T_{eff}), and *Gaia* parallax (distance) measurements were combined. Stellar parameters (including T_{eff}) were obtained from high-precision spectroscopy and used for the stellar atmospheric model. This was combined with spectral energy distributions to measure F_{bol}. By introducing the distance measured by *Gaia*, the stellar radius could be calculated. Once stellar radius was calculated, it was used in the radius ratio ($R_{\mathrm{p}}/R_{\star}$) to produce the planetary radius. Error propagation was used instead of anything more complex, and it was noted that this potentially caused an underestimation for uncertainties. Although it was not the most precise of the studies examined, its empirical approach improves its accuracy. Therefore, if the results within this work are consistent with the 2017 paper it lends credibility to this study.

This chapter is structured to first discuss the data quality and initial depth results followed by a discussion on the radius measurements for each system. Afterwards, there is a brief analysis of the transit time variations and updated ephemerides. The chapter concludes with a section on the recommendations for future studies and the limitations faced within this work.

5.1 WASP-3

5.1.1 *TESS* and *CHEOPS* analysis

The analysis was able to cover all four *CHEOPS* datasets available on DACE, as they all contained part of the transit. Two of the four datasets covered full transits, while the other two covered about half a transit each. Overall, the four datasets were able to cover the entire transit, which is shown in Figure A.2. Compared to the quality of the data for the other systems, WASP-3 had the best *CHEOPS* data. It also had the best quality *TESS* data, with forty-four transits used. Using `lmfit` and `MultiVisit` on *TESS* and *CHEOPS* data, respectively, produced good fits according to the RMS. Figures A.1 and A.2 depict the closeness of the fits to the data. From the transit coverage and RMS, accurate results would be expected from both analyses.

The *CHEOPS* and *TESS* depth results in Table 4.2 do not agree, with a standardised difference of -2.95. There is no obvious cause for the difference, as both *CHEOPS* and *TESS* data cover the transit well with good fits. The most logical conclusion is that the difference in results comes from the inherent ambiguity of the code which, while allowing the fit to adapt to the data, can cause the variability of results.

The results for the *CHEOPS* depth and *TESS* depth measurements are nearly equidistant from the literature mean, although the *CHEOPS* result is below and the *TESS* result is above the mean. Given the poor agreement between the *TESS* and *CHEOPS* results, as well as their deviation from the literature mean, this calls into question which measurement is the most reliable. With such a small pool of data,

no certainties can be made. While it is possible that *CHEOPS* underestimated depth through over-correction, it is not unlikely that previous studies have also encountered this inaccuracy. This could especially be the case for studies which face high levels of contamination, such as ground-based observations. Currently, there are no reasons to suspect inaccuracies in the *TESS* results, however further studies would be required to confirm that this is true.

The t-value for *TESS* is significant, which is in part due to the precision the measurement obtained. Meanwhile, the *CHEOPS* t-value was within a reasonable range ($|t| < 3$). The *TESS* depth measurement agrees more closely with Stassun et al. [2017] and Rostron et al. [2014] than with Pollacco et al. [2008]. The agreement with literature values shows the reliability of the *TESS* analysis results, and further supports their use as priors on the *CHEOPS* analysis. The *CHEOPS* result agrees with Pollacco et al. [2008] within its uncertainty. Given the uncertainties are carefully handled in `pycheops`, the precision remains correct regardless of if the results are accurate within the context of the literature. Therefore, the results can still be considered reliable despite disagreements with the literature.

Both the results of *CHEOPS* and *TESS* provide rough estimates of depth. As both depth measurements are within 0.05% of the literature mean, neither should be immediately disregarded. With only four available depth measurements on the Exoplanet Archive, further studies would be required to understand this work's results in the context of literature.

Future studies should confirm whether the quality of data or analysis method are determining factors in the variation of results. Without knowing the extent of the accuracy of the depth measurements in this study, the reliability of the subsequent radius measurements is not entirely clear. Furthermore, the radius measurements obtained using the *CHEOPS* analysis are affected by the uncertainty of both the *TESS* and *CHEOPS* data, which introduces additional variables to the reliability of the results.

5.1.2   Radius

The stellar radius value calculated using the *TESS* data was lower than those of the literature used to compare the planetary radius measurements, however it was within the range of uncertainty for Stassun et al. [2017] and Pollacco et al. [2008]. Table 4.6 shows that the planetary radius measurement produced using the *TESS* analysis agreed well with the literature, while the *CHEOPS* radius measurement fell slightly below the literature estimations. As mentioned in Chapter 4, the analysis did not use the most precise stellar radius value. The value calculated was 1.28 ± 0.03 R$_{\odot}$, which produced the planetary radius values in Table 4.5 (1.349 ± 0.031 R$_{\mathrm{Jup}}$ and 1.292 ± 0.035 R$_{\mathrm{Jup}}$). The paper which presents the most precise radius measurements is a *Spitzer* study [Rostron et al., 2014]. Using the most precise stellar radius value available (1.36 ± 0.02 R$_{\odot}$ [Rostron et al., 2014]) produced a more precise value for planetary radius: 1.429 ± 0.021 R$_{\mathrm{Jup}}$. This result for planetary radius supersedes the precision of the most precise value found in the Exoplanet Archive as of July 2023.

5.2   WASP-14

5.2.1   *TESS* and *CHEOPS* analysis

WASP-14 used both available datasets, one of which contained around a half a transit and one with a little less than half. This is comparatively poor against the quality of the other systems. The *TESS* data, however, made up for the quality of the *CHEOPS* data. With six datasets, the *TESS* analysis produced results of similar precision as WASP-29. This could indicate that at a certain point increasing the number of datasets no longer has a major impact on the precision of the *TESS* results. Figure A.3 shows a very close fit, with the smallest RMS of any *TESS* fit, and Figure A.4 is similarly well-fit. Given the lack of transit coverage in the *CHEOPS* data, the accuracy of the transit fit is likely influenced by the width and impact parameter priors from the *TESS* analysis.

The standardised difference between the *TESS* and *CHEOPS* depths was extremely small, furthering the hypothesis of the influence of *TESS* priors. The precision of both results caused the t-values for *TESS* and *CHEOPS* to be extremely large. Despite not using the *TESS* depth itself as a prior on the *CHEOPS* analysis, width and impact parameter were used as priors. This could have contributed to the final analysis presenting a similarly underestimated depth measurement.

Both depths measured from *CHEOPS* and *TESS* were small compared to literature values, by a significant margin. The two literature values are the only depth measurements for WASP-14 on the Exoplanet Archive. This small data pool makes it difficult to determine which depth estimate is more reliable. If the *CHEOPS* measurements are assumed to likely be underestimates, that would suggest the *TESS* measurement here is also an underestimate. On the other hand, the close agreement between *TESS* and *CHEOPS* could suggest that the *CHEOPS* underestimation does not always occur. Without a deeper study and a larger data pool, a conclusion cannot be reached.

5.2.2   Radius

The stellar radius calculated from the mean stellar density, 1.41 ± 0.04 R$_\odot$, agrees well with the average value of the wider literature available on the Exoplanet Archive. The radius measurements for WASP-14 both agree well with the literature values, and with one another. However, the literature values create a wide range in which the *TESS* and *CHEOPS* results can fall, so the agreement between *CHEOPS* and *TESS* is more significant than the literature agreement. While the *CHEOPS* planetary radius has the same precision as Wong et al. [2015], the measurement made with *TESS* is the most precise value compared to all literature on the Exoplanet Archive. Furthermore, the method used to calculate errors in this study is robust and not likely to underestimate uncertainties. Without any evidence to suggest inaccuracies in the *TESS* measurements, it can be concluded that the planetary radius measurement 1.348 ± 0.034 R$_{\text{Jup}}$ is the most precise value as of July 2023.

5.3 WASP-16

5.3.1 *TESS* and *CHEOPS* analysis

Of all systems in this study, WASP-16 contained the poorest quality data. There were three datasets available on DACE, however only one contained part of a transit. *TESS* provided six datasets, all of which were usable. Figure A.5 manages to fit the data, and Figure A.6 shows a fairly good fit, despite the lack of data. Looking into the RMS of the *TESS* transit, it was twice that of the RMS for WASP-14 despite both containing 6 transits each. This suggests that the number of transits alone cannot determine how well `pycheops` will be able to fit data. WASP-16b has a short transit duration and high impact factor. The short length of t_F could lead to fewer data points available to estimate transit parameters, which would affect both *TESS* and *CHEOPS* analyses. Likewise, the importance of the number of transits analysed should not be negated. A wider data pool is required to determine the importance of how many transits are used as well as how the quality and coverage of the data. Furthermore, an investigation on the effect of the system parameters (transit duration, impact factor, etc.) could yield significant results.

The depth values for *TESS* and *CHEOPS* did not agree, with a significant margin between the two. According to the difference with the literature mean in Table 4.3, as well as Figure 4.1, the *CHEOPS* result was more accurate than the *TESS* depth result. The t-value was also better for the *CHEOPS* depth. The *TESS* t-value was 3.952, which is considered a significant deviation from the literature mean. Concluding that the *CHEOPS* measurement is more accurate than *TESS* overlooks the possible *CHEOPS* underestimation as well as assuming the literature values are correct. Once again, increasing the observations of this system is required to draw conclusions on the reliability of the measurements and the literature values.

5.3.2 Radius

WASP-16b radius results were calculated using a stellar radius of 1.06 ± 0.03 R$_\odot$, which itself agreed with the literature. The planetary radius estimates agree within a reasonable range, with the *TESS* radius more similar to the larger literature values and the *CHEOPS* estimate falling closer to the literature average. Both radius measurements obtained with *CHEOPS* (1.138 ± 0.036 R$_{\mathrm{Jup}}$) and *TESS* (1.208 ± 0.037 R$_{\mathrm{Jup}}$) were more precise than the literature values. Despite the unknown reliability of the *CHEOPS* accuracy, its radius measurement of 1.138 ± 0.036 R$_{\mathrm{Jup}}$ is the most precise and accurate measurement as of July 2023.

5.4 WASP-24

5.4.1 *TESS* and *CHEOPS* analysis

DACE had four datasets for WASP-24, three of which had nearly full transits, and one of which was unusable. This was coupled with four *TESS* transits. There seems to be a limit reached here, where the precision of the *TESS* depth drops dramatically compared to all other systems. As it has the least amount of *TESS* data, this could be indicating that there are too few datasets to make precise measurements. This hypothesis could be studied further to determine if a lower limit exists. Combining the lack of data with the low quality, as evidenced by both Figure A.7 and its RMS value, would produce the decreased *TESS* precision.

The *CHEOPS* depth agrees well with the *TESS* value, according to Table 4.3 there is a standardised difference of -0.16, and it is also precise. Based on the noise seen in Figure A.8 as well as the RMS, the precision for the *CHEOPS* measurement does not come from using high quality data. The coverage seen in Figure A.8 produced from the three nearly full transits could be evidence towards the importance of the amount of data used. It could also be argued that because there is an excess of noise throughout the transit, `pycheops` does not over-correct and "fit out" the transit signal.

The high level of noise in both the *TESS* and *CHEOPS* data should be investigated further. Given the age of the host star would allow WASP-24b to have a fairly large moon, as discussed in Weidner and Horne [2010], the flux variations seen across multiple instruments could be an indicator of a possible physical perturbation in the system. Figure B.1 shows how the noise appears in consecutive *TESS* transits. Conclusive interpretations cannot be made through this data alone, however it is a point of interest. Additional studies of this system would add clarity to the abnormally high flux variations and how it affects the radius measurement.

5.4.2   Radius

The stellar radius used to calculate the planetary radius value was estimated to be $1.28\pm0.08\,\mathrm{R_\odot}$, which agreed with Southworth et al. [2014] and Street et al. [2010] within its uncertainty. *TESS* and *CHEOPS* agreed on their planetary radius measurements with $1.302 \pm 0.094\,\mathrm{R_{Jup}}$ and $1.290 \pm 0.082\,\mathrm{R_{Jup}}$, respectively. Although they are not close to the most precise measurement, the radius estimates for WASP-24b agree with the literature. The lack of precision is most likely from the few *TESS* transits available, however the accuracy was unaffected. It is surprising to see the accuracy of the radius measurement, given the high variation of flux and high RMS. Again, more investigation is required to understand why this has occurred.

5.5   WASP-29

5.5.1   *TESS* and *CHEOPS* analysis

Both available datasets for WASP-29 on DACE were used. One had a full transit and one had about half, however both datasets were spotty. Similar to WASP-14 and WASP-16, only around half of the data points were during the transit. The many gaps in the data make the already poor quality data even harder to analyse. As for *TESS*, all of the eleven available datasets were used. The coverage of data throughout both

TESS and *CHEOPS* observations are well-fit, as depicted in Figures A.9 and A.10. Interestingly, despite having poorer coverage of the transit and a less precise result, the *CHEOPS* analysis estimated depth more accurately than the *TESS* analysis. The low RMS in Table 4.1 is another indication that the analysis fits the data well.

The *TESS* depth uncertainty is similar to that of WASP-14 (which analysed 6 transits) and falls between the uncertainties for WASP-3 (44 transits) and WASP-16 (6 transits analysed). This potentially supports the correlation between the number of transits analysed and the precision of depth measurements. The uncertainty in the WASP-29 depth measurement with *CHEOPS* is higher than all other systems, with a similar error as WASP-16 (analysed 1 transit). It is possibly because of gaps in the data which hinder the ability to more precisely measure depth. Studying this system further could help add clarity to the cause for the drop in precision.

There is a reasonably sized gap between the *CHEOPS* and *TESS* measurements, and is the only system for which the *CHEOPS* result was higher than *TESS*. The *CHEOPS* measurement aligns well with the literature values, with a t-value of 0.028, whereas the t-value for *TESS* is considered significantly large at -4.173. If the *TESS* results are considered more reliable than the *CHEOPS* measurements, then it is unknown what would cause the overestimation in both the *CHEOPS* and literature values. As it is unlikely that the *CHEOPS* and literature values coincidentally overestimated the depth for this system only, it is possible the *TESS* results are not more reliable than the other measurements.

5.5.2   Radius

The stellar radius, calculated from the *TESS* light curve and mass estimate, was within a reasonable range compared to literature values. The radius results for WASP-29b follow the same pattern the depth measurements saw: the results within this study do not agree with each other. The *TESS* radius estimate was below the range of literature values, however it was within a reasonable distance from the literature. The *CHEOPS* radius measurement on the other hand was in agreement with all literature values.

While the *CHEOPS* radius estimate, 0.792 ± 0.030 R$_{\text{Jup}}$, was more precise than the literature, the *TESS* estimate, 0.758 ± 0.016 R$_{\text{Jup}}$ is the most precise planetary radius estimation (as of July 2023). Given the behaviour of the depth measurements and the close agreement between the *CHEOPS* and literature results, there is hesitation to conclude the *TESS* radius is the most reliable result.

5.6   WASP-74

5.6.1   *CHEOPS* analysis

Two of the three available DACE datasets were used for WASP-74. Like WASP-29, one was a full transit and one was about half of a transit. No *TESS* datasets were available for WASP-74, so priors were produced from the reference paper found on TEPCat [Mancini et al., 2019]. Figure A.11 shows a close fit to the data, possibly enhanced by the minimal curvature seen in the transit as well as the thorough coverage.

The depth measurement is smaller than the literature mean, and not as precise. With a difference of over ten times the literature depth, there is significant disagreement in the measurement and literature. The t-value confirms the substantial divergence, with a value of -3.671. This is an indication that using only two low-quality *CHEOPS* datasets is not enough to make a reliable measurement. An investigation would be useful to uncover if improving the method for analysing *CHEOPS* filler programme data would lead to more reliable measurements.

5.6.2   Radius

Without *TESS* analysis results, the radius estimation was made using the *CHEOPS* result. While the depth measurement is not as accurate or precise as other studies, the radius measurement falls within the range presented by the literature. It uses the same value for stellar radius as the 2019 paper [Mancini et al., 2019], the most precise paper, so it cannot exceed that precision at this time.

5.7   TTV

While TTV plots can be used to discover possible physical perturbations to a system, they are also effective in determining if the ephemeris should be updated. Regardless of the cause of TTV, accurate measurements of the ephemeris are vital to accurately fitting data and therefore should be as up-to-date as possible. Within this study, the variations ranged from less than two seconds on average to over four minutes. The systems which required an updated ephemeris the most were WASP-14, WASP-16, and WASP-24. Unlike WASP-3 and WASP-29 these systems did not vary around the calculated mid-transit time. Conclusions regarding the cause of any of the variations could not be made, given the limited amount of data available. The significant variations is both transit time and flux for WASP-24 could suggest a physical cause, however more investigation is required to make any robust hypothesis.

5.8   Recommendations

There is room for the method created in this study to be improved. Using a better method for noise correction, such as the PIPE PSF photometry, would greatly increase the accuracy of these results. This could have improved the reliability of the *CHEOPS* measurements. It is highly recommended that future analysis of filler programme data use analysis methods which are able to correct for noise without fitting out the transit signal in the process.

The main limiting factor of this study was the amount of available data with which to work. This left gaps in the conclusions that could be reached. Despite determining that data from the filler programme could produce precise planetary radius results, the reliability of the results is questionable. A worthwhile future study would look into this in order to inform the cause of the inaccurate depth measurements. The main hypothesis for the depth underestimation is the over-correction of noise. Using a wider data pool would help to determine if this is a viable theory.

One final note on recommendations for the future relates to ensuring the filler programme observes systems during a transit. Fourteen datasets were analysed, despite DACE providing eighteen. The missing four did not cover transits, and so did not provide any information. While four datasets may not seem to be many, it would have greatly increased accuracy. Had the two unusable WASP-16 datasets been transits, a conclusion regarding the precision limit might have been reached.

6　Conclusion

The main questions in this study are as follows.

1. Can *CHEOPS* filler programme data produce accurate radius measurements?

2. Is the precision of the results comparable to published literature?

3. Is there a quantifiable amount of data required in order to obtain this precision?

After examining the results for each system in this work, it can be concluded that filler programme data can produce literature quality results using one or more datasets. This is only the case, however, when the *CHEOPS* data is analysed in conjunction with high-quality *TESS* data. The planetary radius measurements found within this study are all within a normal range of accuracy compared to literature values. The findings in Chapters 4 and 5 show two-thirds of the literature values fall within $2\ \sigma$ of the radius results, and 80% of the literature estimates agree with the results within their respective ranges of uncertainty. These are clear indications that the results of this study are aligned with the available literature. This conclusion is, however, dependent on the assumed accuracy of the literature. Given the minimal literature available, continued research is recommended to solidify this result.

The precision of the results varies depending on the quality of data provided, both in the number of datasets as well as the coverage of transit. Despite variation, the precision and accuracy of the results in Tables 4.6 through 4.11 are comparable to literature values. Planetary radius measurements for WASP-3b, WASP-14b, WASP-16b, and WASP-29b were found to be the most precise estimates available according to the Exoplanet Archive in July 2023 (1.429 ± 0.021 R$_{\mathrm{Jup}}$, 1.348 ± 0.034 R$_{\mathrm{Jup}}$, 1.138 ± 0.036 R$_{\mathrm{Jup}}$, and 0.758 ± 0.016 R$_{\mathrm{Jup}}$, respectively). The radius measurements for WASP-24b and WASP-74b were not more precise than the literature, however they were within the range of precision found in the literature.

This study shows that the amount of data used, and its quality, impacts the precision of the results. From the findings in this work, as little as one *CHEOPS* dataset could potentially produce literature-comparable precision, if analysed properly. The two systems which did not produce planetary radius results more precise than the literature were also the systems which analysed the least *TESS* data. WASP-24 analysed four *TESS* datasets and WASP-74 did not contain any *TESS* analysis, while all other systems analysed at least six *TESS* datasets. The lack of *TESS* data, and subsequently the low precision of the *TESS* analysis results, impacted the overall precision of the radius measurements. Given the amount of *CHEOPS* data available for these two systems were comparatively high, this could be evidence for the importance of high-quality priors in the *CHEOPS* data analysis. Assuming this, the amount of *CHEOPS* data can be as little as one dataset, if at least six *TESS* datasets are analysed and used as priors during the *CHEOPS* analysis.

Alternatively, WASP-24 and WASP-74 could have been outliers and the amount of *TESS* data does not have a significant impact on the precision of the results. The data for WASP-24b was shown to have a high level of noise in the transit, which could have been the determining factor for the low precision. WASP-74b obtained a planetary radius measurement almost as precise as the most precise literature value and was the third most precise radius measurement in this study. With the small data pool, it is difficult to separate potential trends from outliers. Additional investigation should be conducted to confirm the number of *TESS* datasets required to make precise planetary radius measurements using *CHEOPS* data. Currently, these results suggest that at least six *TESS* datasets are required to analyse the *CHEOPS* data precisely.

Continued analysis is required to confirm how reliably the *CHEOPS* data can be analysed to produce high-quality radius results. The PIPE PSF photometry is one potential alternative method for accurately analysing the filler programme data. Additionally, there are factors beyond only the number of datasets used which impact the accuracy and precision of the results. One potential factor is the combination of transit width and impact parameter to provide enough data within the transit to accurately measure transit parameters.

The agreement of the *TESS* radius measurements with literature, both planetary and stellar radius, shows the reliability of the *TESS* data analysis. The majority of the *CHEOPS* planetary radius results agreed with the *TESS* results within their uncertainties, as well as with the literature. Therefore, it can be concluded that the *CHEOPS* results were at the very least good estimates of planetary radius for the systems in this study.

In order to reach these conclusions, it was necessary to create a bespoke method based in `pycheops`. The *TESS* data were analysed inside the *CHEOPS*-focused `pycheops` with the assistance of `pycdata`. Doing so allowed for a homogeneous study of *TESS* and *CHEOPS* transits as well as enabling *TESS* analysis results to be used as priors on *CHEOPS* light curve analyses. The use of *TESS* results or *Spitzer* values in the analysis of *CHEOPS* data was integral to obtaining meaningful results. Often only partially covering transits, the filler programme data required priors on the parameters it struggled to model (width and impact parameter). Introducing priors for these parameters allowed the *CHEOPS* analysis to focus on determining accurate and precise depth values.

Given the limited quality of *CHEOPS* filler programme data, it was not expected for the results to be an improvement on published results. With the high-precision observations *CHEOPS* makes, the expectation was potentially good radius estimations but with a lower precision than previous papers. Once the method for analysing the filler programme observations is proven to be reliable and robust, the data will produce literature-quality radius measurements.

Further studies are recommended to conclusively determine what factors affect the accuracy and precision of the results, and improve the analysis method. WASP-3 could be a reasonable place to start because it is known to produce precise results and has a large amount of both *TESS* and *CHEOPS* data, as well as a reasonable amount of literature for comparison. The method presented in this work was designed specifically for this type of work, so it would be useful to use it as a starting point. If this method is used there are a number of improvements which could be made in order to increase accuracy, such as using PIPE PSF photometry.

The *CHEOPS* filler programme data can produce publishable quality results for planetary radius, when given high-quality data as priors. *TESS* data can be analysed and used as priors on *CHEOPS* data analysis to improve the quality of results and fill the gaps created by the low-priority *CHEOPS* observations. The *TESS* data can also be analysed alone to produce publishable-quality results. To conclude, if the *CHEOPS* data analysis can be proven reliable, as little as one *CHEOPS* dataset analysed in conjunction with at least six *TESS* datasets can produce results of a higher precision than current literature. Therefore, more filler observations should be added to the observation schedule of *CHEOPS* to increase the efficiency of observing time allocation.

A TESS and CHEOPS transit fits

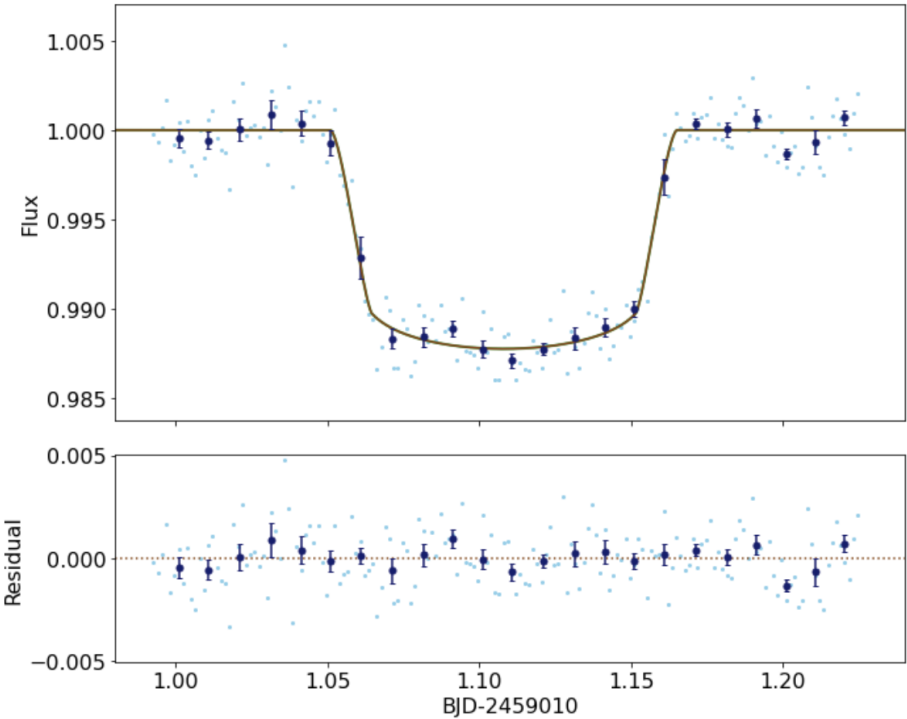Figure A.1: Typical *TESS* transit curve of WASP-3 with `lmfit` model. *Upper panel:* Cyan points are the data collected from MAST. These data are binned over 0.01 phase units. Overlaid are overlapping green and brown lines which represent the best-fit transit model and the model with instrumental trends, respectively. *Lower panel:* Residuals of the best-fit model, with the same meanings for cyan and dark blue.
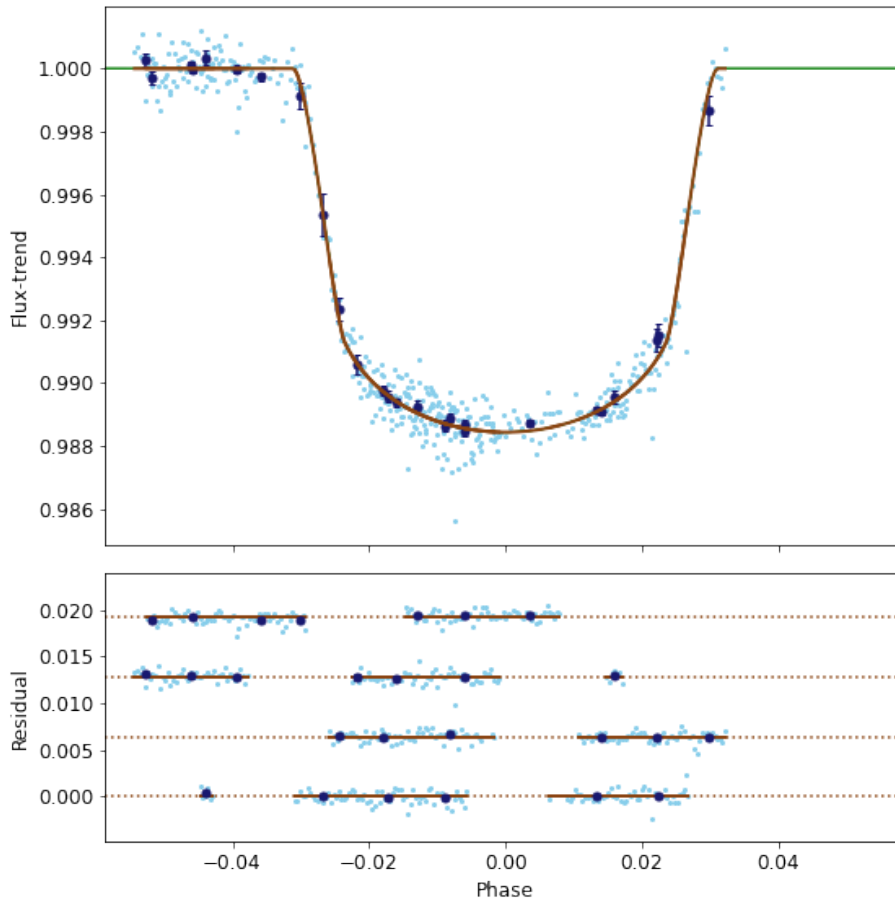
Figure A.2: `MultiVisit` plot for WASP-3. *Upper panel:* Phase-folded results from `MultiVisit`. Cyan points are the data following corrections and detrending. The dark blue points are data binned over 0.01 phase units. The green line is the best-fit model, while the brown line is the model after removing all trends. *Lower panel:* The residuals from the plot above for each dataset offset by multiples of 0.006 units.
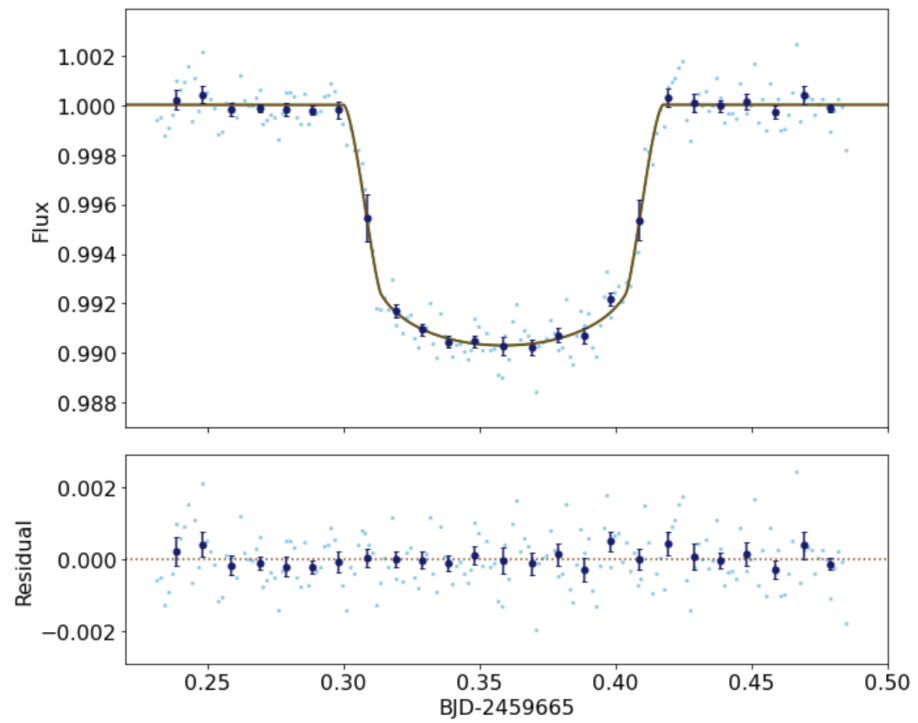
Figure A.3: A *TESS* plot for WASP-14. *Upper panel:* Cyan points are data, with data binned over 0.01 phase units in dark blue. Again, the overlapping green and brown lines are the model and the model with trends, respectively. *Lower panel:* The residuals from above, with cyan and dark blue points having the above meaning.
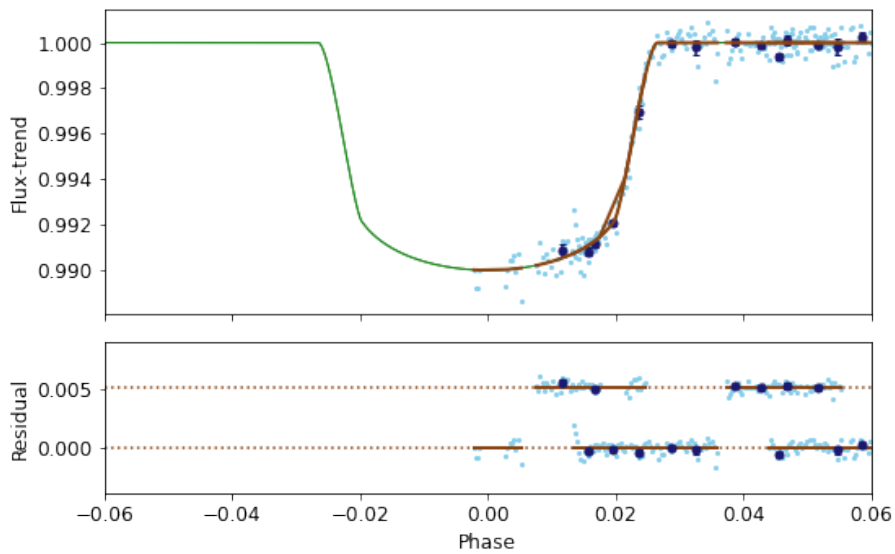
Figure A.4: `MultiVisit` plot for WASP-14. *Upper panel:* Data are shown in cyan, with data binned over 0.001 phase units in dark blue. The green line is the model and the brown line is the model after detrending. *Lower panel:* The residuals of the above plot for each dataset offset in intervals of 0.005 units, where cyan and dark blue are the same as above.
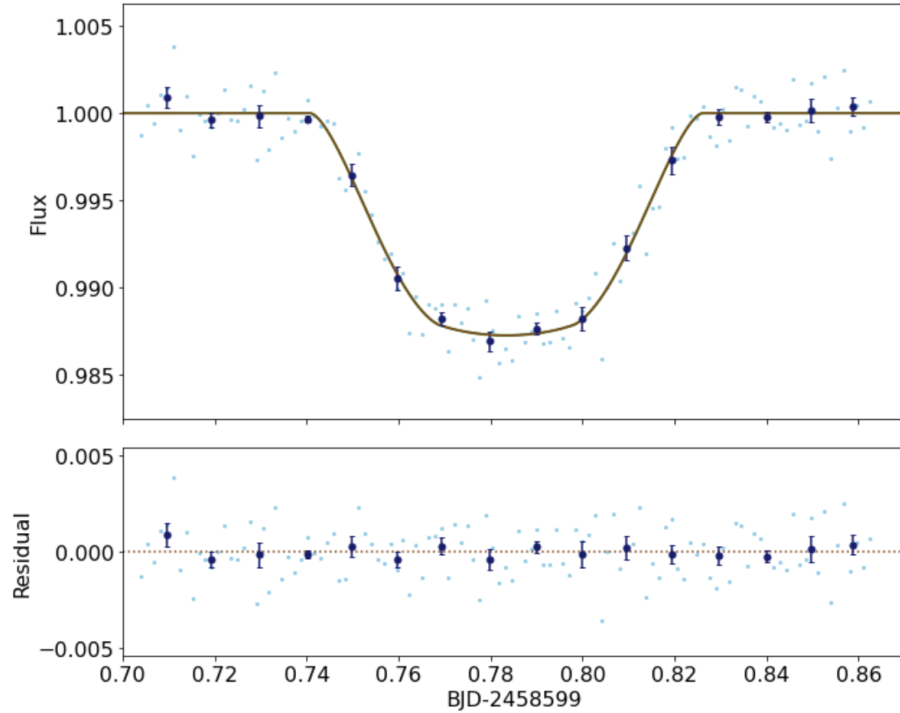
Figure A.5: One of the *TESS* plot for WASP-16. *Upper panel:* `lmfit` plot with the same colour meanings as Figure A.1 and A.3. *Lower panel:* Residuals of the above plot, with the same colours as previous figures.
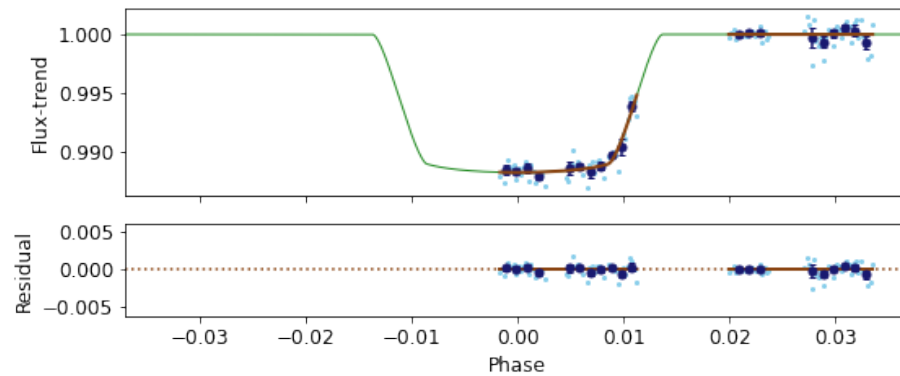
Figure A.6: `MultiVisit` plot for WASP-16. *Upper panel:* `MultiVisit` plot with the same colour scheme as Figure A.4. *Lower panel:* Residuals from above, again with the same colour scheme as Figure A.4, and as only one transit was analysed there is no offset.
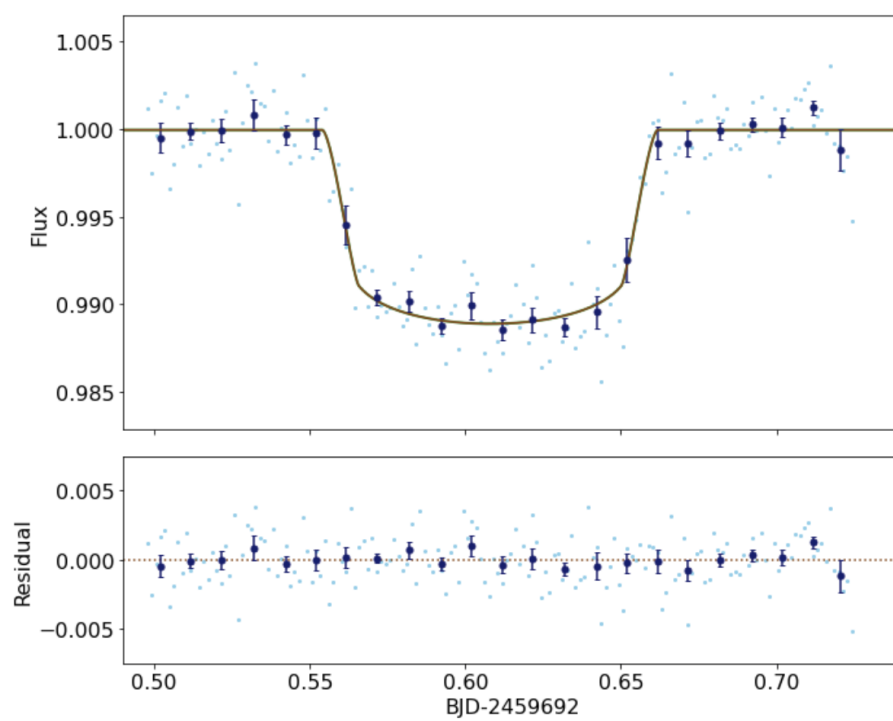
Figure A.7: A typical *TESS* plot for WASP-24. *Upper panel:* `lmfit` plot with the same meanings as Figure A.1. *Lower panel:* Residuals of above plot, again with colours described in Figure A.1.
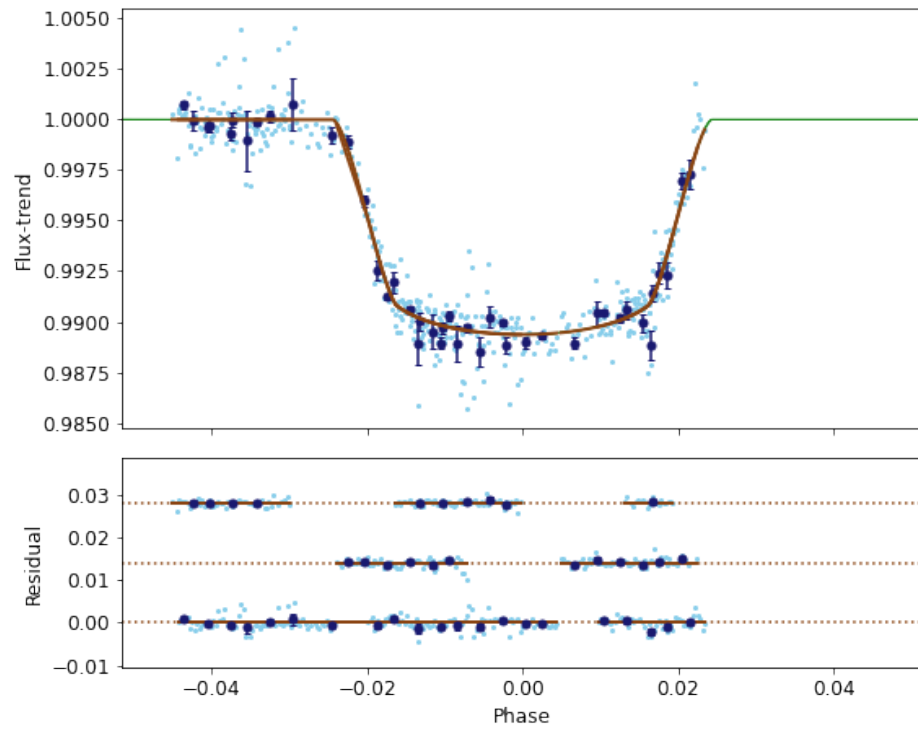
Figure A.8: `MultiVisit` plot for WASP-24. *Upper panel:* `MultiVisit` plot, coloured the same as Figure A.4. *Lower panel:* Residuals from the above plot using the same colours and the datasets offset by 0.0175 units.
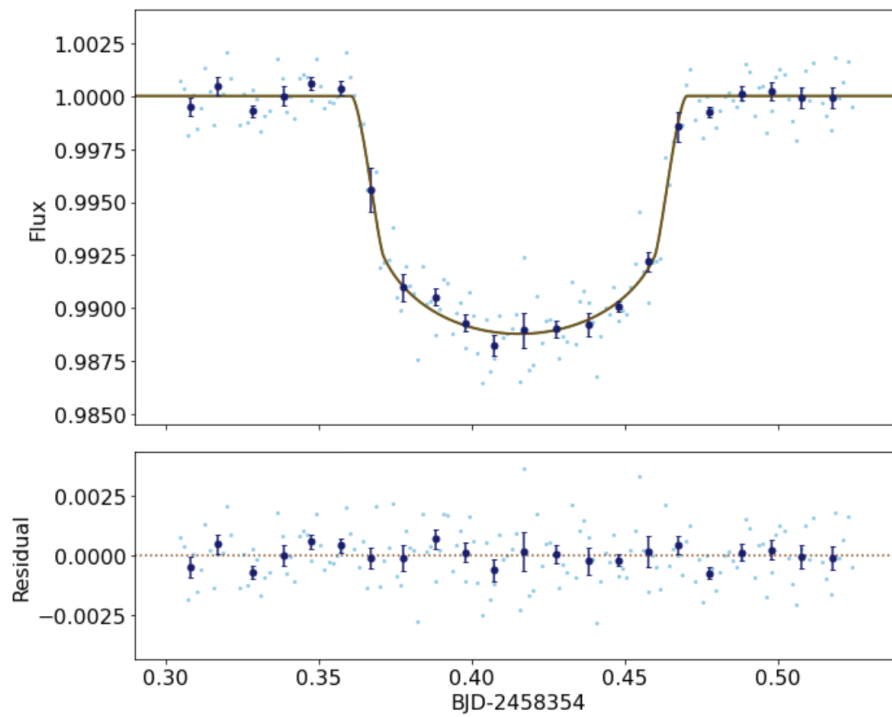
Figure A.9: An example of a *TESS* plot for WASP-29. *Upper panel:* Plot from `lmfit` with the same meanings as Figure A.1. *Lower panel:* Residuals of the above plot, with the same meanings as Figure A.1.
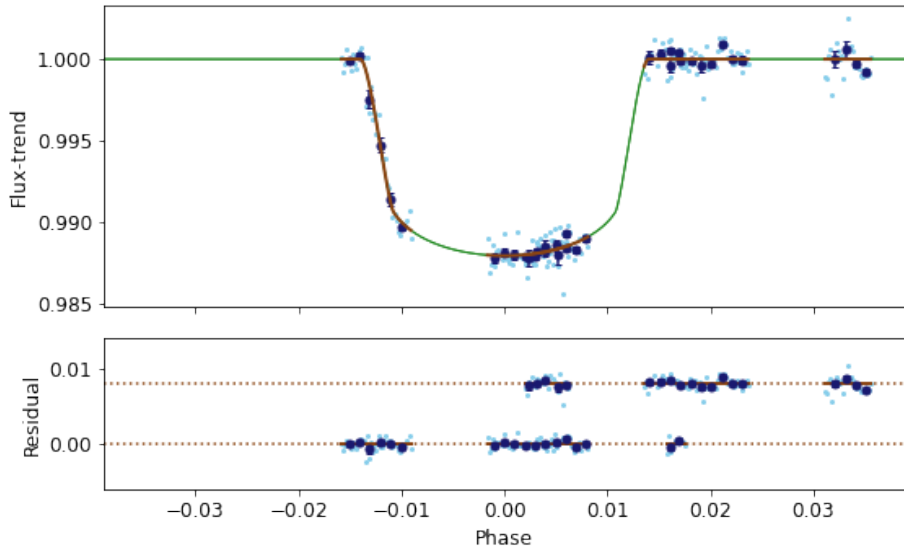
Figure A.10: `MultiVisit` plot for WASP-29. *Upper panel:* Resulting plot from `MultiVisit` with the same colours as described in Figure A.4. *Lower panel:* The residuals from the `MultiVisit` plot above, following the same colour scheme as Figure A.4. The dataset offset is 0.01 units.
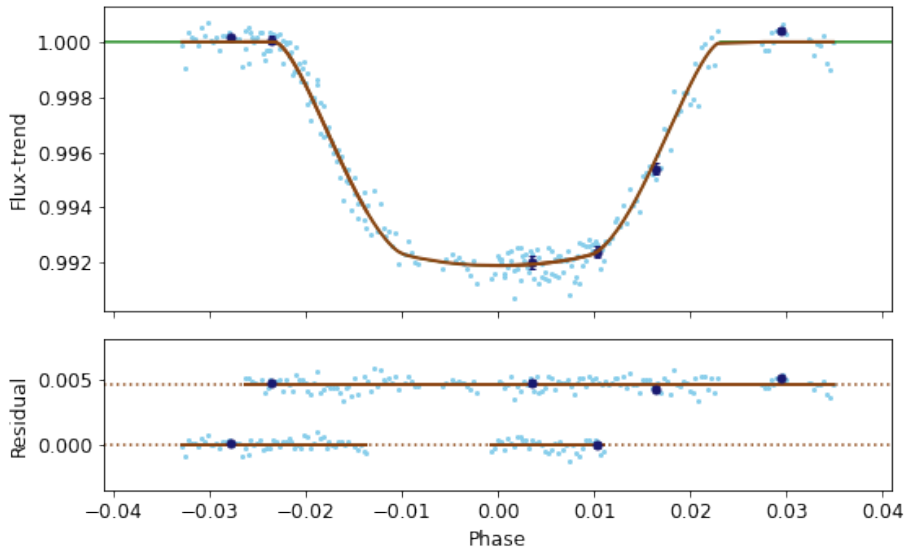
Figure A.11: `MultiVisit` plot for WASP-74. *Upper panel:* The `MultiVisit` plot for WASP-74, with the colour meanings described in Figure A.4. *Lower panel:* The `MultiVisit` plot residuals, with the data offset at 0.005 units and the colours described in Figure A.4.

B WASP-24b flux variations
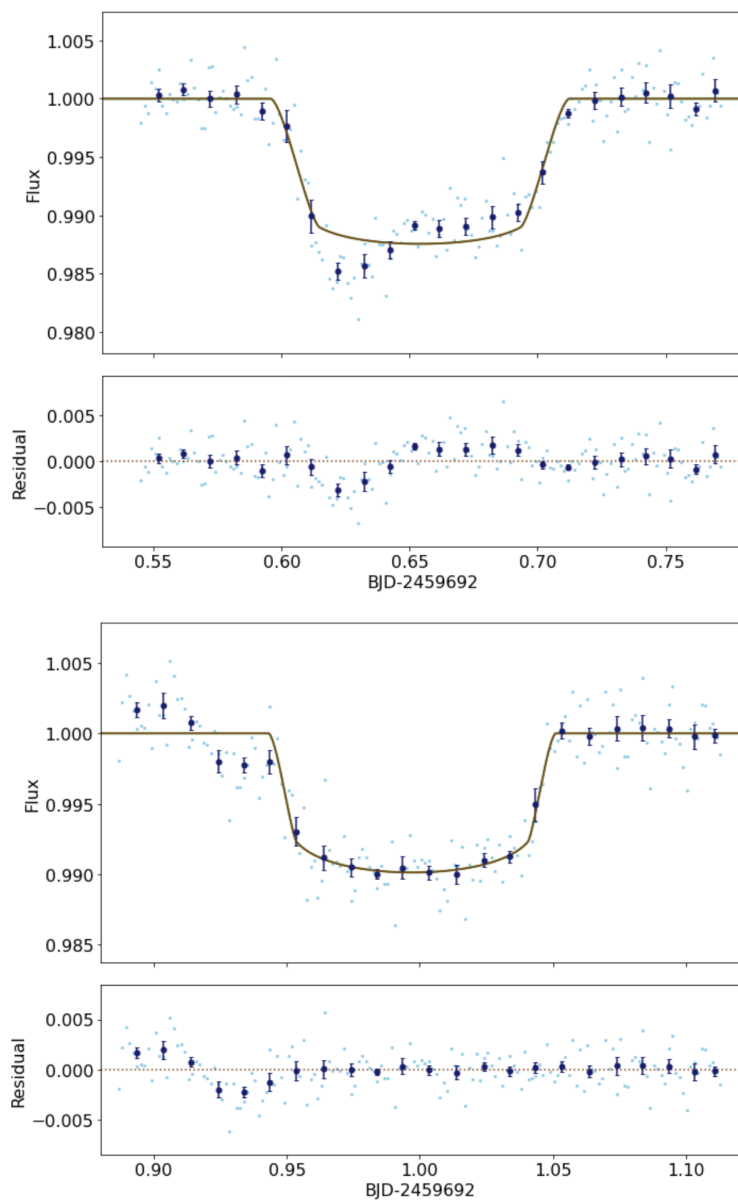
Figure B.1: *TESS* plots for consecutive transits of WASP-24b, depicting the anomalous flux variations. *Upper*: $T_0 = 459714.658$ BJD. *Lower*: $T_0 = 2459717.000$ BJD.

C   Mass-radius plots
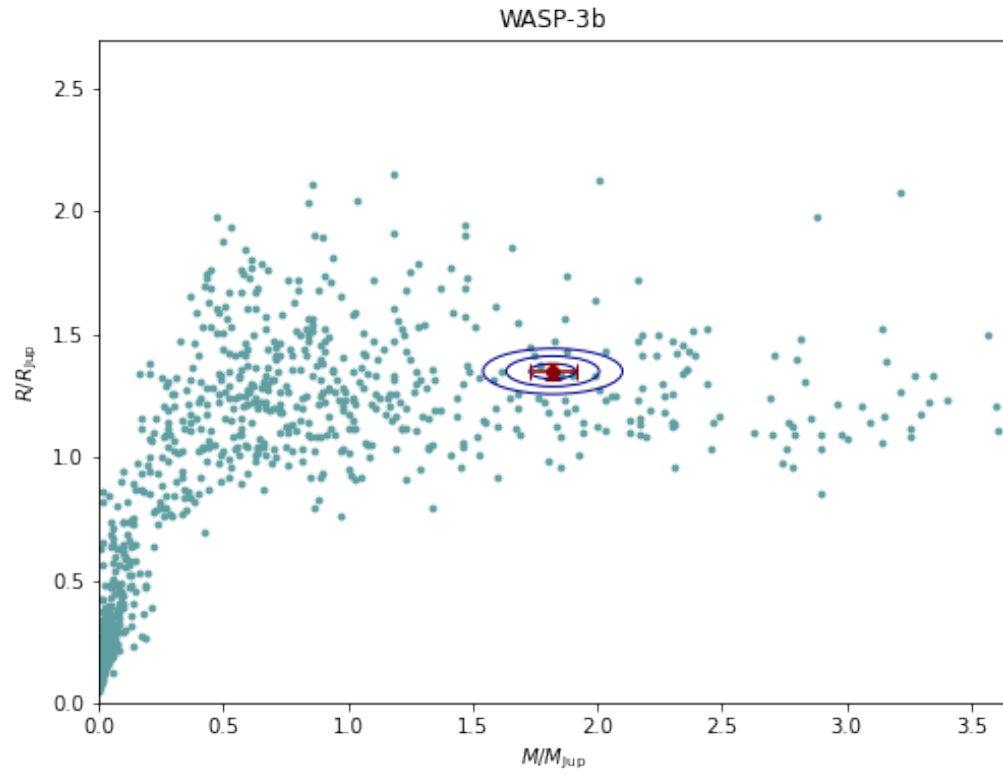
Figure C.1: A plot of the `massradius` result for WASP-3b with known exoplanets.
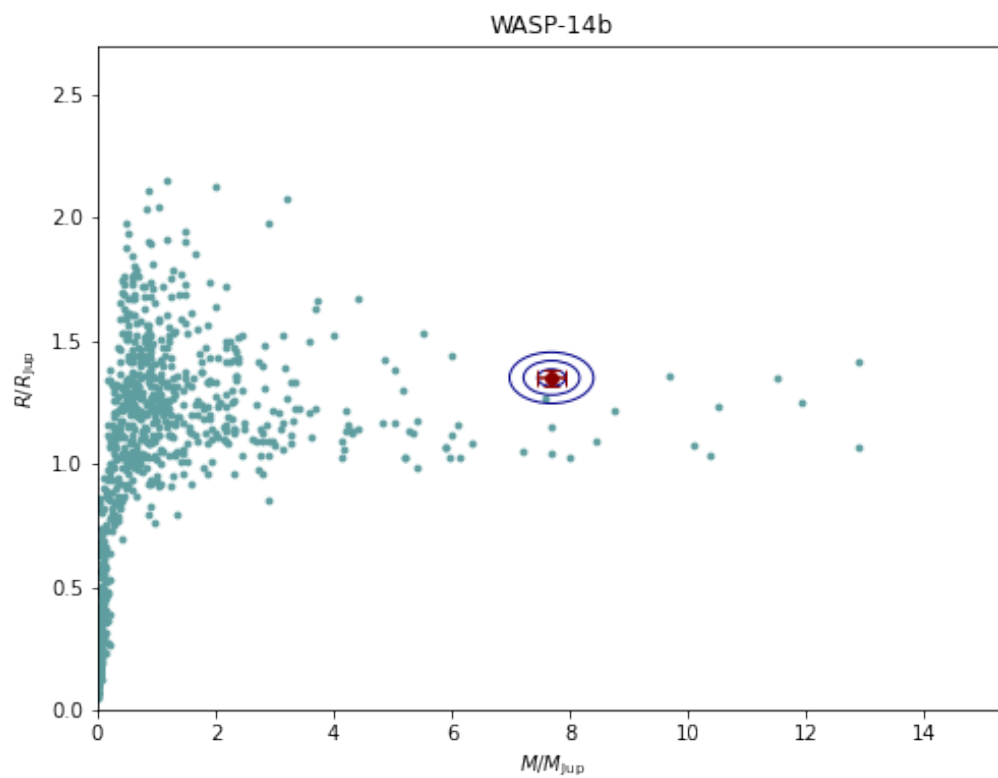
Figure C.2: `massradius` plot for WASP-14b alongside exoplanets found on TEPCat.
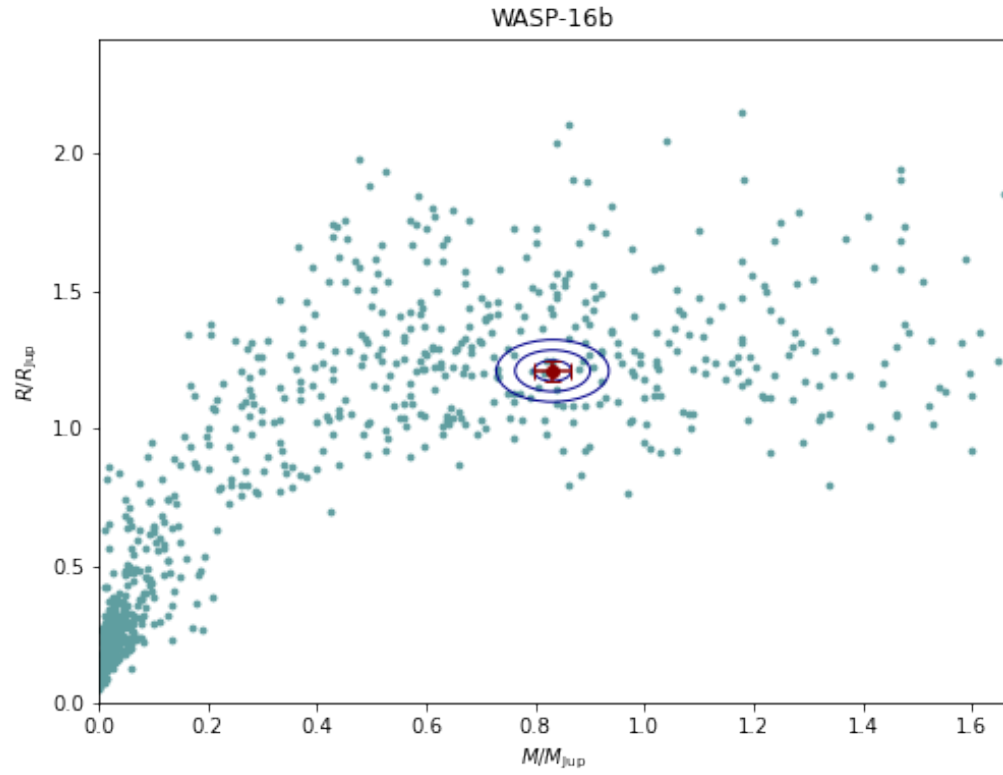
Figure C.3: WASP-16b `massradius` plot compared with known exoplanets.
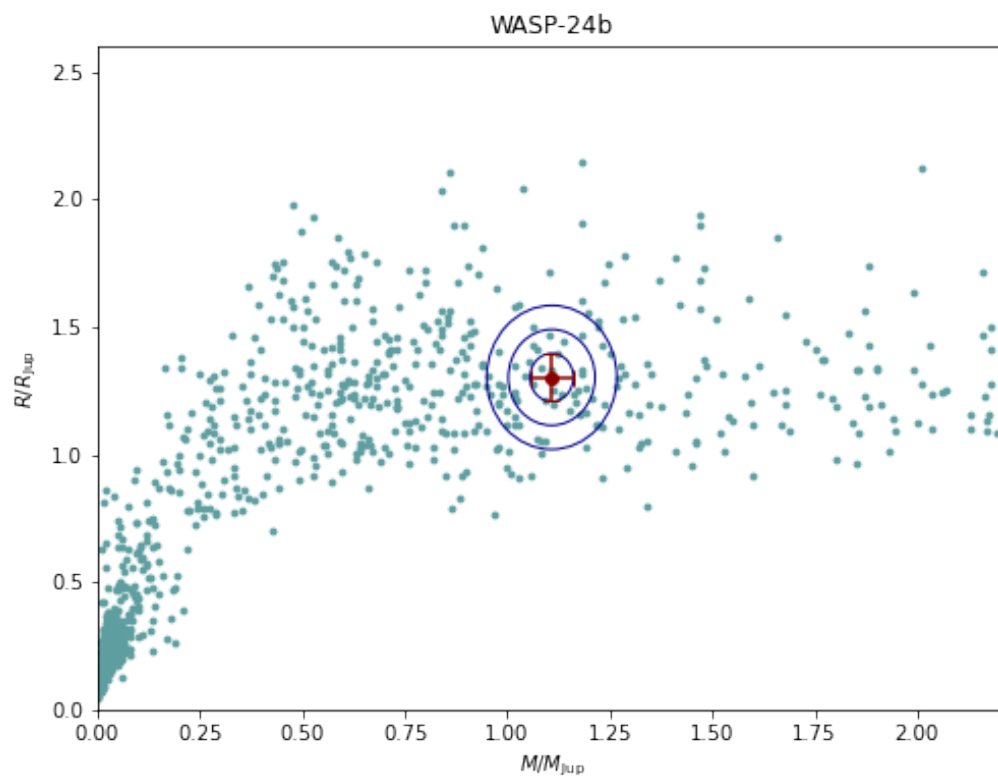
Figure C.4: The results of `massradius` for WASP-24b. Also plotted are known exo-planets from TEPCat.
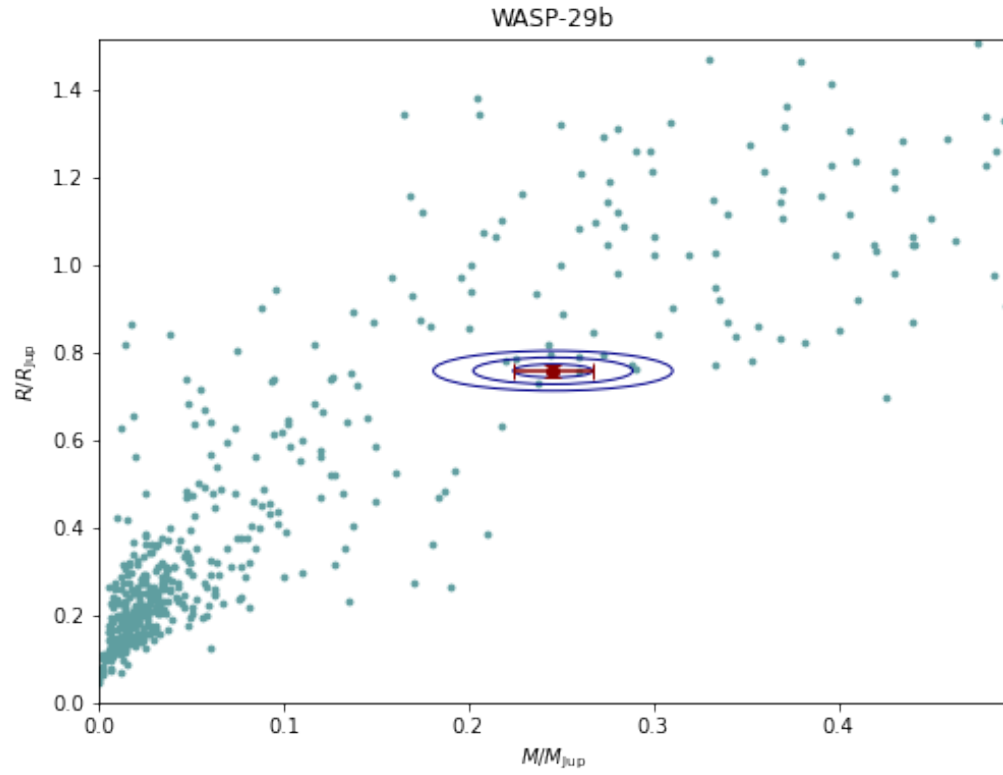
Figure C.5: A plot of the WASP-29b `massradius` result. The mass and radius of known exoplanets are plotted alongside.
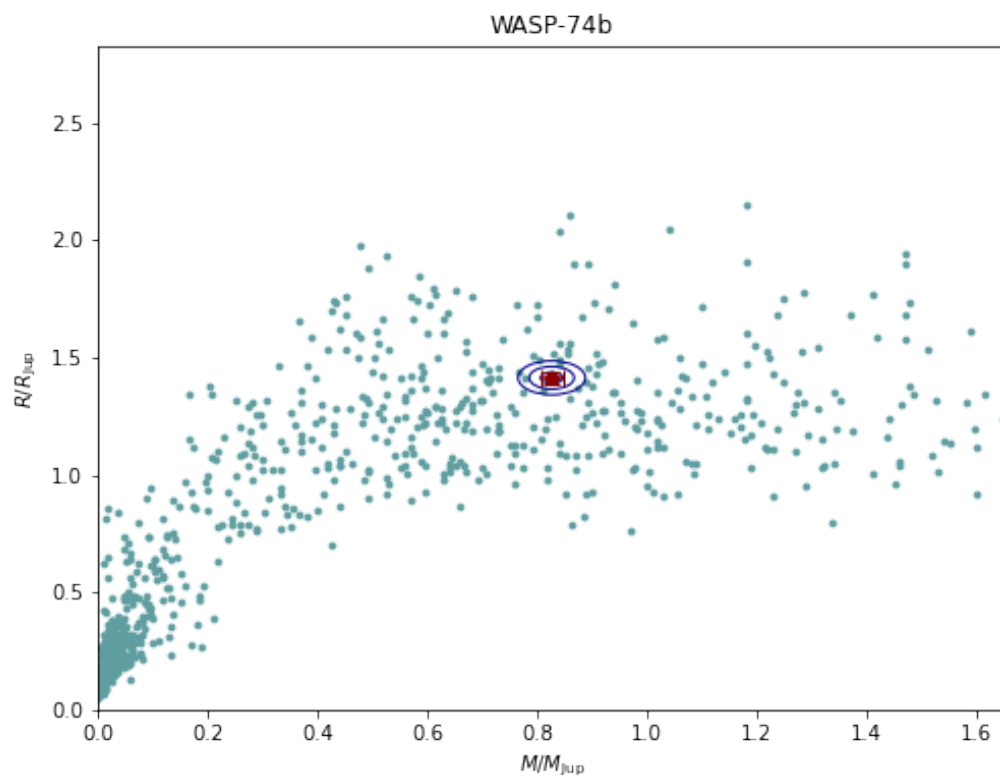
Figure C.6: `massradius` results for WASP-74b using *CHEOPS* data, as no *TESS* data were available. The results are plotted alongside exoplanets from TEPCat.

D   Transit time variation
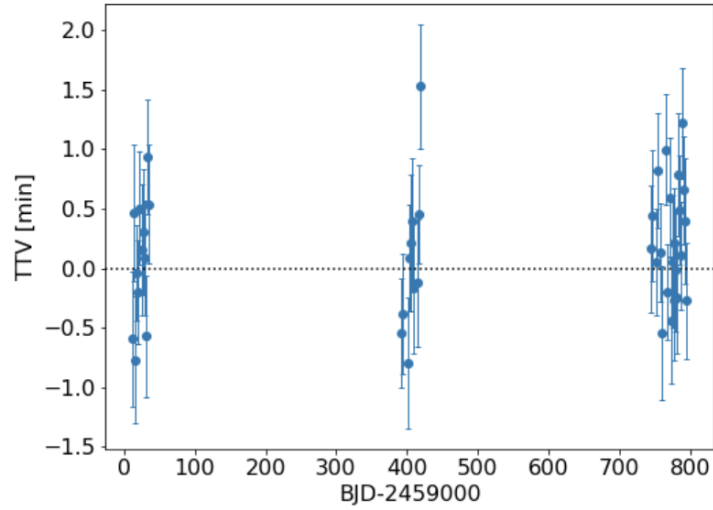
Figure D.1: TTV plot for WASP-3b, given the reference ephemeris from Wong et al. [2021] in BJD of 2455362.76229 ± 0.00009.
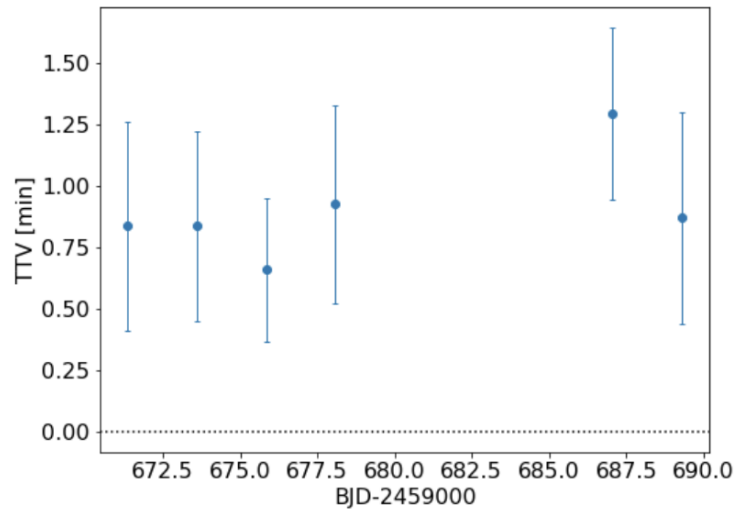
Figure D.2: TTV plot for WASP-14b from 2455632.57865 ± 0.00010 as the ephemeris in BJD of from Baştürk et al. [2022].
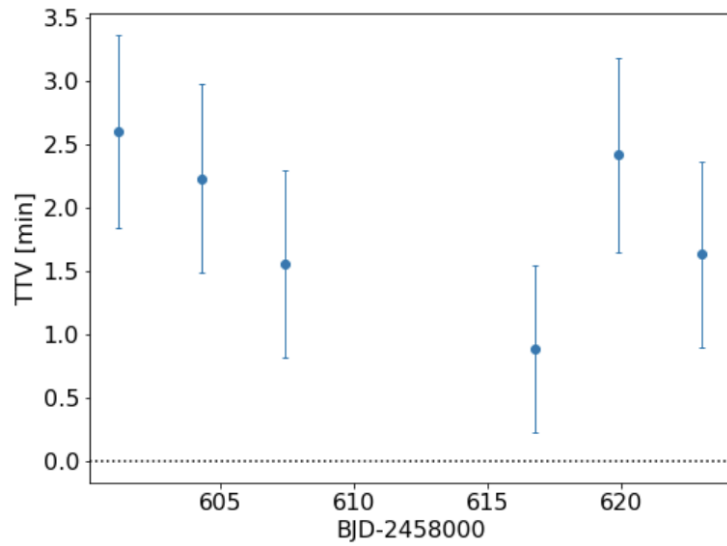
Figure D.3: TTV plot for WASP-16b using the ephemeris 2454584.42898 ± 0.00038 in BJD [Southworth et al., 2013].
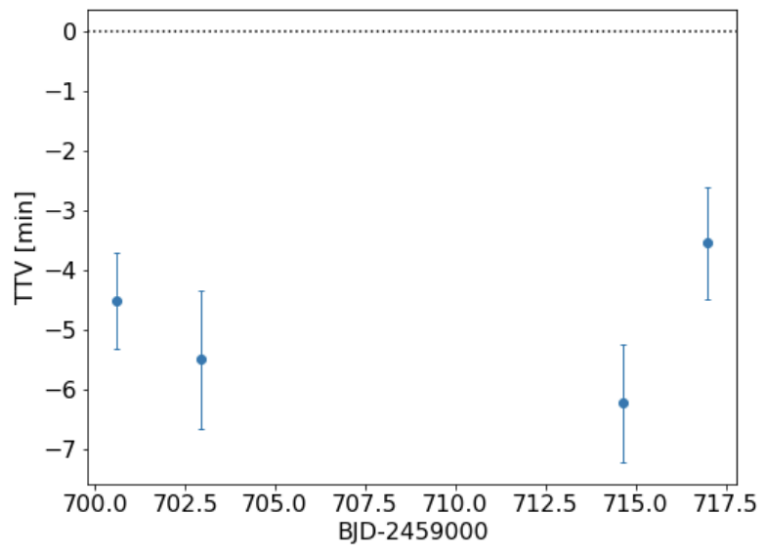
Figure D.4: TTV plot for WASP-24b. The reference ephemeris used to calculate the TTV was 2454945.58944 ± 0.00009 in BJD [Turner et al., 2017].
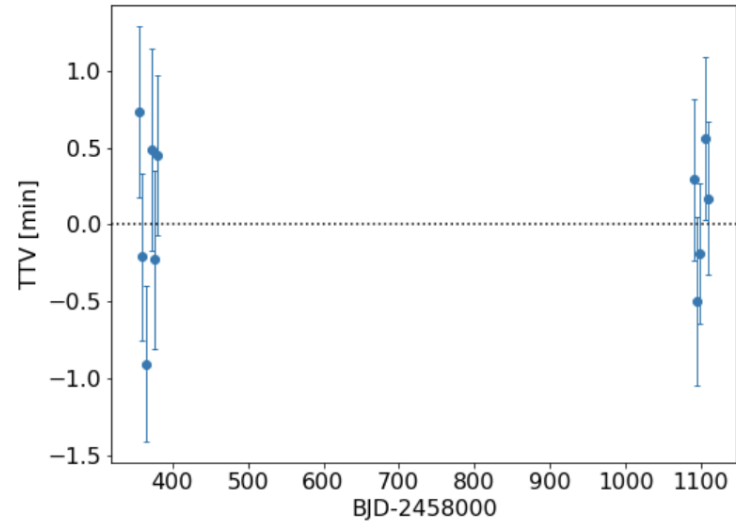
Figure D.5: TTV plot for WASP-29b using 2458356.41487 ± 0.00003 in BJD as the ephemeris from Saha and Sengupta [2021].

Bibliography

Nuno C. Santos, Susana C. C. Barros, Olivier D. S. Demangeon, and João P. Faria. Detection and Characterization Methods of Exoplanets, August 2020. URL https://doi.org/10.1093/acrefore/9780190647926.013.189. ISBN: 9780190647926.

Alapini Odunlade and Aude Ekundayo Pauline. Transiting exoplanets: characterisation in the presence of stellar activity. March 2010. URL https://ore.exeter.ac.uk/repository/handle/10036/104834. Accepted: 2010-06-15T08:00:33Z Publisher: University of Exeter.

P. F. L. Maxted. Comparison of the power-2 limb-darkening law from the STAGGER-grid to *Kepler* light curves of transiting exoplanets. *Astronomy & Astrophysics*, 616: A39, August 2018. ISSN 0004-6361, 1432-0746. doi: 10.1051/0004-6361/201832944. URL https://www.aanda.org/10.1051/0004-6361/201832944.

Keivan G. Stassun, Karen A. Collins, and B. Scott Gaudi. Accurate Empirical Radii and Masses of Planets and Their Host Stars with Gaia Parallaxes. *The Astronomical Journal*, 153:136, March 2017. ISSN 0004-6256. doi: 10.3847/1538-3881/aa5df3. URL https://ui.adsabs.harvard.edu/abs/2017AJ....153..136S. ADS Bibcode: 2017AJ....153..136S.

D. Pollacco, I. Skillen, A. Collier Cameron, B. Loeillet, H. C. Stempels, F. Bouchy, N. P. Gibson, L. Hebb, G. Hebrard, Y. C. Joshi, I. McDonald, B. Smalley, A. M. S. Smith, R. A. Street, S. Udry, R. G. West, D. M. Wilson, P. J. Wheatley, S. Aigrain, C. R. Benn, V. A. Bruce, D. J. Christian, W. I. Clarkson, B. Enoch, A. Evans, A. Fitzsimmons, C. A. Haswell, C. Hellier, S. Hickey, S. T. Hodgkin, K. Horne, M. Hrudkova, J. Irwin, S. R. Kane, F. P. Keenan, T. A. Lister, P. Maxted, M. Mayor, C. Moutou, A. J. Norton, J. P. Osborne, N. Parley, F. Pont, D. Queloz, R. Ryans, and E. Simpson. WASP-3b: a strongly-irradiated transiting gas-giant planet. *Monthly Notices of the Royal Astronomical Society*, 385(3):1576–1584, April 2008. ISSN 0035-

8711, 1365-2966. doi: 10.1111/j.1365-2966.2008.12939.x. URL http://arxiv.org/abs/0711.0126. arXiv:0711.0126 [astro-ph].

Y. C. Joshi, D. Pollacco, A. Collier Cameron, I. Skillen, E. Simpson, I. Steele, R. A. Street, H. C. Stempels, D. J. Christian, L. Hebb, F. Bouchy, N. P. Gibson, G. Hébrard, F. P. Keenan, B. Loeillet, J. Meaburn, C. Moutou, B. Smalley, I. Todd, R. G. West, D. R. Anderson, S. Bentley, B. Enoch, C. A. Haswell, C. Hellier, K. Horne, J. Irwin, T. A. Lister, I. McDonald, P. Maxted, M. Mayor, A. J. Norton, N. Parley, C. Perrier, F. Pont, D. Queloz, R. Ryans, A. M. S. Smith, S. Udry, P. J. Wheatley, and D. M. Wilson. WASP-14b: 7.3 MJ transiting planet in an eccentric orbit. *Monthly Notices of the Royal Astronomical Society*, 392(4):1532–1538, February 2009. ISSN 0035-8711. doi: 10.1111/j.1365-2966.2008.14178.x. URL https://doi.org/10.1111/j.1365-2966.2008.14178.x.

T. A. Lister, D. R. Anderson, M. Gillon, L. Hebb, B. S. Smalley, A. H. M. J. Triaud, A. Collier Cameron, D. M. Wilson, R. G. West, S. J. Bentley, D. J. Christian, R. Enoch, C. A. Haswell, C. Hellier, K. Horne, J. Irwin, Y. C. Joshi, S. R. Kane, M. Mayor, P. F. L. Maxted, A. J. Norton, N. Parley, F. Pepe, D. Pollacco, D. Queloz, R. Ryans, D. Segransan, I. Skillen, R. A. Street, I. Todd, S. Udry, and P. J. Wheatley. WASP-16b: A new Jupiter-like planet transiting a southern solar analog. *The Astrophysical Journal*, 703(1):752–756, September 2009. ISSN 0004-637X, 1538-4357. doi: 10.1088/0004-637X/703/1/752. URL http://arxiv.org/abs/0908.0297. arXiv:0908.0297 [astro-ph].

R. A. Street, E. Simpson, S. C. C. Barros, D. Pollacco, Y. Joshi, I. Todd, A. Collier Cameron, B. Enoch, N. Parley, E. Stempels, L. Hebb, A. H. M. J. Triaud, D. Queloz, D. Segransan, F. Pepe, S. Udry, T. A. Lister, É. Depagne, R. G. West, A. J. Norton, B. Smalley, C. Hellier, D. R. Anderson, P. F. L. Maxted, S. J. Bentley, I. Skillen, M. Gillon, P. Wheatley, J. Bento, P. Cathaway-Kjontvedt, and D. J. Christian. WASP-24 b: A New Transiting Close-in Hot Jupiter Orbiting a Late F-star. *The Astrophysical Journal*, 720:337–343, September 2010. ISSN 0004-637X.

doi: 10.1088/0004-637X/720/1/337. URL https://ui.adsabs.harvard.edu/abs/2010ApJ...720..337S. ADS Bibcode: 2010ApJ...720..337S.

Coel Hellier, D. R. Anderson, A. Collier Cameron, M. Gillon, M. Lendl, P. F. L. Maxted, D. Queloz, B. Smalley, A. H. M. J. Triaud, R. G. West, D. J. A. Brown, B. Enoch, T. A. Lister, F. Pepe, D. Pollacco, D. Ségransan, and S. Udry. WASP-29b: A Saturn-sized Transiting Exoplanet. *The Astrophysical Journal*, 723: L60–L63, November 2010. ISSN 0004-637X. doi: 10.1088/2041-8205/723/1/L60. URL https://ui.adsabs.harvard.edu/abs/2010ApJ...723L..60H. ADS Bibcode: 2010ApJ...723L..60H.

Coel Hellier, D. R. Anderson, A. Collier Cameron, L. Delrez, M. Gillon, E. Jehin, M. Lendl, P. F. L. Maxted, F. Pepe, D. Pollacco, D. Queloz, D. Ségransan, B. Smalley, A. M. S. Smith, J. Southworth, A. H. M. J. Triaud, O. D. Turner, S. Udry, and R. G. West. Three WASP-South Transiting Exoplanets: WASP-74b, WASP-83b, and WASP-89b. *The Astronomical Journal*, 150:18, July 2015. ISSN 0004-6256. doi: 10.1088/0004-6256/150/1/18. URL https://ui.adsabs.harvard.edu/abs/2015AJ....150...18H. ADS Bibcode: 2015AJ....150...18H.

Ian Wong, Daniel Kitzmann, Avi Shporer, Kevin Heng, Tara Fetherolf, Björn Benneke, Tansu Daylan, Stephen R. Kane, Roland Vanderspek, Sara Seager, Joshua N. Winn, Jon M. Jenkins, and Eric B. Ting. Visible-light Phase Curves from the Second Year of the TESS Primary Mission. *The Astronomical Journal*, 162:127, October 2021. ISSN 0004-6256. doi: 10.3847/1538-3881/ac0c7d. URL https://ui.adsabs.harvard.edu/abs/2021AJ....162..127W. ADS Bibcode: 2021AJ....162..127W.

Ö. Baştürk, E. M. Esmer, S. Yalçınkaya, Ş. Torun, L. Mancini, F. Helweh, E. Karamanlı, J. Southworth, S. Aliş, A. Wünsche, F. Tezcan, Y. Aladağ, N. Aksaker, E. Tunç, F. Davoudi, S. Fişek, M. Bretton, D. F. Evans, C. Yeşilyaprak, M. Yılmaz, C. T. Tezcan, and K. Yelkenci. Homogeneous transit timing analyses of 10 exoplanet systems. *Monthly Notices of the Royal Astronomical Society*, 512:2062–2081, May 2022. ISSN 0035-8711. doi: 10.1093/mnras/stac592. URL https:

//ui.adsabs.harvard.edu/abs/2022MNRAS.512.2062B. ADS Bibcode: 2022MN-RAS.512.2062B.

John Southworth, L. Mancini, P. Browne, M. Burgdorf, S. Calchi Novati, M. Dominik, T. Gerner, T. C. Hinse, U. G. Jørgensen, N. Kains, D. Ricci, S. Schäfer, F. Schönebeck, J. Tregloan-Reed, K. A. Alsubai, V. Bozza, G. Chen, P. Dodds, S. Dreizler, X. S. Fang, F. Finet, S. H. Gu, S. Hardis, K. Harpsøe, Th. Henning, M. Hundertmark, J. Jessen-Hansen, E. Kerins, H. Kjeldsen, C. Liebig, M. N. Lund, M. Lundkvist, M. Mathiasen, N. Nikolov, M. T. Penny, S. Proft, S. Rahvar, K. Sahu, G. Scarpetta, J. Skottfelt, C. Snodgrass, J. Surdej, and O. Wertz. High-precision photometry by telescope defocusing - V. WASP-15 and WASP-16. *Monthly Notices of the Royal Astronomical Society*, 434:1300–1308, September 2013. ISSN 0035-8711. doi: 10.1093/mnras/stt1089. URL https://ui.adsabs.harvard.edu/abs/2013MNRAS.434.1300S. ADS Bibcode: 2013MNRAS.434.1300S.

Jake D. Turner, Robin M. Leiter, Lauren I. Biddle, Kyle A. Pearson, Kevin K. Hardegree-Ullman, Robert M. Thompson, Johanna K. Teske, Ian T. Cates, Kendall L. Cook, Michael P. Berube, Megan N. Nieberding, Christen K. Jones, Brandon Raphael, Spencer Wallace, Zachary T. Watson, and Robert E. Johnson. Investigating the physical properties of transiting hot Jupiters with the 1.5-m Kuiper Telescope. *Monthly Notices of the Royal Astronomical Society*, 472:3871–3886, December 2017. ISSN 0035-8711. doi: 10.1093/mnras/stx2221. URL https://ui.adsabs.harvard.edu/abs/2017MNRAS.472.3871T. ADS Bibcode: 2017MN-RAS.472.3871T.

Suman Saha and Sujan Sengupta. Critical Analysis of TESS Transit Photometric Data: Improved Physical Properties for Five Exoplanets. *The Astronomical Journal*, 162(5):221, November 2021. ISSN 0004-6256, 1538-3881. doi: 10.3847/1538-3881/ac294d. URL http://arxiv.org/abs/2109.11366. arXiv: 2109.11366.

L. Mancini, J. Southworth, P. Mollière, J. Tregloan-Reed, I. G. Juvan, G. Chen, P. Sarkis, I. Bruni, S. Ciceri, M. I. Andersen, V. Bozza, D. M. Bramich, M. Burgdorf,

G. D'Ago, M. Dominik, D. F. Evans, R. Figuera Jaimes, L. Fossati, Th Henning, T. C. Hinse, M. Hundertmark, U. G. Jørgensen, E. Kerins, H. Korhonen, M. Küffmeier, P. Longa, N. Peixinho, A. Popovas, M. Rabus, S. Rahvar, J. Skottfelt, C. Snodgrass, R. Tronsgaard, Y. Wang, and O. Wertz. Physical properties and transmission spectrum of the WASP-74 planetary system from multiband photometry. *Monthly Notices of the Royal Astronomical Society*, 485:5168–5179, June 2019. ISSN 0035-8711. doi: 10.1093/mnras/stz661. URL https://ui.adsabs.harvard.edu/abs/2019MNRAS.485.5168M. ADS Bibcode: 2019MNRAS.485.5168M.

John W. Rostron, Peter J. Wheatley, David R. Anderson, Andrew Collier Cameron, Jonathan J. Fortney, Joseph Harrington, Heather A. Knutson, and Don L. Pollacco. The thermal emission of the exoplanet WASP-3b. *Monthly Notices of the Royal Astronomical Society*, 441:3666–3678, July 2014. ISSN 0035-8711. doi: 10.1093/mnras/stu814. URL https://ui.adsabs.harvard.edu/abs/2014MNRAS.441.3666R. ADS Bibcode: 2014MNRAS.441.3666R.

Ian Wong, Heather A. Knutson, Nikole K. Lewis, Tiffany Kataria, Adam Burrows, Jonathan J. Fortney, Joel Schwartz, Eric Agol, Nicolas B. Cowan, Drake Deming, Jean-Michel Désert, Benjamin J. Fulton, Andrew W. Howard, Jonathan Langton, Gregory Laughlin, Adam P. Showman, and Kamen Todorov. 3.6 and 4.5 m Phase Curves of the Highly Irradiated Eccentric Hot Jupiter WASP-14b. *The Astrophysical Journal*, 811:122, October 2015. ISSN 0004-637X. doi: 10.1088/0004-637X/811/2/122. URL https://ui.adsabs.harvard.edu/abs/2015ApJ...811..122W. ADS Bibcode: 2015ApJ...811..122W.

John Southworth, T. C. Hinse, M. Burgdorf, S. Calchi Novati, M. Dominik, P. Galianni, T. Gerner, E. Giannini, S. H. Gu, M. Hundertmark, U. G. Jørgensen, D. Juncher, E. Kerins, L. Mancini, M. Rabus, D. Ricci, S. Schäfer, J. Skottfelt, J. Tregloan-Reed, X. B. Wang, O. Wertz, K. A. Alsubai, J. M. Andersen, V. Bozza, D. M. Bramich, P. Browne, S. Ciceri, G. D'Ago, Y. Damerdji, C. Diehl, P. Dodds, A. Elyiv, X. S.

Fang, F. Finet, R. Figuera Jaimes, S. Hardis, K. Harpsøe, J. Jessen-Hansen, N. Kains, H. Kjeldsen, H. Korhonen, C. Liebig, M. N. Lund, M. Lundkvist, M. Mathiasen, M. T. Penny, A. Popovas, S. Prof., S. Rahvar, K. Sahu, G. Scarpetta, R. W. Schmidt, F. Schönebeck, C. Snodgrass, R. A. Street, J. Surdej, Y. Tsapras, and C. Vilela. High-precision photometry by telescope defocussing - VI. WASP-24, WASP-25 and WASP-26. *Monthly Notices of the Royal Astronomical Society*, 444:776–789, October 2014. ISSN 0035-8711. doi: 10.1093/mnras/stu1492. URL https://ui.adsabs. harvard.edu/abs/2014MNRAS.444..776S. ADS Bibcode: 2014MNRAS.444..776S.

N. P. Gibson, S. Aigrain, J. K. Barstow, T. M. Evans, L. N. Fletcher, and P. G. J. Irwin. A Gemini ground-based transmission spectrum of WASP-29b: a featureless spectrum from 515 to 720 nm. *Monthly Notices of the Royal Astronomical Society*, 428:3680–3692, February 2013. ISSN 0035-8711. doi: 10.1093/mnras/sts307. URL https://ui.adsabs.harvard.edu/abs/2013MNRAS.428.3680G. ADS Bibcode: 2013MNRAS.428.3680G.

A. Wolszczan and D. A. Frail. A planetary system around the millisecond pulsar PSR1257 + 12. *Nature*, 355(6356):145–147, January 1992. ISSN 1476-4687. doi: 10.1038/355145a0. URL https://www.nature.com/articles/355145a0. Number: 6356 Publisher: Nature Publishing Group.

Michel Mayor and Didier Queloz. A Jupiter-mass companion to a solar-type star. *Nature*, 378(6555):355–359, November 1995. ISSN 1476-4687. doi: 10.1038/378355a0. URL https://www.nature.com/articles/378355a0. Number: 6555 Publisher: Nature Publishing Group.

William Borucki, David Koch, Natalie Batalha, Douglas Caldwell, Jorgen Christensen-Dalsgaard, William D. Cochran, Edward Dunham, Thomas N. Gautier, John Geary, Ronald Gilliland, Jon Jenkins, Hans Kjeldsen, Jack J. Lissauer, and Jason Rowe. KE-PLER: Search for Earth-Size Planets in the Habitable Zone. 253:289–299, February 2009. doi: 10.1017/S1743921308026513. URL https://ui.adsabs.harvard.edu/

abs/2009IAUS..253..289B. Conference Name: Transiting Planets ADS Bibcode: 2009IAUS..253..289B.

George R. Ricker, Joshua N. Winn, Roland Vanderspek, David W. Latham, Gáspár Á. Bakos, Jacob L. Bean, Zachory K. Berta-Thompson, Timothy M. Brown, Lars Buchhave, Nathaniel R. Butler, R. Paul Butler, William J. Chaplin, David Charbonneau, Jørgen Christensen-Dalsgaard, Mark Clampin, Drake Deming, John Doty, Nathan De Lee, Courtney Dressing, Edward W. Dunham, Michael Endl, Francois Fressin, Jian Ge, Thomas Henning, Matthew J. Holman, Andrew W. Howard, Shigeru Ida, Jon M. Jenkins, Garrett Jernigan, John Asher Johnson, Lisa Kaltenegger, Nobuyuki Kawai, Hans Kjeldsen, Gregory Laughlin, Alan M. Levine, Douglas Lin, Jack J. Lissauer, Phillip MacQueen, Geoffrey Marcy, Peter R. McCullough, Timothy D. Morton, Norio Narita, Martin Paegert, Enric Palle, Francesco Pepe, Joshua Pepper, Andreas Quirrenbach, Stephen A. Rinehart, Dimitar Sasselov, Bun'ei Sato, Sara Seager, Alessandro Sozzetti, Keivan G. Stassun, Peter Sullivan, Andrew Szentgyorgyi, Guillermo Torres, Stephane Udry, and Joel Villasenor. Transiting Exoplanet Survey Satellite (TESS). *Journal of Astronomical Telescopes, Instruments, and Systems*, 1:014003, January 2015. doi: 10.1117/1.JATIS.1.1.014003. URL https://ui.adsabs.harvard.edu/abs/2015JATIS...1a4003R. ADS Bibcode: 2015JATIS...1a4003R.

E. Gaidos, D. Kitzmann, and K. Heng. Exoplanet characterization by multi-observatory transit photometry with TESS and CHEOPS. *Monthly Notices of the Royal Astronomical Society*, 468:3418–3427, July 2017. ISSN 0035-8711. doi: 10.1093/mnras/stx615. URL https://ui.adsabs.harvard.edu/abs/2017MNRAS.468.3418G. ADS Bibcode: 2017MNRAS.468.3418G.

W. Benz, C. Broeg, A. Fortier, N. Rando, T. Beck, M. Beck, D. Queloz, D. Ehrenreich, P. F. L. Maxted, K. G. Isaak, N. Billot, Y. Alibert, R. Alonso, C. António, J. Asquier, T. Bandy, T. Bárczy, D. Barrado, S. C. C. Barros, W. Baumjohann, A. Bekkelien, M. Bergomi, F. Biondi, X. Bonfils, L. Borsato, A. Brandeker, M. D.

Busch, J. Cabrera, V. Cessa, S. Charnoz, B. Chazelas, A. Collier Cameron, C. Corral Van Damme, D. Cortes, M. B. Davies, M. Deleuil, A. Deline, L. Delrez, O. Demangeon, B. O. Demory, A. Erikson, J. Farinato, L. Fossati, M. Fridlund, D. Futyan, D. Gandolfi, A. Garcia Munoz, M. Gillon, P. Guterman, A. Gutierrez, J. Hasiba, K. Heng, E. Hernandez, S. Hoyer, L. L. Kiss, Z. Kovacs, T. Kuntzer, J. Laskar, A. Lecavelier des Etangs, M. Lendl, A. López, I. Lora, C. Lovis, T. Lüftinger, D. Magrin, L. Malvasio, L. Marafatto, H. Michaelis, D. de Miguel, D. Modrego, M. Munari, V. Nascimbeni, G. Olofsson, H. Ottacher, R. Ottensamer, I. Pagano, R. Palacios, E. Pallé, G. Peter, D. Piazza, G. Piotto, A. Pizarro, D. Pollaco, R. Ragazzoni, F. Ratti, H. Rauer, I. Ribas, M. Rieder, R. Rohlfs, F. Safa, M. Salatti, N. C. Santos, G. Scandariato, D. Ségransan, A. E. Simon, A. M. S. Smith, M. Sordet, S. G. Sousa, M. Steller, G. M. Szabó, J. Szoke, N. Thomas, M. Tschentscher, S. Udry, V. Van Grootel, V. Viotto, I. Walter, N. A. Walton, F. Wildi, and D. Wolter. The CHEOPS mission. *Experimental Astronomy*, 51:109–151, February 2021. ISSN 0922-6435. doi: 10.1007/s10686-020-09679-4. URL https://ui.adsabs.harvard.edu/abs/2021ExA....51..109B. ADS Bibcode: 2021ExA....51..109B.

C. Broeg, W. Benz, N. Thomas, and Cheops Team. The CHEOPS mission. *Contributions of the Astronomical Observatory Skalnate Pleso*, 43:498–498, March 2014. ISSN 0583-466X. URL https://ui.adsabs.harvard.edu/abs/2014CoSka..43..498B. ADS Bibcode: 2014CoSka..43..498B.

Willy Benz, David Ehrenreich, and Kate Isaak. *CHEOPS: CHaracterizing ExOPlanets Satellite*. January 2018. doi: 10.1007/978-3-319-55333-7_84. URL https://ui.adsabs.harvard.edu/abs/2018haex.bookE..84B. Pages: 84 Publication Title: Handbook of Exoplanets ADS Bibcode: 2018haex.bookE..84B.

Z. Garai, T. Pribulla, J. Kovács, Gy M. Szabó, A. Claret, R. Komžík, and E. Kundra. Rapidly rotating stars and their transiting planets: KELT-17b, KELT-19Ab, and KELT-21b in the CHEOPS and TESS era. *Monthly Notices of the Royal Astronomical Society*, 513:2822–2840, June 2022. ISSN 0035-8711. doi: 10.

1093/mnras/stac1095.   URL https://ui.adsabs.harvard.edu/abs/2022MNRAS.
513.2822G. ADS Bibcode: 2022MNRAS.513.2822G.

Dominic Oddo, Diana Dragomir, Alexis Brandeker, Hugh P. Osborn, Karen Collins,
Keivan Stassun, Nicola Astudillo-Defru, Allyson Bieryla, Steve B. Howell, David R.
Ciardi, Samuel Quinn, Jose M. Almenara, Cesar Briceno, Kevin I. Collins, Kni-
cole D. Colon, Dennis M. Conti, Nicolas Crouzet, Elise Furlan, Tianjun Gan, Crys-
tal L. Gnilka, Robert F. Goeke, Erica Gonzales, Mallory Harris, Jon M. Jenkins,
Eric L. N. Jensen, David Latham, Nicholas Law, Michael B. Lund, Andrew W.
Mann, Bob Massey, Felipe Murgas, George Ricker, Howard M. Relles, Pamela Row-
den, Richard P. Schwarz, Joshua Schlieder, Avi Shporer, Sara Seager, Gregor Srdoc,
Guillermo Torres, Joseph D. Twicken, Roland Vanderspek, Joshua N. Winn, and
Carl Ziegler. Characterization of a set of small planets with TESS and CHEOPS
and an analysis of photometric performance. *The Astronomical Journal*, 165(3):134,
March 2023. ISSN 0004-6256, 1538-3881. doi: 10.3847/1538-3881/acb4e3. URL
http://arxiv.org/abs/2301.08162. arXiv:2301.08162 [astro-ph].

M. Lendl, Sz. Csizmadia, A. Deline, L. Fossati, D. Kitzmann, K. Heng, S. Hoyer,
S. Salmon, W. Benz, C. Broeg, D. Ehrenreich, A. Fortier, D. Queloz, A. Bonfanti,
A. Brandeker, A. Collier Cameron, L. Delrez, A. Garcia Muñoz, M. J. Hooton,
P. F. L. Maxted, B. M. Morris, V. Van Grootel, T. G. Wilson, Y. Alibert, R. Alonso,
J. Asquier, T. Bandy, T. Bárczy, D. Barrado, S. C. C. Barros, W. Baumjohann,
M. Beck, T. Beck, A. Bekkelien, M. Bergomi, N. Billot, F. Biondi, X. Bonfils,
V. Bourrier, M. D. Busch, J. Cabrera, V. Cessa, S. Charnoz, B. Chazelas, C. Cor-
ral Van Damme, M. B. Davies, M. Deleuil, O. D. S. Demangeon, B. O. Demory,
A. Erikson, J. Farinato, M. Fridlund, D. Futyan, D. Gandolfi, M. Gillon, P. Guter-
man, J. Hasiba, E. Hernandez, K. G. Isaak, L. Kiss, T. Kuntzer, A. Lecavelier des
Etangs, T. Lüftinger, J. Laskar, C. Lovis, D. Magrin, L. Malvasio, L. Marafatto,
H. Michaelis, M. Munari, V. Nascimbeni, G. Olofsson, H. Ottacher, R. Ottensamer,
I. Pagano, E. Pallé, G. Peter, D. Piazza, G. Piotto, D. Pollacco, F. Ratti, H. Rauer,
R. Ragazzoni, N. Rando, I. Ribas, M. Rieder, R. Rohlfs, F. Safa, N. C. Santos,

G. Scandariato, D. Ségransan, A. E. Simon, V. Singh, A. M. S. Smith, M. Sordet, S. G. Sousa, M. Steller, Gy. M. Szabó, N. Thomas, M. Tschentscher, S. Udry, V. Viotto, I. Walter, N. A. Walton, F. Wildi, and D. Wolter. The hot dayside and asymmetric transit of WASP-189 b seen by CHEOPS. *Astronomy and Astrophysics*, 643:A94, November 2020. ISSN 0004-6361. doi: 10.1051/0004-6361/202038677. URL https://ui.adsabs.harvard.edu/abs/2020A&A...643A..94L. ADS Bibcode: 2020A&A...643A..94L.

Thomas G. Wilson, Elisa Goffo, Yann Alibert, Davide Gandolfi, Andrea Bonfanti, Carina M. Persson, Andrew Collier Cameron, Malcolm Fridlund, Luca Fossati, Judith Korth, Willy Benz, Adrien Deline, Hans-Gustav Florén, Pascal Guterman, Vardan Adibekyan, Matthew J. Hooton, Sergio Hoyer, Adrien Leleu, Alexander James Mustill, Sébastien Salmon, Sérgio G. Sousa, Olga Suarez, Lyu Abe, Abdelkrim Agabi, Roi Alonso, Guillem Anglada, Joel Asquier, Tamas Bárczy, David Barrado Navascues, Susana C. C. Barros, Wolfgang Baumjohann, Mathias Beck, Thomas Beck, Nicolas Billot, Xavier Bonfils, Alexis Brandeker, Christopher Broeg, Edward M. Bryant, Matthew R. Burleigh, Marco Buttu, Juan Cabrera, Sébastien Charnoz, David R. Ciardi, Ryan Cloutier, William D. Cochran, Karen A. Collins, Knicole D. Colón, Nicolas Crouzet, Szilard Csizmadia, Melvyn B. Davies, Magali Deleuil, Laetitia Delrez, Olivier Demangeon, Brice-Olivier Demory, Diana Dragomir, Georgina Dransfield, David Ehrenreich, Anders Erikson, Andrea Fortier, Tianjun Gan, Samuel Gill, Michaël Gillon, Crystal L. Gnilka, Nolan Grieves, Sascha Grziwa, Manuel Güdel, Tristan Guillot, Jonas Haldemann, Kevin Heng, Keith Horne, Steve B. Howell, Kate G. Isaak, Jon M. Jenkins, Eric L. N. Jensen, Laszlo Kiss, Gaia Lacedelli, Kristine Lam, Jacques Laskar, David W. Latham, Alain Lecavelier des Etangs, Monika Lendl, Kathryn V. Lester, Alan M. Levine, John Livingston, Christophe Lovis, Rafael Luque, Demetrio Magrin, Wenceslas Marie-Sainte, Pierre F. L. Maxted, Andrew W. Mayo, Brian McLean, Marko Mecina, Djamel Mékarnia, Valerio Nascimbeni, Louise D. Nielsen, Göran Olofsson, Hugh P. Osborn, Hannah L. M. Osborne, Roland Ottensamer, Isabella Pagano, Enric Pallé,

Gisbert Peter, Giampaolo Piotto, Don Pollacco, Didier Queloz, Roberto Ragazzoni, Nicola Rando, Heike Rauer, Seth Redfield, Ignasi Ribas, George R. Ricker, Martin Rieder, Nuno C. Santos, Gaetano Scandariato, François-Xavier Schmider, Richard P. Schwarz, Nicholas J. Scott, Sara Seager, Damien Ségransan, Luisa Maria Serrano, Attila E. Simon, Alexis M. S. Smith, Manfred Steller, Chris Stockdale, Gyula Szabó, Nicolas Thomas, Eric B. Ting, Amaury H. M. J. Triaud, Stéphane Udry, Vincent Van Eylen, Valérie Van Grootel, Roland K. Vanderspek, Valentina Viotto, Nicholas Walton, and Joshua N. Winn. A pair of sub-Neptunes transiting the bright K-dwarf TOI-1064 characterized with CHEOPS. *Monthly Notices of the Royal Astronomical Society*, 511:1043–1071, March 2022. ISSN 0035-8711. doi: 10.1093/mnras/stab3799. URL https://ui.adsabs.harvard.edu/abs/2022MNRAS.511.1043W. ADS Bibcode: 2022MNRAS.511.1043W.

D. K. Sing, F. Pont, S. Aigrain, D. Charbonneau, J. M. Désert, N. Gibson, R. Gilliland, W. Hayek, G. Henry, H. Knutson, A. Lecavelier Des Etangs, T. Mazeh, and A. Shporer. Hubble Space Telescope transmission spectroscopy of the exoplanet HD 189733b: high-altitude atmospheric haze in the optical and near-ultraviolet with STIS. *Monthly Notices of the Royal Astronomical Society*, 416:1443–1455, September 2011. ISSN 0035-8711. doi: 10.1111/j.1365-2966.2011.19142.x. URL https://ui.adsabs.harvard.edu/abs/2011MNRAS.416.1443S. ADS Bibcode: 2011MNRAS.416.1443S.

George R. Ricker, Joshua N. Winn, Roland Vanderspek, David W. Latham, Gáspár Á Bakos, Jacob L. Bean, Zachory K. Berta-Thompson, Timothy M. Brown, Lars Buchhave, Nathaniel R. Butler, R. Paul Butler, William J. Chaplin, David B. Charbonneau, Jørgen Christensen-Dalsgaard, Mark Clampin, Drake Deming, John P. Doty, Nathan De Lee, Courtney Dressing, Edward W. Dunham, Michael Endl, François Fressin, Jian Ge, Thomas Henning, Matthew J. Holman, Andrew W. Howard, Shigeru Ida, Jon M. Jenkins, Garrett Jernigan, John Asher Johnson, Lisa Kaltenegger, Nobuyuki Kawai, Hans Kjeldsen, Gregory Laughlin, Alan M. Levine, Douglas Lin, Jack J. Lissauer, Phillip MacQueen, Geoffrey Marcy, Peter R. McCul-

lough, Timothy D. Morton, Norio Narita, Martin Paegert, Enric Palle, Francesco Pepe, Joshua Pepper, Andreas Quirrenbach, Stephen A. Rinehart, Dimitar Sasselov, Bun'ei Sato, Sara Seager, Alessandro Sozzetti, Keivan G. Stassun, Peter Sullivan, Andrew Szentgyorgyi, Guillermo Torres, Stephane Udry, and Joel Villasenor. Transiting Exoplanet Survey Satellite. *Journal of Astronomical Telescopes, Instruments, and Systems*, 1(1):014003, October 2014. ISSN 2329-4124, 2329-4221. doi: 10.1117/1.JATIS.1.1.014003. URL https://www.spiedigitallibrary.org/journals/Journal-of-Astronomical-Telescopes-Instruments-and-Systems/volume-1/issue-1/014003/Transiting-Exoplanet-Survey-Satellite/10.1117/1.JATIS.1.1.014003.full. Publisher: SPIE.

A. Deline, D. Queloz, B. Chazelas, M. Sordet, F. Wildi, A. Fortier, C. Broeg, D. Futyan, and W. Benz. Expected performances of the Characterising Exoplanet Satellite (CHEOPS). I. Photometric performances from ground-based calibration. *Astronomy and Astrophysics*, 635:A22, March 2020. ISSN 0004-6361. doi: 10.1051/0004-6361/201935977. URL https://ui.adsabs.harvard.edu/abs/2020A&A...635A..22D. ADS Bibcode: 2020A&A...635A..22D.

Penny D. Sackett. Searching for Unseen Planets Via Occultation and Microlensing. In J.-M. Mariotti and D. Alloin, editors, *Planets Outside the Solar System: Theory and Observations*, NATO Science Series, pages 189–228. Springer Netherlands, Dordrecht, 1999. ISBN 978-94-011-4623-4. doi: 10.1007/978-94-011-4623-4_14. URL https://doi.org/10.1007/978-94-011-4623-4_14.

Jason T. Wright and B. Scott Gaudi. *Exoplanet Detection Methods*. January 2013. doi: 10.1007/978-94-007-5606-9_10. URL https://ui.adsabs.harvard.edu/abs/2013pss3.book..489W. Pages: 489 Publication Title: Planets, Stars and Stellar Systems. Volume 3: Solar and Stellar Planetary Systems ADS Bibcode: 2013pss3.book..489W.

Joshua N. Winn and Daniel C. Fabrycky. The Occurrence and Architecture of Exoplanetary Systems. *Annual Review of Astronomy and Astrophysics*, 53(1):409–447, Au-

gust 2015. ISSN 0066-4146, 1545-4282. doi: 10.1146/annurev-astro-082214-122246. URL http://arxiv.org/abs/1410.4199. arXiv:1410.4199 [astro-ph].

Joshua A. Carter, Jennifer C. Yee, Jason Eastman, B. Scott Gaudi, and Joshua N. Winn. Analytic Approximations for Transit Light-Curve Observables, Uncertainties, and Covariances. *The Astrophysical Journal*, 689:499–512, December 2008. ISSN 0004-637X. doi: 10.1086/592321. URL https://ui.adsabs.harvard.edu/abs/2008ApJ...689..499C. ADS Bibcode: 2008ApJ...689..499C.

Natalia M. Guerrero, S. Seager, Chelsea X. Huang, Andrew Vanderburg, Aylin Garcia Soto, Ismael Mireles, Katharine Hesse, William Fong, Ana Glidden, Avi Shporer, David W. Latham, Karen A. Collins, Samuel N. Quinn, Jennifer Burt, Diana Dragomir, Ian Crossfield, Roland Vanderspek, Michael Fausnaugh, Christopher J. Burke, George Ricker, Tansu Daylan, Zahra Essack, Maximilian N. Günther, Hugh P. Osborn, Joshua Pepper, Pamela Rowden, Lizhou Sha, Steven Villanueva Jr., Daniel A. Yahalomi, Liang Yu, Sarah Ballard, Natalie M. Batalha, David Berardo, Ashley Chontos, Jason A. Dittmann, Gilbert A. Esquerdo, Thomas Mikal-Evans, Rahul Jayaraman, Akshata Krishnamurthy, Dana R. Louie, Nicholas Mehrle, Prajwal Niraula, Benjamin V. Rackham, Joseph E. Rodriguez, Stephen J. L. Rowden, Clara Sousa-Silva, David Watanabe, Ian Wong, Zhuchang Zhan, Goran Zivanovic, Jessie L. Christiansen, David R. Ciardi, Melanie A. Swain, Michael B. Lund, Susan E. Mullally, Scott W. Fleming, David R. Rodriguez, Patricia T. Boyd, Elisa V. Quintana, Thomas Barclay, Knicole D. Colón, S. A. Rinehart, Joshua E. Schlieder, Mark Clampin, Jon M. Jenkins, Joseph D. Twicken, Douglas A. Caldwell, Jeffrey L. Coughlin, Chris Henze, Jack J. Lissauer, Robert L. Morris, Mark E. Rose, Jeffrey C. Smith, Peter Tenenbaum, Eric B. Ting, Bill Wohler, G. Á Bakos, Jacob L. Bean, Zachory K. Berta-Thompson, Allyson Bieryla, Luke G. Bouma, Lars A. Buchhave, Nathaniel Butler, David Charbonneau, John P. Doty, Jian Ge, Matthew J. Holman, Andrew W. Howard, Lisa Kaltenegger, Stephen R. Kane, Hans Kjeldsen, Laura Kreidberg, Douglas N. C. Lin, Charlotte Minsky, Norio Narita, Martin Paegert, András Pál, Enric Palle, Dimitar D. Sasselov, Alton Spencer, Alessandro Sozzetti,

Keivan G. Stassun, Guillermo Torres, Stephane Udry, and Joshua N. Winn. The TESS Objects of Interest Catalog from the TESS Prime Mission, March 2021. URL http://arxiv.org/abs/2103.12538. arXiv:2103.12538 [astro-ph].

Thomas Barclay, Joshua Pepper, and Elisa V. Quintana. A Revised Exoplanet Yield from the Transiting Exoplanet Survey Satellite (TESS). *The Astrophysical Journal Supplement Series*, 239(1):2, October 2018. ISSN 1538-4365. doi: 10.3847/1538-4365/aae3e9. URL http://arxiv.org/abs/1804.05050. arXiv:1804.05050 [astro-ph].

T. Beck, L. Gambicorti, C. Broeg, V. Cessa, A. Fortier, D. Piazza, D. Ehrenreich, D. Magrin, J. Y. Plesseria, G. Peter, I. Pagano, M. Steller, Z. Kovacs, R. Ragazzoni, F. Wildi, and W. Benz. The CHEOPS (characterising exoplanet satellite) mission: telescope optical design, development status and main technical and programmatic challenges. In *International Conference on Space Optics — ICSO 2016*, volume 10562, pages 352–359. SPIE, September 2017a. doi: 10.1117/12.2296216. URL https://doi.org/10.1117/12.2296216.

Daniel Bayliss, Sean M. O'Brien, Edward Bryant, Peter Wheatley, Richard West, James McCormac, Paul Chote, Sam Gill, David R. Anderson, Adam Wise, Ines Juvan-Beaulieu, Colin Coates, Edward Gillen, Alexis M. S. Smith, James S. Jenkins, Maximiliano Moyano, Douglas R. Alves, Matthew R. Burleigh, Michael R. Goad, Sarah L. Casewell, Jack Acton, Rosanna L. Tilbrook, Beth A. Henderson, and Alicia Kendall. High precision ground-based CCD photometry from the Next Generation Transit Survey. 12191:121911A, August 2022. doi: 10.1117/12.2628966. URL https://ui.adsabs.harvard.edu/abs/2022SPIE12191E..1AB. Conference Name: X-Ray, Optical, and Infrared Detectors for Astronomy X ADS Bibcode: 2022SPIE12191E..1AB.

T. Beck, C. Broeg, D. Ehrenreich, G. Peter, D. Magrin, J.-Y. Plesseria, J. Szoke, F. Wildi, Virginie Cessa, W. Benz, A. Fortier, I. Pagano, M. Steller, N. Thomas, and R. Ragazzoni. CHEOPS: a space telescope for ultra-high precision photometry

of exoplanet transits. In Bruno Cugny, Zoran Sodnik, and Nikos Karafolas, editors, *International Conference on Space Optics — ICSO 2014*, page 104, Tenerife, Canary Islands, Spain, November 2017b. SPIE. ISBN 978-1-5106-1615-8 978-1-5106-1616-5. doi: 10.1117/12.2304164. URL https://doi.org/10.1117/12.2304164.

S. Hoyer, P. Guterman, O. Demangeon, S. G. Sousa, M. Deleuil, J. C. Meunier, and W. Benz. Expected performances of the Characterising Exoplanet Satellite (CHEOPS). III. Data reduction pipeline: architecture and simulated performances. *Astronomy and Astrophysics*, 635:A24, March 2020. ISSN 0004-6361. doi: 10.1051/0004-6361/201936325. URL https://ui.adsabs.harvard.edu/abs/2020A&A...635A..24H. ADS Bibcode: 2020A&A...635A..24H.

G. S. Da Costa. Basic Photometry Techniques. 23:90, January 1992. URL https://ui.adsabs.harvard.edu/abs/1992ASPC...23...90D. Conference Name: Astronomical CCD Observing and Reduction Techniques ADS Bibcode: 1992ASPC...23...90D.

K. J. Mighell. CCD Aperture Photometry. 189:50, January 1999. URL https://ui.adsabs.harvard.edu/abs/1999ASPC..189...50M. Conference Name: Precision CCD Photometry ADS Bibcode: 1999ASPC..189...50M.

P. F. L. Maxted, D. Ehrenreich, T. G. Wilson, Y. Alibert, A. Collier Cameron, S. Hoyer, S. G. Sousa, G. Olofsson, A. Bekkelien, A. Deline, L. Delrez, A. Bonfanti, L. Borsato, R. Alonso, G. Anglada Escudé, D. Barrado, S. C. C. Barros, W. Baumjohann, M. Beck, T. Beck, W. Benz, N. Billot, F. Biondi, X. Bonfils, A. Brandeker, C. Broeg, T. Bárczy, J. Cabrera, S. Charnoz, C. Corral Van Damme, Sz Csizmadia, M. B. Davies, M. Deleuil, O. D. S. Demangeon, B. O. Demory, A. Erikson, H. G. Florén, A. Fortier, L. Fossati, M. Fridlund, D. Futyan, D. Gandolfi, M. Gillon, M. Guedel, P. Guterman, K. Heng, K. G. Isaak, L. Kiss, J. Laskar, A. Lecavelier des Etangs, M. Lendl, C. Lovis, D. Magrin, V. Nascimbeni, R. Ottensamer, I. Pagano, E. Pallé, G. Peter, G. Piotto, D. Pollacco, F. J. Pozuelos, D. Queloz, R. Ragazzoni, N. Rando, H. Rauer, C. Reimers, I. Ribas, N. C. Santos, G. Scandariato, A. E. Simon, A. M. S. Smith, M. Steller, M. I. Swayne,

Gy M. Szabó, D. Ségransan, N. Thomas, S. Udry, V. Van Grootel, and N. A. Walton. Analysis of Early Science observations with the CHaracterising ExOPlanets Satellite (CHEOPS) using PYCHEOPS. *Monthly Notices of the Royal Astronomical Society*, November 2021. ISSN 0035-8711. doi: 10.1093/mnras/stab3371. URL https://ui.adsabs.harvard.edu/abs/2021MNRAS.tmp.3057M. ADS Bibcode: 2021MNRAS.tmp.3057M.

O. Barragán, D. J. Armstrong, D. Gandolfi, I. Carleo, A. A. Vidotto, C. Villarreal D'Angelo, A. Oklopčić, H. Isaacson, D. Oddo, K. Collins, M. Fridlund, S. G. Sousa, C. M. Persson, C. Hellier, S. Howell, A. Howard, S. Redfield, N. Eisner, I. Y. Georgieva, D. Dragomir, D. Bayliss, L. D. Nielsen, B. Klein, S. Aigrain, M. Zhang, J. Teske, J. D. Twicken, J. Jenkins, M. Esposito, V. Van Eylen, F. Rodler, V. Adibekyan, J. Alarcon, D. R. Anderson, J. M. Akana Murphy, D. Barrado, S. C. C. Barros, B. Benneke, F. Bouchy, E. M. Bryant, R. P. Butler, J. Burt, J. Cabrera, S. Casewell, P. Chaturvedi, R. Cloutier, W. D. Cochran, J. Crane, I. Crossfield, N. Crouzet, K. I. Collins, F. Dai, H. J. Deeg, A. Deline, O. D. S. Demangeon, X. Dumusque, P. Figueira, E. Furlan, C. Gnilka, M. R. Goad, E. Goffo, F. Gutiérrez-Canales, A. Hadjigeorghiou, Z. Hartman, A. P. Hatzes, M. Harris, B. Henderson, T. Hirano, S. Hojjatpanah, S. Hoyer, P. Kabáth, J. Korth, J. Lillo-Box, R. Luque, M. Marmier, T. Močnik, A. Muresan, F. Murgas, E. Nagel, H. L. M. Osborne, A. Osborn, H. P. Osborn, E. Palle, M. Raimbault, G. R. Ricker, R. A. Rubenzahl, C. Stockdale, N. C. Santos, N. Scott, R. P. Schwarz, S. Shectman, M. Raimbault, S. Seager, D. Ségransan, L. M. Serrano, M. Skarka, A. M. S. Smith, J. Šubjak, T. G. Tan, S. Udry, C. Watson, P. J. Wheatley, R. West, J. N. Winn, S. X. Wang, A. Wolfgang, and C. Ziegler. The young HD 73583 (TOI-560) planetary system: two 10-M mini-Neptunes transiting a 500-Myr-old, bright, and active K dwarf. *Monthly Notices of the Royal Astronomical Society*, 514:1606–1627, August 2022. ISSN 0035-8711. doi: 10.1093/mnras/stac638. URL https://ui.adsabs.harvard.edu/abs/2022MNRAS.514.1606B. ADS Bibcode: 2022MNRAS.514.1606B.

A. Bonfanti, L. Delrez, M. J. Hooton, T. G. Wilson, L. Fossati, Y. Alibert, S. Hoyer, A. J. Mustill, H. P. Osborn, V. Adibekyan, D. Gandolfi, S. Salmon, S. G. Sousa, A. Tuson, V. Van Grootel, J. Cabrera, V. Nascimbeni, P. F. L. Maxted, S. C. C. Barros, N. Billot, X. Bonfils, L. Borsato, C. Broeg, M. B. Davies, M. Deleuil, O. D. S. Demangeon, M. Fridlund, G. Lacedelli, M. Lendl, C. Persson, N. C. Santos, G. Scandariato, Gy. M. Szabó, A. Collier Cameron, S. Udry, W. Benz, M. Beck, D. Ehrenreich, A. Fortier, K. G. Isaak, D. Queloz, R. Alonso, J. Asquier, T. Bandy, T. Bárczy, D. Barrado, O. Barragán, W. Baumjohann, T. Beck, A. Bekkelien, M. Bergomi, A. Brandeker, M. D. Busch, V. Cessa, S. Charnoz, B. Chazelas, C. Corral Van Damme, B. O. Demory, A. Erikson, J. Farinato, D. Futyan, A. Garcia Muñoz, M. Gillon, M. Guedel, P. Guterman, J. Hasiba, K. Heng, E. Hernandez, L. Kiss, T. Kuntzer, J. Laskar, A. Lecavelier des Etangs, C. Lovis, D. Magrin, L. Malvasio, L. Marafatto, H. Michaelis, M. Munari, G. Olofsson, H. Ottacher, R. Ottensamer, I. Pagano, E. Pallé, G. Peter, D. Piazza, G. Piotto, D. Pollacco, R. Ragazzoni, N. Rando, F. Ratti, H. Rauer, I. Ribas, M. Rieder, R. Rohlfs, F. Safa, M. Salatti, D. Ségransan, A. E. Simon, A. M. S. Smith, M. Sordet, M. Steller, N. Thomas, M. Tschentscher, V. Van Eylen, V. Viotto, I. Walter, N. A. Walton, F. Wildi, and D. Wolter. CHEOPS observations of the HD 108236 planetary system: a fifth planet, improved ephemerides, and planetary radii. *Astronomy and Astrophysics*, 646:A157, February 2021. ISSN 0004-6361. doi: 10.1051/0004-6361/202039608. URL https://ui.adsabs.harvard.edu/abs/2021A&A...646A.157B. ADS Bibcode: 2021A&A...646A.157B.

Robert Lea. Europe's exoplanet-hunting CHEOPS mission extended through 2026, March 2023. URL https://www.space.com/esa-cheops-exoplanet-mission-extension-2026.

S. Seager and G. Mallén-Ornelas. A Unique Solution of Planet and Star Parameters from an Extrasolar Planet Transit Light Curve. *The Astrophysical Journal*, 585:1038–1055, March 2003. ISSN 0004-637X. doi: 10.1086/346105.

URL https://ui.adsabs.harvard.edu/abs/2003ApJ...585.1038S. ADS Bibcode: 2003ApJ...585.1038S.

B. Enoch, A. Collier Cameron, N. R. Parley, and L. Hebb. An Improved Method for Estimating the Masses of Stars with Transiting Planets. *Astronomy and Astrophysics*, 516:A33, June 2010. ISSN 0004-6361, 1432-0746. doi: 10.1051/0004-6361/201014326. URL http://arxiv.org/abs/1004.1991. arXiv:1004.1991 [astro-ph].

F. Bouchy. ELODIE metallicity-biased search for transiting Hot Jupiters - II. A very hot Jupiter transiting the bright K star HD 189733 | Astronomy & Astrophysics (A&A), 2005. URL https://www.aanda.org/articles/aa/abs/2005/46/aahi291/aahi291.html.

Guillermo Torres, Joshua N. Winn, and Matthew J. Holman. Improved Parameters for Extrasolar Transiting Planets. *The Astrophysical Journal*, 677:1324–1342, April 2008a. ISSN 0004-637X. doi: 10.1086/529429. URL https://ui.adsabs.harvard.edu/abs/2008ApJ...677.1324T. ADS Bibcode: 2008ApJ...677.1324T.

David M. Kipping. Transiting planets – light-curve analysis for eccentric orbits. *Monthly Notices of the Royal Astronomical Society*, 389(3):1383–1390, September 2008. ISSN 0035-8711. doi: 10.1111/j.1365-2966.2008.13658.x. URL https://doi.org/10.1111/j.1365-2966.2008.13658.x.

S. Seager, L. J. Richardson, B. M. S. Hansen, K. Menou, J. Y. K. Cho, and D. Deming. On the Dayside Thermal Emission of Hot Jupiters. *The Astrophysical Journal*, 632:1122–1131, October 2005. ISSN 0004-637X. doi: 10.1086/444411. URL https://ui.adsabs.harvard.edu/abs/2005ApJ...632.1122S. ADS Bibcode: 2005ApJ...632.1122S.

Sz Csizmadia, Th Pasternacki, C. Dreyer, J. Cabrera, A. Erikson, and H. Rauer. The effect of stellar limb darkening values on the accuracy of the planet radii derived from photometric transit observations. *Astronomy & Astrophysics*, 549:A9, January 2013. ISSN 0004-6361, 1432-0746. doi: 10.1051/0004-6361/201219888. URL https://

www.aanda.org/articles/aa/abs/2013/01/aa19888-12/aa19888-12.html. Publisher: EDP Sciences.

René Heller. Analytic solutions to the maximum and average exoplanet transit depth for common stellar limb darkening laws. *Astronomy and Astrophysics*, 623:A137, March 2019. ISSN 0004-6361. doi: 10.1051/0004-6361/201834620. URL https://ui.adsabs.harvard.edu/abs/2019A&A...623A.137H/abstract.

Michael Hippke and René Heller. Optimized transit detection algorithm to search for periodic transits of small planets. *Astronomy and Astrophysics*, 623:A39, March 2019. ISSN 0004-6361. doi: 10.1051/0004-6361/201834672. URL https://ui.adsabs.harvard.edu/abs/2019A&A...623A..39H/abstract.

Joshua N. Winn. Measuring accurate transit parameters. *Proceedings of the International Astronomical Union*, 4(S253):99–109, May 2008. ISSN 1743-9213, 1743-9221. doi: 10.1017/S174392130802629X. URL http://arxiv.org/abs/0807.4929. arXiv: 0807.4929.

C. Lovis and D. Fischer. *Radial Velocity Techniques for Exoplanets*. December 2010. URL https://ui.adsabs.harvard.edu/abs/2010exop.book...27L. Pages: 27-53 Publication Title: Exoplanets ADS Bibcode: 2010exop.book...27L.

John Southworth, Peter J. Wheatley, and Giles Sams. A method for the direct determination of the surface gravities of transiting extrasolar planets. *Monthly Notices of the Royal Astronomical Society: Letters*, 379(1):L11–L15, July 2007. ISSN 1745-3925. doi: 10.1111/j.1745-3933.2007.00324.x. URL https://doi.org/10.1111/j.1745-3933.2007.00324.x.

I. Boisse, F. Bouchy, G. Hébrard, X. Bonfils, N. Santos, and S. Vauclair. Disentangling between stellar activity and planetary signals. *Astronomy and Astrophysics*, 528:A4, April 2011. ISSN 0004-6361. doi: 10.1051/0004-6361/201014354. URL https://ui.adsabs.harvard.edu/abs/2011A&A...528A...4B/abstract.

John Southworth. Homogeneous studies of transiting extrasolar planets - I. Light-curve analyses. *Monthly Notices of the Royal Astronomical Society*, 386:1644–1666, May 2008. ISSN 0035-8711. doi: 10.1111/j.1365-2966.2008.13145.x. URL https://ui.adsabs.harvard.edu/abs/2008MNRAS.386.1644S. ADS Bibcode: 2008MN-RAS.386.1644S.

Michael Endl. Chapter 45 - Extrasolar Planets. In Tilman Spohn, Doris Breuer, and Torrence V. Johnson, editors, *Encyclopedia of the Solar System (Third Edition)*, pages 957–977. Elsevier, Boston, January 2014. ISBN 978-0-12-415845-0. doi: 10.1016/B978-0-12-415845-0.00045-1. URL https://www.sciencedirect.com/science/article/pii/B9780124158450000451.

G. Torres, J. Andersen, and A. Giménez. Accurate masses and radii of normal stars: modern results and applications. *Astronomy and Astrophysics Review*, 18(1-2):67–126, February 2010. ISSN 0935-4956. doi: 10.1007/s00159-009-0025-1. URL https://ui.adsabs.harvard.edu/abs/2010A&ARv..18...67T/abstract.

Stéphane Udry and Nuno C. Santos. Statistical Properties of Exoplanets. *Annual Review of Astronomy and Astrophysics*, 45(1):397–439, 2007. doi: 10.1146/annurev.astro.45.051806.110529. URL https://doi.org/10.1146/annurev.astro.45.051806.110529. _eprint: https://doi.org/10.1146/annurev.astro.45.051806.110529.

G. Morello, A. Tsiaras, I. D. Howarth, and D. Homeier. High-precision Stellar Limb-darkening in Exoplanetary Transits. *The Astronomical Journal*, 154:111, September 2017. ISSN 0004-6256. doi: 10.3847/1538-3881/aa8405. URL https://ui.adsabs.harvard.edu/abs/2017AJ....154..111M. ADS Bibcode: 2017AJ....154..111M.

K. Schwarzschild. On the equilibrium of the Sun's atmosphere. *Nachrichten von der Königlichen Gesellschaft der Wissenschaften zu Göttingen. Math.-phys. Klasse*, 195:41–53, January 1906. URL https://ui.adsabs.harvard.edu/abs/1906WisGo.195...41S. ADS Bibcode: 1906WisGo.195...41S.

E. A. Milne. Radiative equilibrium in the outer layers of a star. *Monthly Notices of the Royal Astronomical Society*, 81:361–375, March 1921. ISSN 0035-8711. doi: 10.1093/mnras/81.5.361. URL https://ui.adsabs.harvard.edu/abs/1921MNRAS. .81..361M. ADS Bibcode: 1921MNRAS..81..361M.

Zdenek Kopal. Detailed effects of limb darkening upon light and velocity curves of close binary systems. *Harvard College Observatory Circular*, 454:1–12, January 1950. URL https://ui.adsabs.harvard.edu/abs/1950HarCi.454....1K. ADS Bibcode: 1950HarCi.454....1K.

D. A. Klinglesmith and S. Sobieski. Nonlinear Limb Darkening for Early-Type Stars. *The Astronomical Journal*, 75:175–182, March 1970. ISSN 0004-6256. doi: 10.1086/ 110960. URL https://ui.adsabs.harvard.edu/abs/1970AJ.....75..175K. ADS Bibcode: 1970AJ.....75..175K.

J. Diaz-Cordoves and A. Gimenez. A new nonlinear approximation to the limb-darkening of hot stars. *Astronomy and Astrophysics*, 259(1):227–231, June 1992. ISSN 0004-6361. URL https://ui.adsabs.harvard.edu/abs/1992A&A...259. .227D/abstract.

D. Hestroffer. Centre to limb darkening of stars. New model and application to stellar interferometry. *Astronomy and Astrophysics*, 327:199–206, November 1997. ISSN 0004-6361. URL https://ui.adsabs.harvard.edu/abs/1997A&A...327..199H/ abstract.

A. Claret. A new non-linear limb-darkening law for LTE stellar atmosphere models. Calculations for -5.0 <= log[M/H] <= +1, 2000 K <= T_{eff} <= 50000 K at several surface gravities. *Astronomy and Astrophysics*, 363:1081– 1190, November 2000. ISSN 0004-6361. URL https://ui.adsabs.harvard.edu/ abs/2000A&A...363.1081C/abstract.

T. M. D. Pereira, M. Asplund, R. Collet, I. Thaler, R. Trampedach, and J. Leenaarts. How realistic are solar model atmospheres? *Astronomy & As-*

trophysics, 554:A118, June 2013. ISSN 0004-6361, 1432-0746. doi: 10.1051/ 0004-6361/201321227. URL https://www.aanda.org/articles/aa/abs/2013/06/ aa21227-13/aa21227-13.html. Publisher: EDP Sciences.

Néstor Espinoza and Andrés Jordán. Limb darkening and exoplanets – II. Choosing the best law for optimal retrieval of transit parameters. *Monthly Notices of the Royal Astronomical Society*, 457(4):3573–3581, April 2016. URL https://doi.org/10. 1093/mnras/stw224.

Eric Agol, Jason Steffen, Re'em Sari, and Will Clarkson. On detecting terrestrial planets with timing of giant planet transits. *Monthly Notices of the Royal Astronomical Society*, 359:567–579, May 2005. ISSN 0035-8711. doi: 10.1111/j. 1365-2966.2005.08922.x. URL https://ui.adsabs.harvard.edu/abs/2005MNRAS. 359..567A. ADS Bibcode: 2005MNRAS.359..567A.

Jordi Miralda-Escudé. Orbital Perturbations of Transiting Planets: A Possible Method to Measure Stellar Quadrupoles and to Detect Earth-Mass Planets. *The Astrophysical Journal*, 564:1019–1023, January 2002. ISSN 0004-637X. doi: 10.1086/324279. URL https://ui.adsabs.harvard.edu/abs/2002ApJ...564.1019M. ADS Bibcode: 2002ApJ...564.1019M.

Matthew J. Holman and Norman W. Murray. The Use of Transit Timing to Detect Terrestrial-Mass Extrasolar Planets. *Science*, 307:1288–1291, February 2005. ISSN 0036-8075. doi: 10.1126/science.1107822. URL https://ui.adsabs.harvard.edu/ abs/2005Sci...307.1288H. ADS Bibcode: 2005Sci...307.1288H.

B. Levrard, C. Winisdoerffer, and G. Chabrier. FALLING TRANSITING EXTRA-SOLAR GIANT PLANETS. *The Astrophysical Journal*, 692(1):L9, January 2009. ISSN 0004-637X. doi: 10.1088/0004-637X/692/1/L9. URL https://dx.doi.org/ 10.1088/0004-637X/692/1/L9. Publisher: The American Astronomical Society.

Nevin N. Weinberg, Niyousha Davachi, Reed Essick, Hang Yu, Phil Arras, and Brent Belland. Orbital Decay of Hot Jupiters due to Weakly Nonlinear Tidal Dissipation,

May 2023. URL https://ui.adsabs.harvard.edu/abs/2023arXiv230511974W. Publication Title: arXiv e-prints ADS Bibcode: 2023arXiv230511974W.

P. F. L. Maxted and S. Gill. qpower2: A fast and accurate algorithm for the computation of exoplanet transit light curves with the power-2 limb-darkening law. *Astronomy and Astrophysics*, 622:A33, February 2019. ISSN 0004-6361. doi: 10.1051/0004-6361/201834563. URL https://ui.adsabs.harvard.edu/abs/2019A&A...622A..33M. ADS Bibcode: 2019A&A...622A..33M.

Suman Saha. Precise Transit Photometry Using TESS: Updated Physical Properties for 28 Exoplanets Around Bright Stars, June 2023. URL https://ui.adsabs.harvard.edu/abs/2023arXiv230602951S. Publication Title: arXiv e-prints ADS Bibcode: 2023arXiv230602951S.

Kaisey Mandel and Eric Agol. Analytic Light Curves for Planetary Transit Searches. *The Astrophysical Journal*, 580:L171–L175, December 2002. ISSN 0004-637X. doi: 10.1086/345520. URL https://ui.adsabs.harvard.edu/abs/2002ApJ...580L.171M. ADS Bibcode: 2002ApJ...580L.171M.

Luigi Mancini and John Southworth. Eight years of accurate photometric follow-up of transiting giant exoplanets, May 2016. URL https://ui.adsabs.harvard.edu/abs/2016arXiv160505576M. Publication Title: arXiv e-prints ADS Bibcode: 2016arXiv160505576M.

John Southworth. Homogeneous studies of transiting extrasolar planets - II. Physical properties. *Monthly Notices of the Royal Astronomical Society*, 394:272–294, March 2009. ISSN 0035-8711. doi: 10.1111/j.1365-2966.2008.14274.x. URL https://ui.adsabs.harvard.edu/abs/2009MNRAS.394..272S. ADS Bibcode: 2009MN-RAS.394..272S.

Guillermo Torres, Joshua N. Winn, and Matthew J. Holman. Toward a homogeneous set of transiting planet parameters. *Proceedings of the International Astronomical*

Union, 4(S253):482–485, May 2008b. ISSN 1743-9213, 1743-9221. doi: 10.1017/ S1743921308026999. URL http://arxiv.org/abs/0806.4353. arXiv: 0806.4353.

P. F. L. Maxted, D. Ehrenreich, T. G. Wilson, Y. Alibert, A. Collier Cameron, S. Hoyer, S. G. Sousa, G. Olofsson, A. Bekkelien, A. Deline, L. Delrez, A. Bonfanti, L. Borsato, R. Alonso, G. Anglada Escudé, D. Barrado, S. C. C. Barros, W. Baumjohann, M. Beck, T. Beck, W. Benz, N. Billot, F. Biondi, X. Bonfils, A. Brandeker, C. Broeg, T. Bárczy, J. Cabrera, S. Charnoz, C. Corral Van Damme, Sz Csizmadia, M. B. Davies, M. Deleuil, O. D. S. Demangeon, B.-O. Demory, A. Erikson, H. G. Florén, A. Fortier, L. Fossati, M. Fridlund, D. Futyan, D. Gandolfi, M. Gillon, M. Guedel, P. Guterman, K. Heng, K. G. Isaak, L. Kiss, J. Laskar, A. Lecavelier des Etangs, M. Lendl, C. Lovis, D. Magrin, V. Nascimbeni, R. Ottensamer, I. Pagano, E. Pallé, G. Peter, G. Piotto, D. Pollacco, F. J. Pozuelos, D. Queloz, R. Ragazzoni, N. Rando, H. Rauer, C. Reimers, I. Ribas, S. Salmon, N. C. Santos, G. Scandariato, A. E. Simon, A. M. S. Smith, M. Steller, M. I. Swayne, Gy M. Szabó, D. Ségransan, N. Thomas, S. Udry, V. Van Grootel, and N. A. Walton. Analysis of Early Science observations with the CHaracterising ExOPlanets Satellite (CHEOPS) using pycheops. *Monthly Notices of the Royal Astronomical Society*, 514 (1):77–104, June 2022. ISSN 0035-8711, 1365-2966. doi: 10.1093/mnras/stab3371. URL http://arxiv.org/abs/2111.08828. arXiv:2111.08828 [astro-ph].

Jon M. Jenkins, Joseph D. Twicken, Sean McCauliff, Jennifer Campbell, Dwight Sanderfer, David Lung, Masoud Mansouri-Samani, Forrest Girouard, Peter Tenenbaum, Todd Klaus, Jeffrey C. Smith, Douglas A. Caldwell, A. Dean Chacon, Christopher Henze, Cory Heiges, David W. Latham, Edward Morgan, Daryl Swade, Stephen Rinehart, and Roland Vanderspek. The TESS science processing operations center. In *Software and Cyberinfrastructure for Astronomy IV*, volume 9913, pages 1232–1251. SPIE, August 2016. doi: 10.1117/12.2233418. URL https://www.spiedigitallibrary.org/conference-proceedings-of-spie/ 9913/99133E/The-TESS-science-processing-operations-center/10.1117/12. 2233418.full.

D. K. Sing. Stellar limb-darkening coefficients for CoRot and Kepler. *Astronomy and Astrophysics*, 510:A21, February 2010. ISSN 0004-6361. doi: 10.1051/0004-6361/ 200913675. URL https://ui.adsabs.harvard.edu/abs/2010A&A...510A..21S. ADS Bibcode: 2010A&A...510A..21S.

Z. Magic, A. Chiavassa, R. Collet, and M. Asplund. The Stagger-grid: A grid of 3D stellar atmosphere models. IV. Limb darkening coefficients. *Astronomy and Astrophysics*, 573:A90, January 2015. ISSN 0004-6361. doi: 10.1051/0004-6361/ 201423804. URL https://ui.adsabs.harvard.edu/abs/2015A&A...573A..90M. ADS Bibcode: 2015A&A...573A..90M.

P. F. L. Maxted. Limb darkening measurements from TESS and Kepler light curves of transiting exoplanets. *Monthly Notices of the Royal Astronomical Society*, 519(3): 3723–3735, January 2023. ISSN 0035-8711, 1365-2966. doi: 10.1093/mnras/stac3741. URL http://arxiv.org/abs/2212.09117. arXiv:2212.09117 [astro-ph].

Christopher M. Johns-Krull, Peter R. McCullough, Christopher J. Burke, Jeff A. Valenti, K. A. Janes, J. N. Heasley, L. Prato, R. Bissinger, M. Fleenor, C. N. Foote, E. Garcia-Melendo, B. L. Gary, P. J. Howell, F. Mallia, G. Masi, and T. Vanmunster. XO-3b: A Massive Planet in an Eccentric Orbit Transiting an F5 V Star. *The Astrophysical Journal*, 677:657–670, April 2008. ISSN 0004-637X. doi: 10.1086/528950. URL https://ui.adsabs.harvard.edu/abs/2008ApJ...677..657J. ADS Bibcode: 2008ApJ...677..657J.

Matthew Newville, Till Stensitzki, Daniel B. Allen, and Antonino Ingargiola. LM-FIT: Non-Linear Least-Square Minimization and Curve-Fitting for Python. *Zenodo*, September 2014. doi: 10.5281/zenodo.11813. URL https://ui.adsabs.harvard.edu/abs/2014zndo.....11813N. ADS Bibcode: 2014zndo.....11813N.

Daniel Foreman-Mackey, David W. Hogg, Dustin Lang, and Jonathan Goodman. emcee: The MCMC Hammer. *Publications of the Astronomical Society of the Pacific*, 125(925):306, February 2013. ISSN 1538-3873. doi: 10.1086/670067. URL

https://iopscience.iop.org/article/10.1086/670067/meta. Publisher: IOP Publishing.

G. Maciejewski, D. Dimitrov, R. Neuhaeuser, A. Niedzielski, St Raetz, Ch Ginski, Ch Adam, C. Marka, M. Moualla, and M. Mugrauer. Transit timing variation in exoplanet WASP-3b. *Monthly Notices of the Royal Astronomical Society*, 407(4): 2625–2631, July 2010. ISSN 00358711. doi: 10.1111/j.1365-2966.2010.17099.x. URL http://arxiv.org/abs/1006.1348. arXiv:1006.1348 [astro-ph].

M. Montalto, J. Gregorio, G. Boue', A. Mortier, I. Boisse, M. Oshagh, M. Maturi, P. Figueira, S. Sousa, and N. C. Santos. A new analysis of the WASP-3 system: no evidence for an additional companion. *Monthly Notices of the Royal Astronomical Society*, 427(4):2757–2771, December 2012. ISSN 0035-8711, 1365-2966. doi: 10.1111/j.1365-2966.2012.21926.x. URL http://arxiv.org/abs/1211.0218. arXiv:1211.0218 [astro-ph].

J. W. Rostron and P. J. Wheatley. Dectection of Thermal Emission from WASP-3b. *Proceedings of the International Astronomical Union*, 8 (S299):305–306, June 2013. ISSN 1743-9213, 1743-9221. doi: 10. 1017/S1743921313008715. URL https://www.cambridge.org/core/product/ identifier/S1743921313008715/type/journal_article.

Ming Zhao, Jennifer Milburn, Travis Barman, Sasha Hinkley, Mark R. Swain, Jason Wright, and John D. Monnier. Detection of Ks-band Thermal Emission from WASP-3b. *The Astrophysical Journal*, 748(1):L8, March 2012. ISSN 2041-8205, 2041-8213. doi: 10.1088/2041-8205/748/1/L8. URL http://arxiv.org/abs/1202.3435. arXiv:1202.3435 [astro-ph].

Nawal Husnoo, Frédéric Pont, Guillaume Hébrard, Elaine Simpson, Tsevi Mazeh, François Bouchy, Claire Moutou, Luc Arnold, Isabelle Boisse, Rodrigo F. Díaz, Anne Eggenberger, and Avi Shporer. Orbital eccentricity of WASP-12 and WASP-14 from new radial velocity monitoring with SOPHIE. *Monthly Notices of the*

Royal Astronomical Society, 413:2500–2508, June 2011. ISSN 0035-8711. doi: 10.1111/j.1365-2966.2011.18322.x. URL https://ui.adsabs.harvard.edu/abs/2011MNRAS.413.2500H. ADS Bibcode: 2011MNRAS.413.2500H.

Nikku Madhusudhan. C/O Ratio as a Dimension for Characterizing Exoplanetary Atmospheres. *The Astrophysical Journal*, 758:36, October 2012. ISSN 0004-637X. doi: 10.1088/0004-637X/758/1/36. URL https://ui.adsabs.harvard.edu/abs/2012ApJ...758...36M. ADS Bibcode: 2012ApJ...758...36M.

Jasmina Blecic, Joseph Harrington, Nikku Madhusudhan, Kevin B. Stevenson, Ryan A. Hardy, Patricio E. Cubillos, Matthew Hardin, Christopher J. Campo, William C. Bowman, Sarah Nymeyer, Thomas J. Loredo, David R. Anderson, and Pierre F. L. Maxted. Thermal Emission of WASP-14b Revealed with Three Spitzer Eclipses. *The Astrophysical Journal*, 779:5, December 2013. ISSN 0004-637X. doi: 10.1088/0004-637X/779/1/5. URL https://ui.adsabs.harvard.edu/abs/2013ApJ...779....5B. ADS Bibcode: 2013ApJ...779....5B.

Brian M. Kilpatrick, Nikole K. Lewis, Tiffany Kataria, Drake Deming, James G. Ingalls, Jessica E. Krick, and Gregory S. Tucker. Spitzer Secondary Eclipse Depths with Multiple Intrapixel Sensitivity Correction Methods Observations of WASP-13b, WASP-15b, WASP-16b, WASP-62b, and HAT-P-22b. *The Astronomical Journal*, 153:22, January 2017. ISSN 0004-6256. doi: 10.3847/1538-3881/153/1/22. URL https://ui.adsabs.harvard.edu/abs/2017AJ....153...22K. ADS Bibcode: 2017AJ....153...22K.

E. K. Simpson, D. Pollacco, A. Collier Cameron, G. Hébrard, D. R. Anderson, S. C. C. Barros, I. Boisse, F. Bouchy, F. Faedi, M. Gillon, L. Hebb, F. P. Keenan, G. R. M. Miller, C. Moutou, D. Queloz, I. Skillen, P. Sorensen, H. C. Stempels, A. Triaud, C. A. Watson, and P. A. Wilson. The spin-orbit angles of the transiting exoplanets WASP-1b, WASP-24b, WASP-38b and HAT-P-8b from Rossiter-McLaughlin observations. *Monthly Notices of the Royal Astronomical Society*, 414:3023–3035, July 2011. ISSN 0035-8711. doi: 10.1111/j.1365-2966.2011.18603.x. URL https:

//ui.adsabs.harvard.edu/abs/2011MNRAS.414.3023S. ADS Bibcode: 2011MN-RAS.414.3023S.

A. M. S. Smith, D. R. Anderson, N. Madhusudhan, J. Southworth, A. Collier Cameron, J. Blecic, J. Harrington, C. Hellier, P. F. L. Maxted, D. Pollacco, D. Queloz, B. Smalley, A. H. M. J. Triaud, and P. J. Wheatley. Thermal emission from WASP-24b at 3.6 and 4.5 m. *Astronomy and Astrophysics*, 545:A93, September 2012. ISSN 0004-6361. doi: 10.1051/0004-6361/201219294. URL https://ui.adsabs.harvard.edu/abs/2012A&A...545A..93S. ADS Bibcode: 2012A&A...545A..93S.

C. Weidner and K. Horne. Limits on the orbits and masses of moons around currently-known transiting exoplanets. *Astronomy and Astrophysics*, 521:A76, October 2010. ISSN 0004-6361. doi: 10.1051/0004-6361/201014955. URL https://ui.adsabs.harvard.edu/abs/2010A&A...521A..76W. ADS Bibcode: 2010A&A...521A..76W.

L. A. dos Santos, V. Bourrier, D. Ehrenreich, J. Sanz-Forcada, M. López-Morales, D. K. Sing, A. García Muñoz, G. W. Henry, P. Lavvas, A. Lecavelier des Etangs, T. Mikal-Evans, A. Vidal-Madjar, and H. R. Wakeford. HST PanCET program: non-detection of atmospheric escape in the warm Saturn-sized planet WASP-29 b. *Astronomy & Astrophysics, Volume 649, id.A40, <NUMPAGES>10</NUMPAGES> pp.*, 649:A40, May 2021. ISSN 0004-6361. doi: 10.1051/0004-6361/202140491. URL https://ui.adsabs.harvard.edu/abs/2021A%26A...649A..40D/abstract.

Ian Wong, Yayaati Chachan, Heather A. Knutson, Gregory W. Henry, Danica Adams, Tiffany Kataria, Björn Benneke, Peter Gao, Drake Deming, Mercedes López-Morales, David K. Sing, Munazza K. Alam, Gilda E. Ballester, Joanna K. Barstow, Lars A. Buchhave, Leonardo A. dos Santos, Guangwei Fu, Antonio García Muñoz, Ryan J. MacDonald, Thomas Mikal-Evans, Jorge Sanz-Forcada, and Hannah R. Wakeford. The Hubble PanCET Program: A Featureless Transmission Spectrum for WASP-29b and Evidence of Enhanced Atmospheric Metallicity on WASP-80b. Technical Report arXiv:2205.10765, arXiv, May 2022. URL http://arxiv.org/abs/2205.10765. arXiv:2205.10765 [astro-ph] type: article.

Guangwei Fu, Drake Deming, Erin May, Kevin Stevenson, David K. Sing, Joshua D. Lothringer, H. R. Wakeford, Nikolay Nikolov, Thomas Mikal-Evans, Vincent Bourrier, Leonardo A. dos Santos, Munazza K. Alam, Gregory W. Henry, Antonio García Muñoz, and Mercedes López-Morales. The Hubble PanCET program: Transit and Eclipse Spectroscopy of the Hot-Jupiter WASP-74b. *The Astronomical Journal*, 162:271, December 2021. ISSN 0004-6256. doi: 10.3847/1538-3881/ac3008. URL https://ui.adsabs.harvard.edu/abs/2021AJ....162..271F. ADS Bibcode: 2021AJ....162..271F.

A. Lira-Barria, P. M. Rojo, and R. A. Mendez. Characterization of exoplanetary atmospheres through a model-unbiased spectral survey methodology. *Astronomy and Astrophysics*, 657:A36, January 2022. ISSN 0004-6361. doi: 10.1051/0004-6361/202140494. URL https://ui.adsabs.harvard.edu/abs/2022A&A...657A..36L. ADS Bibcode: 2022A&A...657A..36L.

Petros Spyratos, Nikolay K. Nikolov, Savvas Constantinou, John Southworth, Nikku Madhusudhan, Elyar Sedaghati, David Ehrenreich, and Luigi Mancini. A precise blue-optical transmission spectrum from the ground: evidence for haze in the atmosphere of WASP-74b. *Monthly Notices of the Royal Astronomical Society*, 521: 2163–2180, May 2023. ISSN 0035-8711. doi: 10.1093/mnras/stad637. URL https://ui.adsabs.harvard.edu/abs/2023MNRAS.521.2163S. ADS Bibcode: 2023MNRAS.521.2163S.

N. Buchschacher, D. Ségransan, S. Udry, and R. Díaz. Data and Analysis Center for Exoplanets. 495:7, September 2015. URL https://ui.adsabs.harvard.edu/abs/2015ASPC..495....7B. Conference Name: Astronomical Data Analysis Software an Systems XXIV (ADASS XXIV) ADS Bibcode: 2015ASPC..495....7B.

R. L. Akeson, X. Chen, D. Ciardi, M. Crane, J. Good, M. Harbut, E. Jackson, S. R. Kane, A. C. Laity, S. Leifer, M. Lynn, D. L. McElroy, M. Papin, P. Plavchan, S. V. Ramírez, R. Rey, K. von Braun, M. Wittman, M. Abajian, B. Ali, C. Beichman, A. Beekley, G. B. Berriman, S. Berukoff, G. Bryden, B. Chan, S. Groom,

C. Lau, A. N. Payne, M. Regelson, M. Saucedo, M. Schmitz, J. Stauffer, P. Wyatt, and A. Zhang. The NASA Exoplanet Archive: Data and Tools for Exoplanet Research. *Publications of the Astronomical Society of the Pacific*, 125:989, August 2013. ISSN 0004-6280. doi: 10.1086/672273. URL https://ui.adsabs.harvard.edu/abs/2013PASP..125..989A. ADS Bibcode: 2013PASP..125..989A.

John Southworth. Homogeneous studies of transiting extrasolar planets - IV. Thirty systems with space-based light curves. *Monthly Notices of the Royal Astronomical Society*, 417:2166–2196, November 2011. ISSN 0035-8711. doi: 10.1111/j.1365-2966.2011.19399.x. URL https://ui.adsabs.harvard.edu/abs/2011MNRAS.417.2166S. ADS Bibcode: 2011MNRAS.417.2166S.

N. C. Santos, S. G. Sousa, A. Mortier, V. Neves, V. Adibekyan, M. Tsantaki, E. Delgado Mena, X. Bonfils, G. Israelian, M. Mayor, and S. Udry. SWEET-Cat: A catalogue of parameters for Stars With ExoplanETs. I. New atmospheric parameters and masses for 48 stars with planets. *Astronomy and Astrophysics*, 556:A150, August 2013. ISSN 0004-6361. doi: 10.1051/0004-6361/201321286. URL https://ui.adsabs.harvard.edu/abs/2013A&A...556A.150S. ADS Bibcode: 2013A&A...556A.150S.

Jonathan Goodman and Jonathan Weare. Ensemble samplers with affine invariance. *Communications in Applied Mathematics and Computational Science*, 5:65–80, January 2010. doi: 10.2140/camcos.2010.5.65. URL https://ui.adsabs.harvard.edu/abs/2010CAMCS...5...65G. ADS Bibcode: 2010CAMCS...5...65G.

Rodrigo Luger, Daniel Foreman-Mackey, and David W. Hogg. Linear Models for Systematics and Nuisances. *Research Notes of the American Astronomical Society*, 1:7, December 2017. ISSN 2515-5172. doi: 10.3847/2515-5172/aa96b5. URL https://ui.adsabs.harvard.edu/abs/2017RNAAS...1....7L. ADS Bibcode: 2017RNAAS...1....7L.

David M. Kipping. Binning is sinning: morphological light-curve distortions due to finite integration time. *Monthly Notices of the Royal Astronomical Society*, 408:

1758–1769, November 2010. ISSN 0035-8711. doi: 10.1111/j.1365-2966.2010.17242.x. URL https://ui.adsabs.harvard.edu/abs/2010MNRAS.408.1758K. ADS Bibcode: 2010MNRAS.408.1758K.

Steve B. Howell, Charlie Sobeck, Michael Haas, Martin Still, Thomas Barclay, Fergal Mullally, John Troeltzsch, Suzanne Aigrain, Stephen T. Bryson, Doug Caldwell, William J. Chaplin, William D. Cochran, Daniel Huber, Geoffrey W. Marcy, Andrea Miglio, Joan R. Najita, Marcie Smith, J. D. Twicken, and Jonathan J. Fortney. The K2 Mission: Characterization and Early Results. *Publications of the Astronomical Society of the Pacific*, 126:398, April 2014. ISSN 0004-6280. doi: 10.1086/676406. URL https://ui.adsabs.harvard.edu/abs/2014PASP..126..398H. ADS Bibcode: 2014PASP..126..398H.

Pía Cortés-Zuleta, Patricio Rojo, Songhu Wang, Tobias C. Hinse, Sergio Hoyer, Bastian Sanhueza, Patricio Correa-Amaro, and Julio Albornoz. TraMoS. V. Updated ephemeris and multi-epoch monitoring of the hot Jupiters WASP-18Ab, WASP-19b, and WASP-77Ab. *Astronomy and Astrophysics*, 636:A98, April 2020. ISSN 0004-6361. doi: 10.1051/0004-6361/201936279. URL https://ui.adsabs.harvard.edu/abs/2020A&A...636A..98C/abstract.